NTNU

Norwegian University of
Science and Technology

Active Control of Reactive Power in a Modern Electrical Rail Vehicle

Eivind Toreid

Master of Science in Electric Power Engineering
Submission date: June 2011
Supervisor: Kjetil Uhlen, ELKRAFT

Norwegian University of Science and Technology
Department of Electric Power Engineering

Problem Description

The master thesis is a further investigation of control schemes for reactive power proposed in a project fall semester 2010. The control schemes were intended to reduce line losses and increase available power to the vehicle.

The control schemes for reactive power were designed assuming the electric traction power system was fed by one or more stiff voltage sources. The master thesis should investigate the performance of the proposed control schemes in a system supplied by rotary converters instead of stiff voltage sources.

The thesis should investigate the proposed control schemes with respect to low frequency stability in system consisting of a rotary converter and a modern electrical rail vehicle; voltage stability and power oscillations. The control schemes are to be implemented in a simplified vehicle model for testing.

A complete simulation model of a real vehicle is normally not available from the manufacturer, as this would include industrial secrets. It should be investigated how low frequency stability analyses can be performed without the complete vehicle model, only with the steady state characteristics and the input admittance in the low frequency domain at the interface between the vehicle and the power system. The simplified vehicle model mentioned above and dynamic behaviour should be used as reference, comparing the results from the vehicle model and the results based on its frequency response.

Assignment given: 18 January 2011
Supervisor: Prof. Kjetil Uhlen

Abstract

Modern electrical rail vehicles employ four-quadrant voltage source converters, which allow independent control of real and reactive power. This thesis focuses the control of reactive power at the vehicle regarding load flow and stability.

Settings for power factor as a function of voltage were proposed in a project fall 2010, aiming to reduce line loss and increase transmission capacity. This thesis is mainly a further investigation of some of the settings proposed.

One of the proposed settings for controlling reactive power is found to reduce the load of a rotary converter station in the range of 0-3 %. Total system losses are reduced by 0.21-0.33 %.

During traction, the problematic issue regarding stability is found to be speed oscillations of the rotary converter. Controlling reactive power is found to have a limited damping effect on speed oscillations of a rotary converter. Other works have investigated how speed oscillations of the rotary converter can be damped by controlling the real power of the vehicle; the real power control is found to have a clearly better effect than reactive.

During no-load operation, the problematic issue regarding stability is found to be oscillations caused by the vehicle and its control system. The vehicle control system and its response to the line voltage may cause instability, especially at long line lengths, regardless of any rotary converter. As reactive power has a significant effect on the line voltage, reactive power may be controlled in a manner increasing the damping of such oscillations significantly.

Finally the thesis describes how a simulation model of a modern electrical rail vehicle for stability analysis can be made from the steady state characteristics and the input admittance of the vehicle, without knowing the complete vehicle model.

The settings which where proposed and investigated in this project are optimized for a system fed by stiff voltage sources, not by rotary converters, and a more complete optimization for a system fed by rotary converters would be of interest.

Keywords:

Reactive power, modern rail vehicle, advanced rail vehicle, railway, locomotive, SIMPOW, low frequency stability, impedance modelling, equivalent admittance-based load

Acknowledgements

First I would like to thank my advisor, Prof. Kjetil Uhlen, and Dr. Steinar Danielsen, for their guidance and feedback to my work.

I would also like to thank the Norwegian National Rail Administration, for providing simulation software, models and input parameters, and Frank Martinsen, for teaching me how to use the simulation software during my work summer 2010.

Last but not least I would like to thank Chuleeporn Toreid, for her support and patience with me during this work. Without you, this project would not have been what it is.

Eivind Toreid

Contents

List of symbols

C	Capacitance
E	Energy
F	Force, tractive effort
f	Frequency
g	Acceleration of gravity, 9.81 m/s^2
I	Current, RMS-value
$[I]$	Identity matrix
i	Current, instantaneous value
j	Imaginary unit $\sqrt{-1}$
L	Inductance
l	Line length
M	Mass
MP	Real power's voltage dependency
P	Real (active) power
Q	Reactive power
R	Resistance
S	Track gradient in per mille, apparent power
s	Laplace variable
T	Torque, time in time constants
t	Time as variable
U	Voltage, RMS-value
u	Voltage, instantaneous value
v	Speed
X	Reactance
Y	Admittance
Z	Impedance
α	Adhesion coefficient
δ	Voltage angle at node
η	Efficiency
λ	Eigenvalue
θ_Z	Angle
θ_Z	Impedance angle, < 0 capacitive, > 0 inductive

θ_Y	Admittance angle, > 0 capacitive, < 0 inductive
Φ	Magnetic flux
ϕ	Load angle, < 0 capacitive, > 0 inductive
ω	Angular speed
x^{ref}	Reference value, set point
x_0	Initial value
Δx	Change of value

Phasor quantities are indicated as $\bar{Z}$.

Chapter 1

Introduction

1.1 Motivation

Modern electrical rail vehicles employ self-commutated converters, which allow independent control of real and reactive power. The real power is normally given by the tractive work to be done, but the reactive power can be utilized according to what is useful for the vehicle and the power system.

In a weak and heavily loaded network, the real power may have to be reduced to avoid an unacceptable voltage drop. Optimal control of reactive power enable higher real power capacity - capacity for more or more powerful trains, allowing reduced driving times or higher load capacity. Capacity could otherwise be increased by reducing the line impedance or building new converter stations, but these measures are expensive and require long time for realization.

From basic theory of AC systems, reactive power is known to have significant effect on the line voltage. Higher power factor and line voltage will allow the same power to be taken out at a lower current. As resistive losses are proportional to the square of the current, lower currents will reduce the transmission losses. During regenerative braking, the line voltage will increase. Regenerative braking is not permitted at line voltage above a certain limit. Reactive power may be consumed during regenerative braking, to ensure real power is not limited.

1.2 Scope of Work

A project was done the fall semester 2010 ([5]), investigating the effect of reactive power control regarding available power at the vehicle and losses. Two new control

schemes were proposed for traction. For regenerative braking, one new control scheme was proposed. This thesis will further investigate one of the control schemes for traction. The attention is mostly given to the distribution of load between converter stations, and the effect on voltage and rotor angle stability.

1.2.1 Research Questions

- What is the effect of the reactive power control schemes proposed, when operated in an interconnected system fed by rotary converters, with respect to losses and distribution of load between the converter stations?
- What is the effect on stability of the control schemes proposed? Are modifications of the control schemes required, in order to be acceptable regarding stability.
- How can stability be investigated without having a complete simulation model of the vehicle, only a steady state model and the frequency response at the interface between the vehicle and the power system? An equivalent dynamic model of the load for the simulation software SIMPOW is to be made, enabling the simulations to be run finding e.g. time domain responses and eigenvalues.

1.2.2 Outline of Report

The outline of the report is as follows:

- Chapter 1 introduces the project, giving the background and establishing questions to be investigated. The structure and limitations of the work are given, as well as an overview of some previous research on the field.
- Chapter 2 gives a basic description of electric traction power systems. The description of the power supply emphasizes the power supply by rotary converters as implemented in Norway, with modern electrical rail vehicles as load.
- Chapter 3 is a summary of a project performed fall semester 2010. In this project, control schemes for reactive power was developed for a system fed by stiff voltage sources and investigated regarding capacity and losses.
- Chapter 4 describes the performance of the control schemes suggested in chapter 3 in a system fed by rotary converters.
- Chapter 5 investigates some of the control schemes for traction suggested in chapter 3 regarding stability. A power oscillation damper is introduced, modulating reactive power attempting to improve the system stability.

- Chapter 6 describes the modelling of a load to be equivalent to the complete vehicle model, based in the operating point and the vehicle admittance seen from the power system.
- Chapter 7 presents answers to the research questions, conclusions and suggestions for further work.

1.2.3 Limitations

Simulations are only performed with one train in the system.

Simulations are only performed for traction and no-load, not for regenerative braking.

The control scheme "Maximum power" proposed in the fall semester (section 3.2.1 and [5]) is not considered any further. This control scheme is closely connected to the limitation of vehicle current according to the European Standard EN50388:2005, and this limitation is not in focus of this thesis.

Chapter 2

Electric Traction Power Systems

This chapter gives a brief introduction to electric traction power system and some of its components, focusing on the system as used on the Norwegian railways. In this thesis, the term "electric traction[1] power system" is used to describe the total system of components used for the generation/conversion, transmission and consumption og electric energy for railway transport. The majority of the energy and the focus of this thesis is energy used for traction, but energy from the system is also used for auxiliary consumption on board the train, in some cases also for stationary loads.

2.1 Electrification Systems

Electric traction power systems are with few exceptions DC systems or single phase AC, as these require only two conductors to the vehicle. The conductor may be an overhead line, or for lower voltages a conductor rail next to the track (third rail). The rails are used as return conductor. The system voltage of a power system will generally be chosen higher with increasing rated power and transmission distances, to keep losses at an acceptable level. Except from some applications of power electronics, AC is the only practical solution to convert electrical power from one voltage level to another, and this has been and is the main reason for AC electrification of railways.

AC can be transformed from one voltage level to another, and different voltages can be obtained by employing transformers with several inputs or outlets, using a

[1] The word "railway" would perhaps be more self-explanatory than "traction"

tap changer to select between them. Before the development of power electronics, this way was the possibility to supply a stepwise adjustable AC voltage available for the traction motors of a vehicle.

As DC voltages cannot be easily transformed, the line voltage should be in the same range as the voltage of the traction motors. DC is commonly used for tramways and subways, in some countries also for conventional railways. The nominal voltage is in the range 600 V to 3 kV. The low voltage and thereby large current limits the maximum power and largest possible distance between feeding stations [1]. As reactive power does not exist for DC, DC systems will not be treated here.

2.1.1 Low Frequency Systems

A DC motor will keep the direction of torque constant if the direction of both field and armature current is changed simultaneously. A series wound motor can be constructed for running at AC, as the current of the field and armature winding always is the same. But to obtain sparkless commutation, a low frequency is required. Also other measures were required to reduce arcing to an acceptable level, but these will not be described here [1].

Both 25 Hz and 50 Hz/3 = 16 2/3 Hz have been realized at several voltages, but today only the 15 kV/ 16 2/3 Hz is still in use in large extent, as the main system in Norway, Sweden, Germany, Austria and Switzerland.

Centralized Feeding

The term centralized feeding is used to describe an electric traction power system with a high voltage transmission network, supplying single phase low frequency to the overhead line via transformers. Such a system is used in Germany, with a 110 kV network covering most of the country. The system is not synchronous to the public 3-phase 50 Hz grid, but has its own frequency control. Power is partly generated in designated power plants, and partly converted from the public utility.

Decentralized Feeding

The major part of the Norwegian system has a decentralized feeding, although a small 55 kV network exists, covering a region south west of Oslo. The network is partly supplied by rotary converters employing both synchronous motor and generator, which gives a synchronous connection to the public utility. The network has thereby no independent frequency control, as the frequency in steady state is fixed to 1/3 of the frequency of the public utility.

Power is mainly supplied by converter stations along the line. The older converters

are rotary converters, while for the last 20 years, the converter capacity has been increased by the installation of static converters. Static converters will not be treated in this thesis. A small fraction of the power is also supplied by two hydro power plants.

A overview of the railway traction power system is given in figure 2.1. The nominal voltage is 15 kV, but the converter stations normally supply at 16.5 kV, to allow a higher voltage drop in transmission. The system is normally operated interconnected, but sectioning into smaller or larger parts occurs due to maintenance and faults [2].

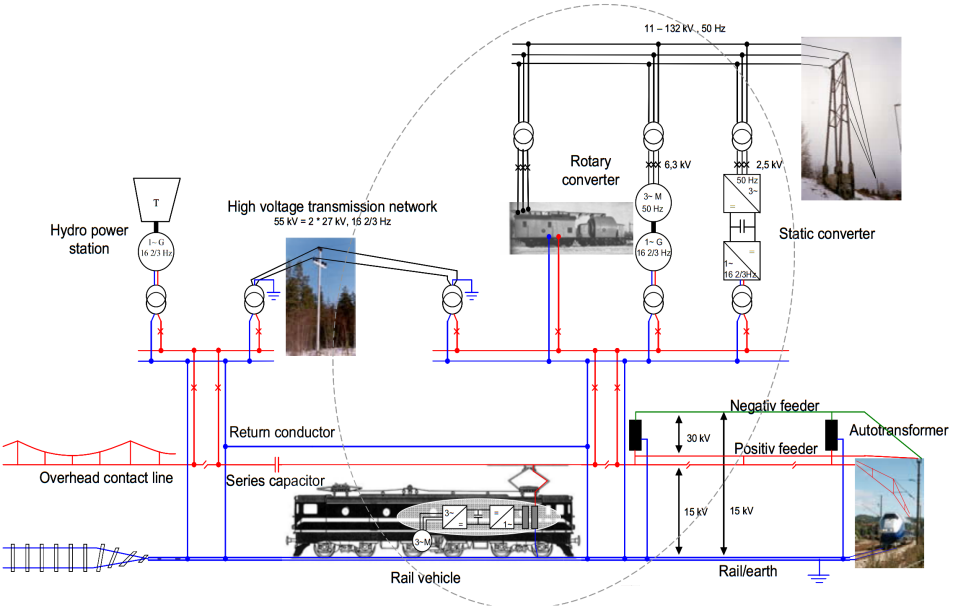

Figure 2.1: An overview the 16 2/3 Hz system [3]

2.1.2 50/60 Hz Systems

With the development of power electronics, AC could be transferred to the vehicle, transformed and rectified before being fed to DC traction motors. The low frequency was no longer needed, and countries starting AC electrification typically after World War II chose the 50 Hz/25 kV system (60 Hz in countries with public 60 Hz grid) [1].

2.2 Rotary Converters

The rotary converters used in Norway consist of a 3-phase synchronous motor for 50 Hz and a single phase synchronous generator for 16 2/3 Hz, connected to a common shaft. The motor is a 12-pole machine, while the generator is a 4-pole machine, which gives as rotational speed of 500 rpm. The motor and the generator are both equipped with field machines and automatic voltage regulators. Synchronous machines are in principle not designated as either motor or generator, and the converters allow reversed power flow, feeding power back from the contact line to the utility.

In a single phase system, the instantaneous power is the product of an alternating current and an alternating voltage, which gives a power pulsating with twice the fundamental frequency, in this case 33 1/3 Hz. The power and thereby torque pulsations are largely absorbed by the rotating mass of the converter, so that the load on the 3-phase system is constant and symmetrical in steady state.

The converter units are normally installed in converter stations with 2 or 3 units, with a size per unit ranging from 3 to 10 MVA. The units are connected and disconnected depending on the load situation to reduce losses. A typical topology of a converter station is shown in figure 2.2. Each unit has a separate transformer on both the 3-phase and single phase side. The 3-phase side is connected to the grid at 11-130 kV, while the single phase transformer is connected to the contact line. Two converter stations are also connected to the 55 kV high voltage line [2].

Both the motor and generator have brushless AC or DC excitation machines. The single phase generator has damper windings, while the 3-phase motor has none.

2.2.1 Operation of Rotary Converters

The operation of synchronous - synchronous converters is mainly governed by two aspects. First, the position of the field windings and thereby the angle of the internal voltages of the motor and the generator are fixed to each other, as they are mechanically coupled. This could otherwise have been used to control torque and thereby real power. Secondly, the sum of real power input of the two machine must be zero in steady state (neglecting losses). Under transient conditions, deviation from zero sum will accelerate or decelerate the rotating mass.

As the real power in a synchronous machine is to large extent driven by the angle difference between the internal voltage and terminal voltage, the two machines will find their respective angles giving equilibrium between incoming and outgoing power. In other words, if the terminal voltage of the single phase side is lagging the terminal voltage of the 3-phase side, power will flow from the 3-phase to the single phase side. During regeneration, power will flow from the single phase to the 3-phase side, requiring the voltage angle on the single phase side to be leading

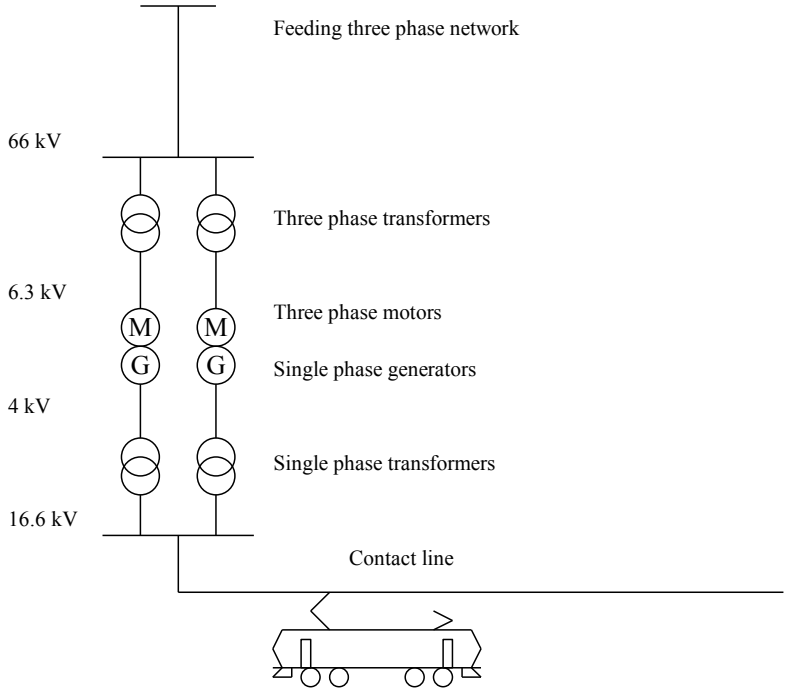

Figure 2.2: Topology of a typical converter station, with 2 rotary converter units (nominal voltages are taken from the rotary converter ASEA Q38 [3]).

the 3-phase voltage.

The automatic voltage regulator of the motor is normally set to maintain unity power factor, ie. no reactive power exchange with the 3-phase grid. The automatic voltage generator of generator is normally set to 16.5 kV upside the step-up transformer, either as a stiff voltage or slightly decreasing voltage with increasing reactive power demand. Decreasing voltage is set to improve the load sharing between the converter stations, as a highly loaded machine will reduce its own terminal voltage, thereby increasing the power flow from nearby converter stations.

The converters can principally be operated in three different modes:

- Interconnected mode - This is the normal operation. The contact line of a larger area is interconnected, and supplied by several converter stations. Most of the railway will be supplied from both sides, which gives a stronger supply to each vehicle than with single sided feeding. Settings for voltage control may be used to share the load between the different converter stations. An example of load sharing between two machines is given in this thesis. As

this operation gives a relatively strong grid, stability is normally a smaller concern.

- Islanded mode - Due to maintenance and fault situations, the contact line is sectioned, which may leave a line section to be supplied from only one converter station. A long line section supplied from one end is the case normally giving the weakest grid seen from the vehicle, and in which stability may be problematic. This is the case chosen for stability analysis in this thesis. The Norwegian National Rail Administration requires a vehicle to be capable of stable operation at a single fed line up to 60 km long [2]. Load sharing is of course not an issue, as the entire section is supplied from one converter station.

- Reactive compensation mode - A synchronous machine may be used for voltage control, only producing or consuming reactive power, without a mechanical load or prime mover. This mode is seldom used, and is not treated any further.

2.3 Modern Electrical Rail Vehicles

The development of high performance power electronics and microcomputers allows the use of compact and robust asynchronous motors for traction of rail vehicles. These vehicles with power electronics, asynchronous motors and computer based control systems are often called modern or advanced electric rail vehicles. Other descriptions may be "inverter locomotive", "4 quadrant converter vehicle" or "asynchronous motor vehicle".

The main components of the modern electric rail vehicle is shown in figure 2.3. There is a step-down transformer, two four-quadrant converters connected by a DC link and asynchronous traction motors. The motor side converter is three-phase, supplying the asynchronous traction motors with variable voltage and frequency. The line side converter is single-phase, and controls the power flow between the grid and the DC-link, depending on the power of the motor side converter.

Seen from the grid, the vehicle appears as a controllable voltage source behind the impedance of the filter and the transformer.

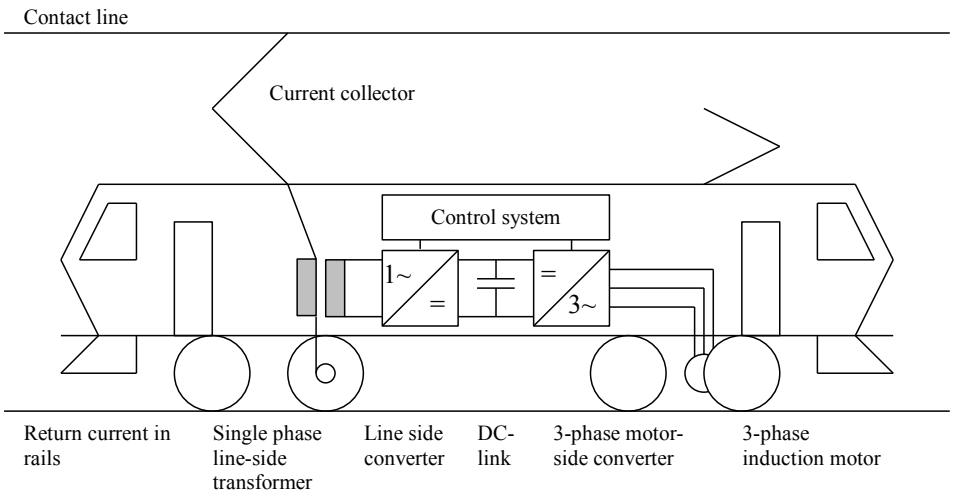

Figure 2.3: The main components of a modern electrical rail vehicle

A sketch of the converter is shown in figure 2.4. The switching elements may be thyristors with quenching circuits, gate turn-off (GTO) thyristors or insulated gate bipolar transistors (IGBTs). The maximum internal voltage of the converter is limited by the DC-link voltage. The maximum current is limited by the thermal limit of the switches. Within these limitations, every current and corresponding real and reactive powers are in principle possible. The real power is given by the tractive work to be done, leaving the reactive power to be controlled for other purposes [3].

As with the rotary converters, one side of the converter is single phase, giving an instantaneous power pulsating with twice the fundamental frequency. The main purpose of the DC-link capacitor is to store energy in the DC-link, absorbing the power pulsations and providing a constant power for the motor side converter. Filters may be included to reduce the harmonics of the DC-link voltage, shown in figure 2.4 as an RCL branch.

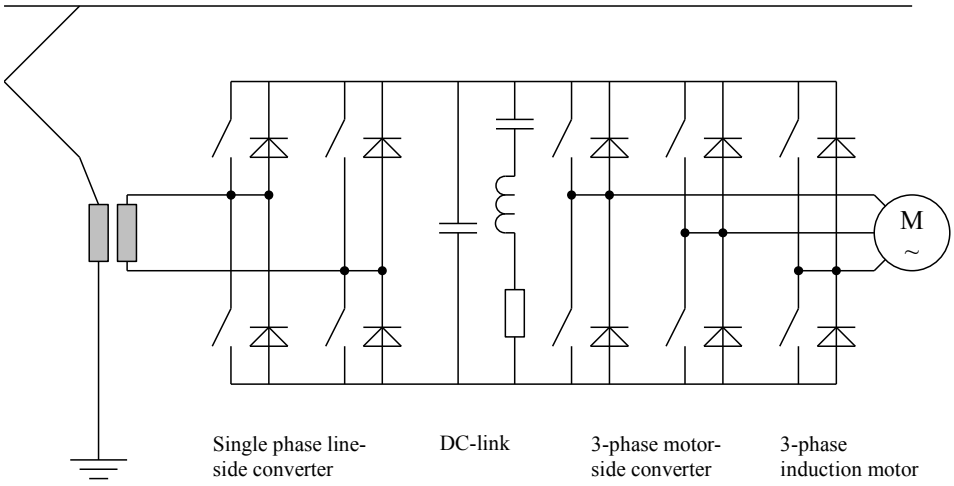

Figure 2.4: Simplified main circuit of a modern electrical rail vehicle

2.3.1 Operation

The main purpose of the circuit shown in figure 2.4 is to provide the traction motors the required power for the train's propulsion. The traction motors are fed with variable voltage and frequency, depending on speed and required torque. When reducing speed or to maintain speed when driving downhill, the motors may be operated as generators, braking the train. The power is fed back to the overhead line, to be used by other trains or fed back to the public grid, so-called regenerative braking. Electric motor drives have a high efficiency, which causes the electric real power to follow the mechanic power closely both during traction and regeneration. During transient conditions, a power unbalance may occur, charging or discharging the DC-link capacitor.

Real and reactive power may be controlled independently by controlling the internal voltage magnitude and angle of the line side converter. Both real and reactive power may be used to control the line voltage, improving stability and protecting the system from voltage collapse. The vehicle's response to varying line voltage may be controlled by settings of the control system.

Generally, reactive power will be fed into the grid when consuming real power (traction) if this is needed to increase the line voltage. Similarly, reactive power may be consumed during regenerative braking to prevent an unacceptable voltage rise.

For moderate power or in a strong network, the real power will normally be kept constant at the level set by the driver, so that a voltage increase results in a current

decrease. In this operation, the motor side converter appears as a constant power DC load at the DC-link. The line side converter should supply or feed back the real power required to keep the DC-link voltage U_d constant.

To distribute power between vehicles and protect a weak network from voltage collapse, regulations require a reduction of vehicle's main current at low voltage, which will limit the power. When available power is limited, this will limit the tractive effort at higher speeds. However, at start-up and low speed, the full tractive force is normally available regardless of line voltage [4].

An example of the steady state characteristics of a real vehicle is shown in the summary of the fall project, in figure 3.5 and 3.9.

Chapter 3

Summary of Fall Project 2010

A project with title "Active Control of Reactive Power in a Modern Electrical Rail Vehicle" [5] was done in the fall semester 2010, as a preliminary project for this thesis. Two new control schemes were proposed for traction, while one new control scheme was proposed for regenerative braking.

The control schemes proposed were implemented in a train model for traffic simulation by SIMPOW/TracFeed, and evaluated regarding driving time and energy consumption.

3.1 Research Objectives and Limitations

3.1.1 Research Questions

- Which use of reactive power allows the maximum power to be transferred to the vehicle, within the technical and formal limitations that apply?
- When desired power is less than the possible transmission capacity (operating in a strong grid or at moderate power), how can reactive power be used to minimize losses?
- How should reactive power be used during regenerative braking, to ensure real power is not limited due to unacceptable voltage rise.

Simulations will be used to investigate the effects of reactive power control, with respect to increased transmission capacity, reduced driving times, reduced losses

and increased amount of energy fed back to the grid during braking.

Transmission capacity and loss are both electrical quantities which can be included in an objective function for optimization, but simulations are required to find the relation between increased transmission capacity and reduced driving time. As the objectives are reduced driving time and reduced losses, there are one optimization function for power transfer, and another one for loss, simply saying that reducing driving time has higher priority than reducing losses. However, to enable some comparison, the different simulation results are compared with respect to energy costs vs. value of reduced driving time.

3.1.2 Applicable Regulations

The following regulations bring about limitations or constraints which the proposed control schemes must comply with.

Permitted Voltages - EN:50163:2004

Electric railways in Norway are subject to the European standard EN50163:2004 [7], which limits allowed voltages at the supply point to the train. The power consumed or fed back by the vehicle shall be limited to ensure that these voltages are not exceeded. A summary of the voltages are given in table 3.1. The standard also specifies permitted interval of temporary voltages. As the power consumption shows large variations, the voltage is allowed to vary relatively much compared to other power systems; 0.8 - 1.15 pu. is allowed permanently.

Table 3.1: Allowed voltages according to EN50163:2004

Lowest non-permanent voltage U_{min2}	Lowest permanent voltage U_{min2}	Nominal voltage U_n	Highest permanent voltage U_{max1}	Highest non-permanent voltage U_{max2}
11000 V	12000 V	15000 V	17250 V	18000 V

Current Limitation - EN:50388:2005

The power limitations to ensure permitted voltages are not exceed are defined in the European standard EN50388:2005 [8]. The vehicle is permitted to draw its nominal current at 14.25 kV (0.95 pu) and above. Below 14.25 kV, the traction current is to be ramped down linearly reaching zero at 11 kV (0.733 pu). It is the magnitude of the current being limited, i.e. the real power for a given voltage may vary depending on the power factor used. The limitation applies to traction

current only, not current for auxiliary power. The current limitation is shown in figure 3.1, together with the same limitation expressed as appearent power.

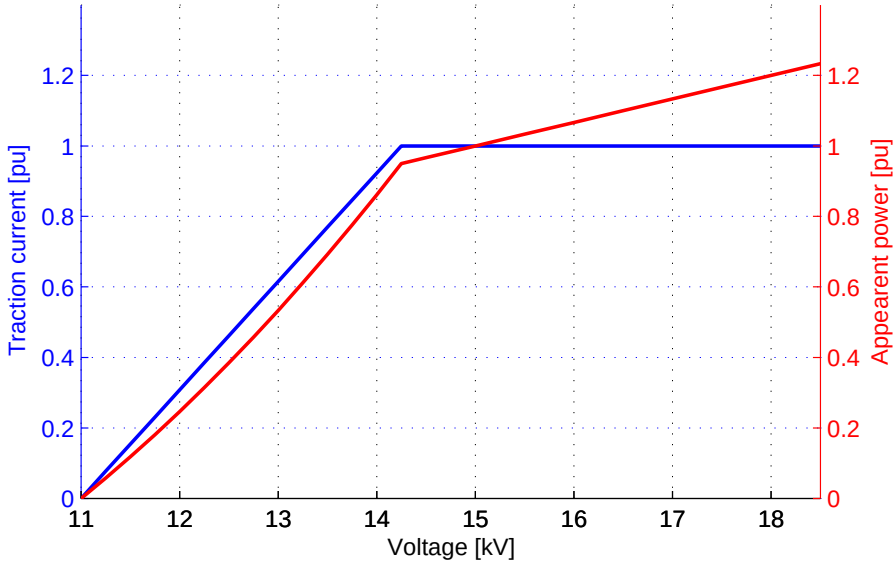

Figure 3.1: The limitation of traction current according to EN50388:2005, represented as current and appearent power as function of voltage. This figure does not apply for regenerative braking

Regenerative braking is not limited at low voltage, but is not permitted at line voltage above $U_{max2} = 18$ kV. No ramp down is specified, but stability requirements shall be fulfilled.

Permitted Power Factor

Permitted power factors for new vehicles are defined in the requirements to rolling stock by the Norwegian National Rail Administration [2], shown in figure 3.2. Power factor is defined for the fundamental frequency, not the total RMS-values. The Norwegian requirements regarding power factor follow EN50388:2005 with minor exceptions. This permits vehicles to use reactive power to control line voltage; using capacitive power factor during traction at low voltage, and inductive power factor during regeneration at high voltages. It is though required that stability is maintained.

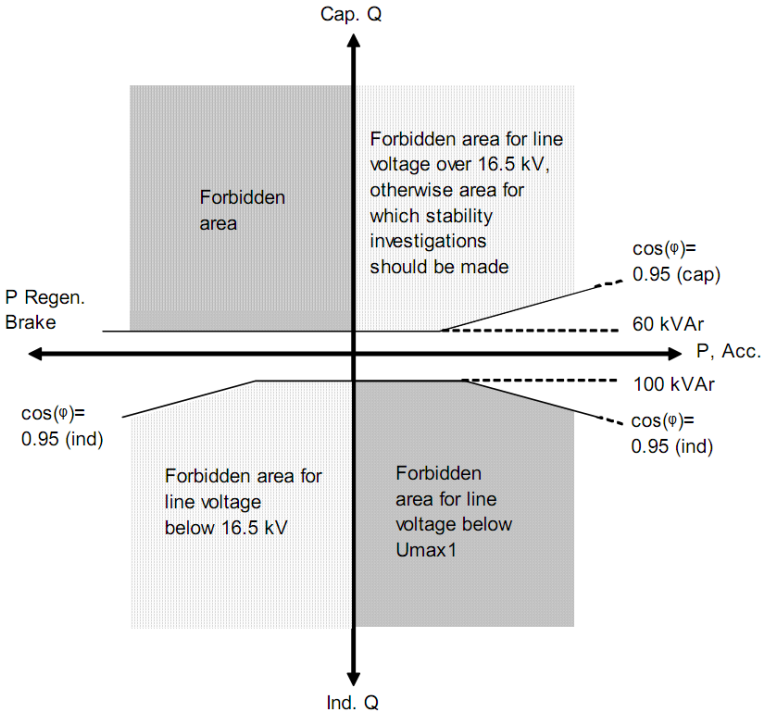

Figure 3.2: Allowed power factor for the fundamental during traction and braking [2].

3.2 Control Schemes Proposed

The control schemes below are found for the following assumptions:

- The electric traction power system consists of overhead line with an impedance of $(0.19 + j0.21)\Omega/km$. The system is fed by one or more voltage stiff sources of 16.5 kV with the same voltage angle. This system may be transformed into a Thevenin equivalent, with a Thevenin voltage of 16.5 kV and a Thevenin impedance $\bar{Z}_{th} = l_{eq} \cdot (0.19 + j0.21)\Omega/km$. l_{eq} indicates the equivalent line length, i.e. the Thevenin impedance has the same impedance as a line with length l_{eq}.

- The rated electric power of the load (a modern electrical rail vehicle) is 6.364 MW and a rated voltage of 15 kV, giving a nominal current of 424.2 A.

- Auxillary power is neglected.

3.2.1 Traction

Minimum loss

The "minimum loss" control scheme is calculated to obtain the lowest line loss for a given power. As line loss at a given network configuration is only depending on the current magnitude ($P_{loss} = I^2 \cdot R$), the lowest loss is obtained by keeping the current magnitude as low as possible. When fed from a constant voltage source, the lowest current for a given power is obtained with unity power factor at the point with constant voltage, the feeding point. When the feeding voltage and X/R ratio or impedance angle θ_{Zline} of the line is known, the load angle ϕ at the load is a function of the voltage at the load, equation 3.1. U_1 is the voltage at the feeding point, assumed to be fixed, while U_2 is the measured voltage at the vehicle's current collector.

$$\phi = \theta_{Zline} - \sin^{-1} \frac{U_1 \sin \theta_{Zline}}{U_2} \tag{3.1}$$

This mode of operation will imply feeding reactive power to cover the line loss (unity power factor at feeding point $\Rightarrow$ all reactive power supplied from vehicle), which will increase the voltage at the load compared to running the load at unity power factor. If the available power to the vehicle is limited due to voltage drop in a long line, this will also increase the available power. If neglecting the current limitation after EN50388 (section 3.1.2), allowing the vehicle to draw its nominal current at any voltage, this is also the load angle giving maximum power to the vehicle.

Maximum power

A MATLAB script was made to find the maximum power possible within EN50388 (section 3.1.2). At voltage at the vehicle above 14.25 kV, the load angle was the same as for "minimum loss". At 14.25 kV and below, maximum power to the vehicle was obtained by feeding back more reactive power than for "minimum loss". This will increase the voltage and thereby make a higher current permitted. At quite a substantial range of line lengths, the maximum power was obtained at the nominal current, supplying reactive power to maintain voltage at 14.25 kV.

Comparison of Control Schemes

The control schemes proposed are compared with two reference cases, unity power factor at any voltage (no reactive power) and the reactive power control scheme from a real locomotive [6]. The available power and within EN50388 and corresponding load angle, with the assumptions from section 3.2, is shown in figure 3.3,

over a line length form 0 to 150 km. The corresponding line voltage and current are shown in figure 3.4.

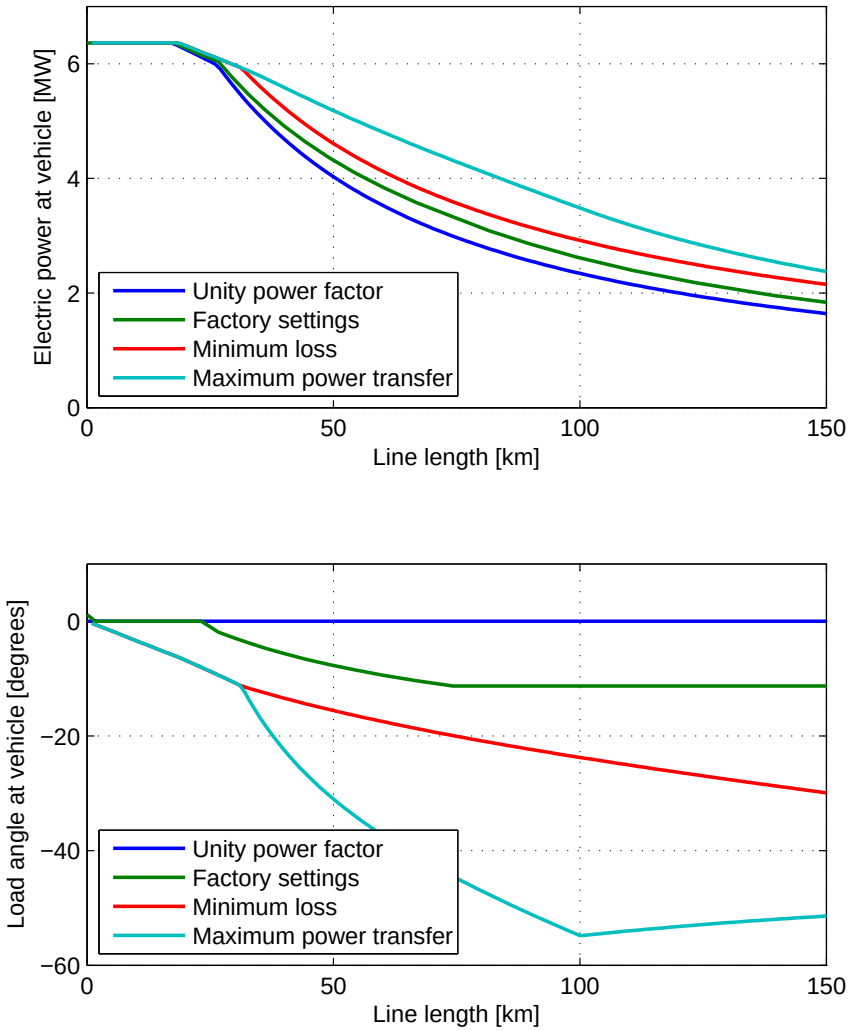

Figure 3.3: Maximum possible power to the vehicle with different uses of reactive power and its corresponding load angle, as a function of line length.

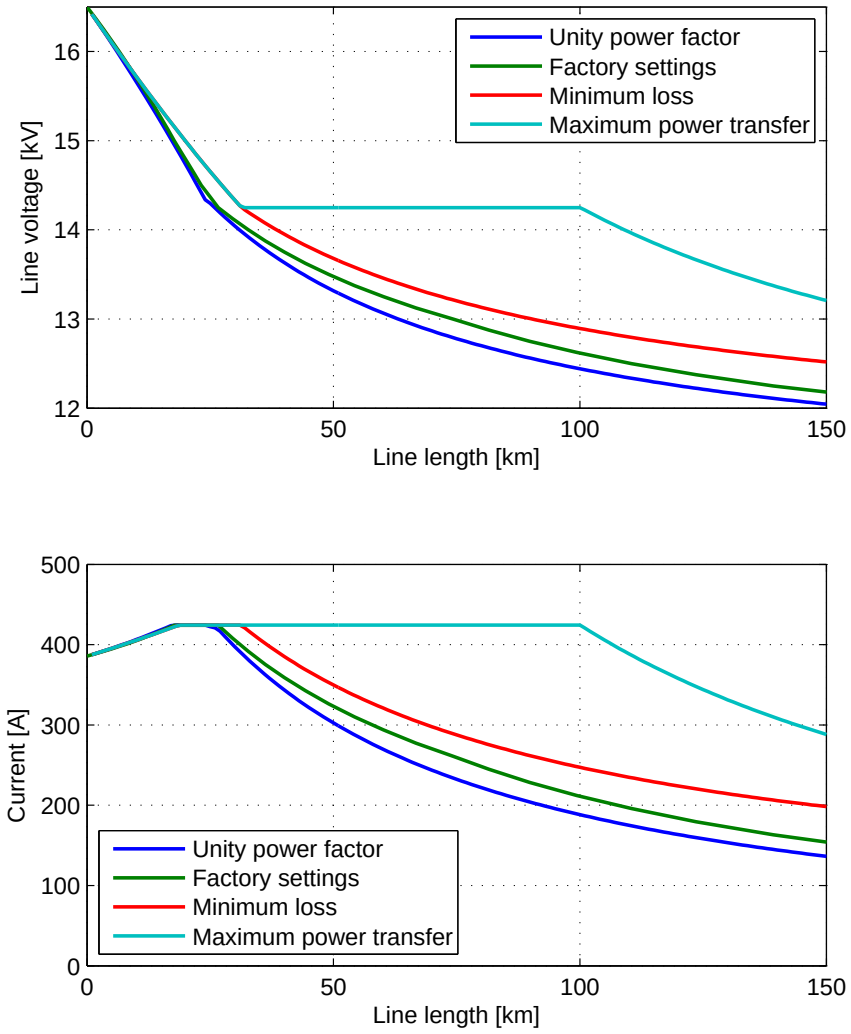

Figure 3.4: Line voltage and current when transferring maximum power with different uses of reactive power, as a function of line length.

To be implemented in a SIMPOW/TracFeed simulation model, the permitted power and load angle are to be given as functions of the line voltage. The data from figure 3.3 and 3.4 are shown as functions of line voltage in figure 3.5. The current and apparent power for a given voltage are the same for all settings, as they are the maximum permitted within EN50388, figure 3.1.

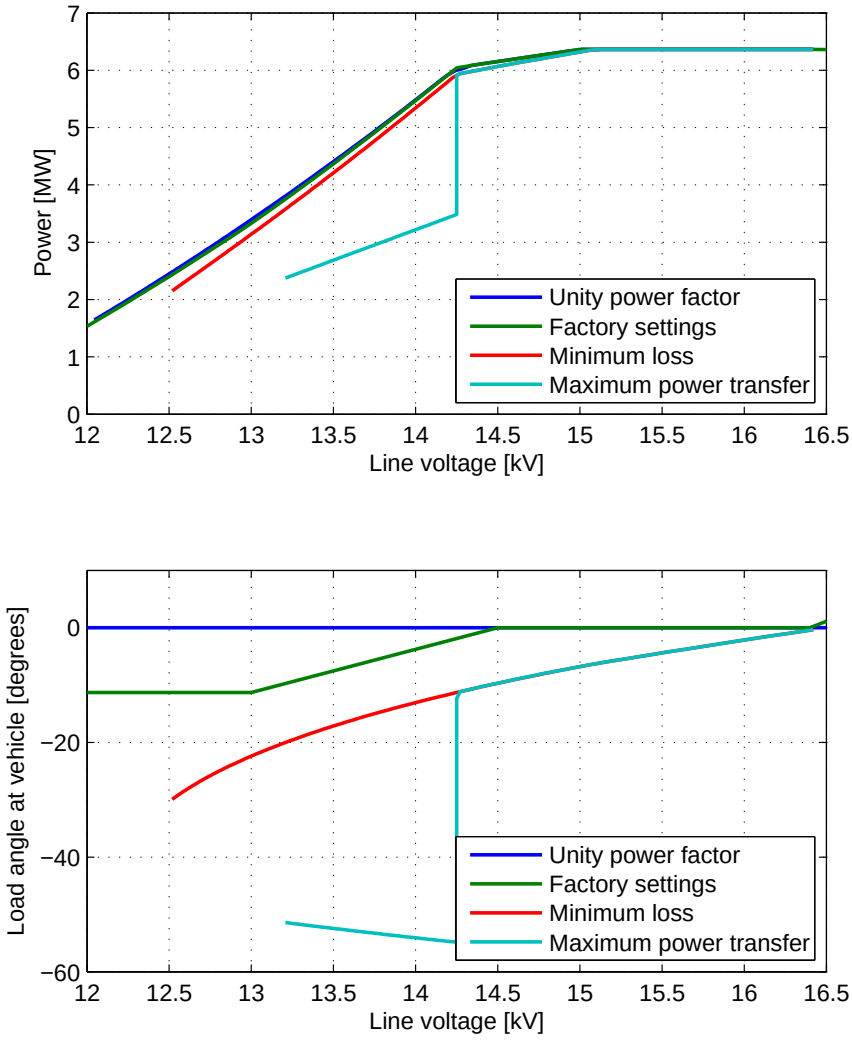

Figure 3.5: Power and load angle as functions of voltage.

Increased amount of reactive power fed into the line will, until a maximum, available power is the nose curve, with the real power as a function of the voltage, normally given for a constant power factor. The distance from the operating point to the tip of the nose curve (maximum power) is an indication for the margin from a voltage collapse for a load with constant power characteristics. At unity power factor, the tip of the nose will occur at about half the no-load voltage, while at a capacitive power factor, it will occur at higher voltage.

The nose curves for 30 km line length are shown in figure 3.6. The nose curve for maximum power and minimum loss are identical, and indicate clearly a higher available power than unity power factor. All operating points have a large margin from the tip.

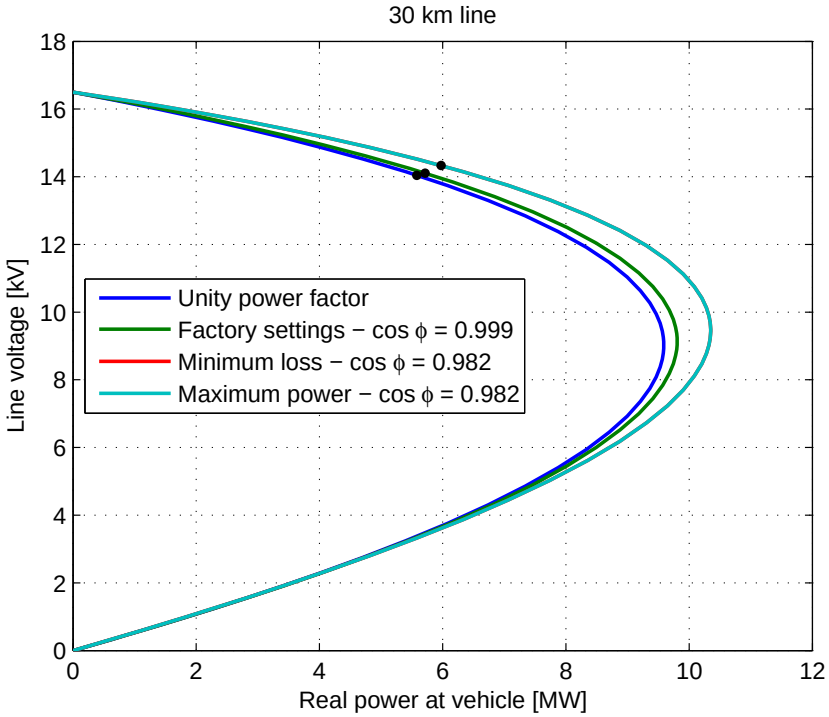

Figure 3.6: Nose curves for 30 km line length with different power factors, power factors used at the operating points of the respective control schemes. The operating points from figure 3.3 and 3.4 are marked with black circles.

At 60 km, figure 3.7, the nose curves clearly show a lower available power than at 30 km, regardless of power factor. Especially the curve for "maximum power" indicate that maximum power occurs at a higher voltage. All operating points have a significant margin to the tip.

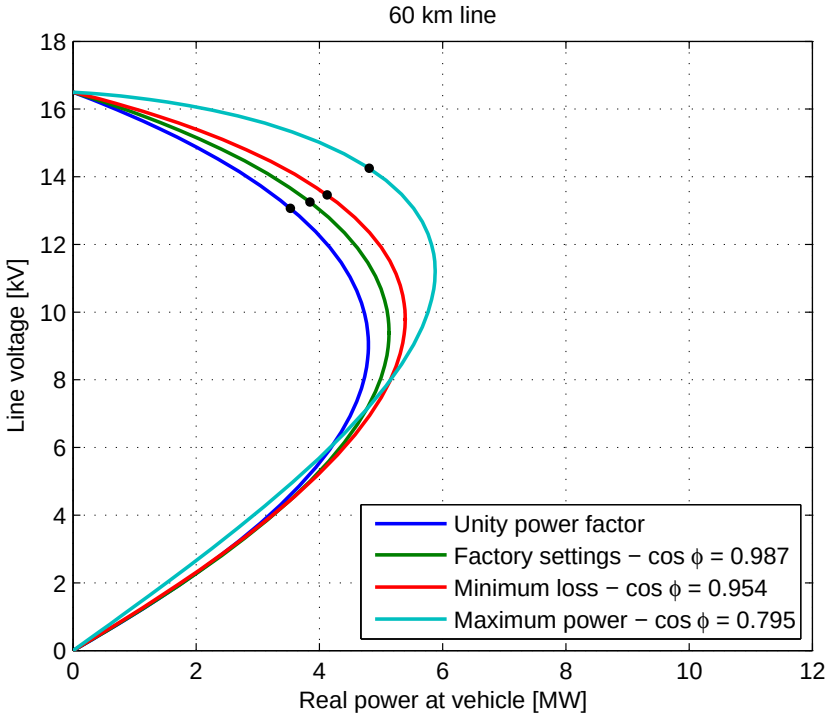

Figure 3.7: Nosecurves for 60 km line length with different power factors, power factors used at the operating points of the respective control schemes. The operating points from figure 3.3 and 3.4 are marked with black circles.

At 120 km, figure 3.8, the nose curve indicate an even lower available power. With "maximum power" characteristics, there is very little margin to the tip of the nose curve, and stable operation may be difficult to obtain. It should also be noted that the nose curve occurs at about 13 kV, which could be considered within the normal operating range. In other words, the voltage indicate that situation is OK, while a there may be a large risk of voltage collapse.

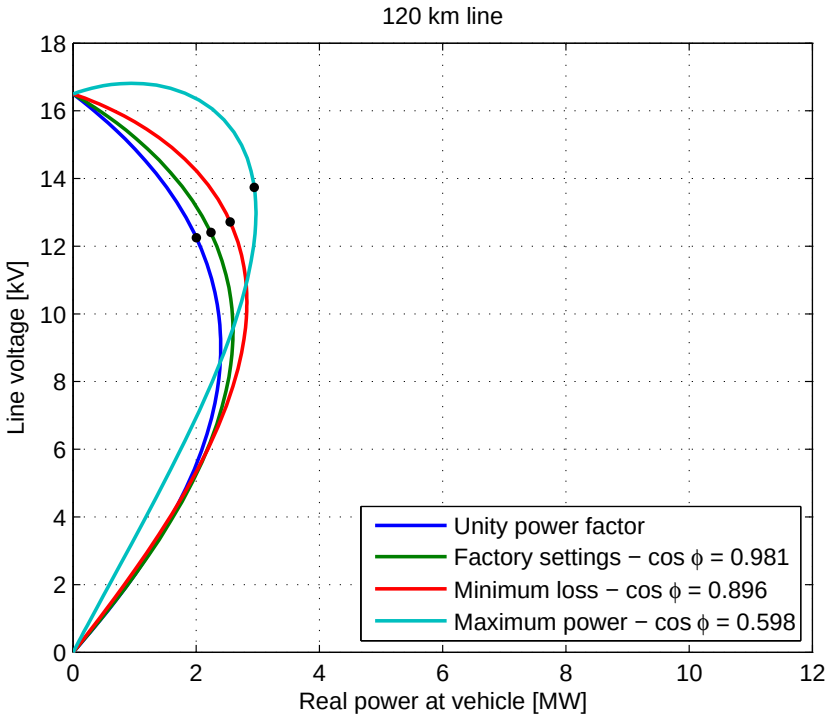

Figure 3.8: Nose curves for 120 km line length with different power factors, power factors used at the operating points of the respective control schemes. The operating points from figure 3.3 and 3.4 are marked with black circles.

3.2.2 Regenerative Braking

The lowest losses for a given power, also during braking, are obtained when the converter station is running at unity power factor, while the vehicle supplies all reactive power. This setting is not permitted during braking, as capacitive power factor is not allowed during regeneration, see figure 3.2. The closest possible would be unity power factor.

However, as regenerative braking is not allowed at line voltages over 18 kV, the voltage must be controlled, either by real or reactive power. To avoid limiting real power, power factor should first be made sufficiently inductive to control the voltage increase, before the real power is reduced. The settings are shown in figure 3.9. With the factory setting, power factor is reduced from unity at 16.5 kV to 0.85 inductive at 17 kV and above. Power is ramped down from full power up to 17 kV to 0 at 18 kV. For unity power factor, the real power ramp down is the same as for factory settings.

A setting for reduced loss during regenerative braking is proposed. Full power at unity power factor is used up to 17.5 kV. From 17.5 kV to 17.75 kV, power factor is ramped down to 0.9. From 17.75 kV to 18 kV, the real power is ramped down from rated value to 0, see figure 3.9.

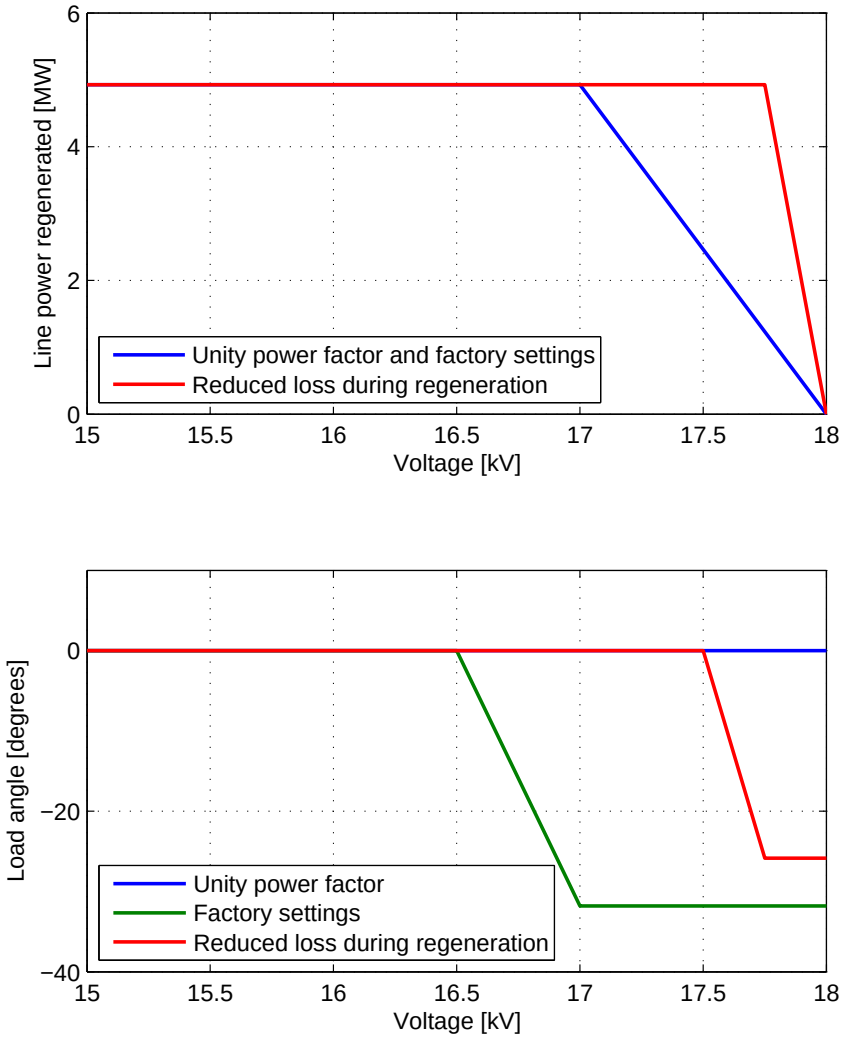

Figure 3.9: Power limitation and reactive power control during braking.

3.3 Simulation Model

The control schemes proposed were implemented in a train model for SIMPOW/TracFeed, and simulated driving from Hønefoss to Nesbyen; a distance of 91.589 km. Power limitation and reactive power settings are described in figure 3.5 and 3.9. The track data and train data is also used in this thesis, shown in figure 4.7 and table A.1. The following combinations of settings for traction and braking were simulated:

1 Unity power factor during both traction and regeneration

2 Factory settings; unity or capacitive during traction, inductive during regeneration

3 Minimum losses; capacitive during traction, unity at regeneration

4 Minimum losses during traction (capacitive), factory settings (inductive) during regeneration

5 Minimum losses during traction (capacitive), settings for reduced loss during regeneration (inductive)

6 Maximum power transfer during traction (capacitive), settings for reduced loss during regeneration (inductive)

The power system was modelled with two different configurations; with the contact line fed from the Nesbyen end and from both ends. The feeding was modelled as stiff voltage sources with the same angle and 16.5 kV. Single sided feeding from Nesbyen was used to give a weak power supply, in which available power at the locomotive is limited, and increased power will give reduced driving time. Double sided feeding was used to give a strong power supply, where power limitation was not an issue, but where reactive power control might reduce losses. All six train models were simulated in both the weak and the strong configuration.

The value of reduced driving time of the train was found to 33100 NOK/hr. The cost of electrical energy out from the converter station line was found to 0.4768 NOK/kWh, while the value of regenerated energy fed back to the converter station was assumed to be 0.333 NOK/kWh.

3.4 Summary of Results

3.4.1 Single Fed Line - Weak Grid

Selected results from the simulations with a single fed line are shown in table 3.2.

Table 3.2: Results of simulation with single fed line. Numbering of simulation cases refer to section 3.3.

Simulation case	1	2	3	4	5	6
Vehicle						
Driving time [s]	4178	4132	4103	4104	4103	4072
Average speed [km/h]	78.9	79.8	80.4	80.3	80.4	81.0
Traction [MWh]	2.4196	2.4643	2.4988	2.5036	2.5037	2.5511
Regeneration [MWh]	-0.3315	-0.4282	-0.3460	-0.4425	-0.4425	-0.4564
Net consumed [MWh]	2.0881	2.0361	2.1528	2.0611	2.0612	2.0947
Average voltage [kV]	15.03	15.09	15.31	15.25	15.31	15.65
Converter station(s)						
Traction [MWh]	2.8000	2.8886	2.9808	2.9867	2.9863	3.2777
Regeneration [MWh]	-0.3103	-0.375	-0.3231	-0.3853	-0.3943	-0.4047
Net supplied [MWh]	2.4897	2.5136	2.6577	2.6014	2.592	2.873
Line						
Loss, traction [MWh]	0.3804	0.4243	0.482	0.4831	0.4826	0.7266
Loss, traction[1] [%]	13.59	14.69	16.17	16.18	16.16	22.17
Loss, regen. [MWh]	0.0212	0.0532	0.0229	0.0572	0.0482	0.0517
Loss, regen.[2] [%]	6.40	12.42	6.62	12.93	10.89	11.33
Total loss [MWh]	0.4016	0.4775	0.5049	0.5403	0.5308	0.7783
Total loss[3] [%]	16.13	19.00	19.00	20.77	20.48	27.09
Benefit vs. case 1						
Saved time [NOK]	-	422.94	689.58	680.39	689.58	974.61
Traction energy [NOK]	-	-42.24	-86.21	-89.02	-88.83	-227.77
Braking energy [NOK]	-	21.55	4.26	24.98	27.97	31.44
Net benefit [NOK]	-	402.24	607.64	616.34	628.73	778.28

Driving Pattern and Vehicle Performance

The driving time is for all cases higher than for the double fed system (table 3.3), which clearly indicates that the weak grid affects train operation. Limited power available will cause reduced acceleration and reduced speed uphill. For constant speed on a relatively flat track, limited power will normally have no effect, as only a moderate power is required for such operation. The driving time differs on the most 106 s between the simulations, indicating that controlling reactive power affects train performance in a weak grid.

[1] % of energy supplied from converter stations during traction
[2] % of energy supplied from vehicle during regeneration
[3] % of net energy supplied from converter station

Traction

Higher acceleration and increased average speed causes only a moderate increase of traction energy consumed by the vehicle. From the slowest (78.9 km/h) to the fastest (81.0 km/h), speed is increased by 2.7 %, while the energy consumed is increased by 131.5 kWh or 5.4 %. The speed of fastest train is 1.5 % higher than for the train with factory settings.

Power at the vehicle is roughly proportional to the current, while line loss is proportional with to the current squared. To transfer a given amount of energy, the lowest losses are obtained at the lowest power possible, i.e. the transfer takes more time. Higher acceleration and increased speed cause higher power transferred over shorter time, and the consequence is higher losses. From the slowest, case 1, to the fastest, case 6, the energy consumed is increased by 131.5 kWh, while the line loss during traction is increased by 346.2 kWh.

Regenerative Braking

Case 1 and 3 use unity power factor during regenerative braking. The energy regenerated is about 100 kWh lower for these cases, compared to the cases 2, 4, 5 and 6, which consume reactive power during regeneration to control line voltage. For cases 1 and 3, the voltage is not controlled by reactive power, which means that real power is limited to avoid unacceptably high voltage. The minor differences in the energy regenerated between case 2, 4 and 5, and 6 are probably caused by different driving pattern.

To limit the losses, the reactive power consumed should only be enough to limit the voltage at an acceptable level. Excess use of reactive power will increase losses. The settings for reduced loss during regeneration accepts up to 17.5 kV before reactive power is used to control voltage, while the factory settings starts using reactive power at 16.5 kV. The effect can be shown by comparing case 4 (factory settings during regeneration) and 5 (reduced loss during regeneration). The energy regenerated from the vehicle is the same, while the line loss during regeneration is 9 kWh lower for case 5, a reduction of 19 %. The reduced losses are, however on the cost of higher deviation from the nominal voltage. Case 4 and 5 are identical during traction, but the average voltage is higher for case 5, which means the voltage during regeneration is higher. Case 6 also uses settings for reduced loss during regeneration, and obtains lower loss than case 4, for more energy transferred.

3.4.2 Double Fed Line - Strong grid

Selected results from the simulations with a double fed line are shown in table 3.3. The detailed results are not included in the appendix, as the weak grid results already illustrate the trains' performance on the full range of line lengths, from 91 km to 0. The differences between the simulation cases are also smaller with a strong grid than a weak.

Table 3.3: Results of simulation with double fed line. Numbering of simulation cases refer to section 3.3.

Simulation case	1	2	3	4	5	6
Vehicle						
Driving time [s]	4030	4030	4030	4030	4030	4030
Average speed [km/h]	81.8	81.8	81.8	81.8	81.8	81.8
Traction [MWh]	2.6578	2.6553	2.6587	2.6620	2.6577	2.6615
Regeneration [MWh]	-0.4639	-0.5041	-0.4639	-0.5043	-0.5044	-0.5041
Net consumed [MWh]	2.1939	2.1512	2.1948	2.1577	2.1533	2.1574
Average voltage [kV]	16.12	16.10	16.16	16.13	16.17	16.16
Converter station(s)						
Traction [MWh]	2.7920	2.7892	2.7920	2.7951	2.7906	2.7946
Regeneration [MWh]	-0.4385	-0.4706	-0.4385	-0.4706	-0.4746	-0.4742
Net supplied [MWh]	2.3535	2.3186	2.3535	2.3245	2.316	2.3204
Line						
Loss, traction [MWh]	0.1342	0.1339	0.1333	0.1331	0.1329	0.1331
Loss, traction[1] [%]	4.81	4.80	4.77	4.76	4.76	4.76
Loss, regen. [MWh]	0.0254	0.0335	0.0254	0.0337	0.0298	0.0299
Loss, regen.[2] [%]	5.48	6.65	5.48	6.68	5.91	5.93
Total loss [MWh]	0.1596	0.1674	0.1587	0.1668	0.1627	0.163
Total loss[3] [%]	6.78	7.22	6.74	7.18	7.03	7.02
Benefit vs. case 1						
Saved time [NOK]	-	0	0	0	0	0
Traction energy [NOK]	-	1.34	0.00	-1.48	0.67	-1.24
Braking energy [NOK]	-	10.69	0.00	10.69	12.02	11.89
Net benefit [NOK]	-	12.02	0.00	9.21	12.69	10.65

[1] % of energy supplied from converter stations during traction
[2] % of energy supplied from vehicle during regeneration
[3] % of net energy supplied from converter station

Driving Pattern and Vehicle Performance

The driving time is the same for all simulation cases, which indicates that the grid configuration is strong enough, not to affect train performance significantly. The traction energy consumption at the vehicle is however slightly different, which may indicate differences in driving pattern causing less than 1 second difference in driving time.

Traction

The energy consumed at by the vehicle during traction differs only 6.7 kWh between the different cases, 0.25 % of the energy consumed during traction. The loss during traction shows a somewhat higher difference, with the highest, case 1 having about 1.3 kWh or 1 % higher loss than the lowest, case 5. Case 1 (unity) and 2 (factory settings) have very similar losses, the same is for the cases 3, 4, 5 and 6.

Regenerative Braking

In the strong grid, the energy regenerated is about 40 kWh lower for cases 1 and 3 (unity power factor during regeneration), compared to the cases 2, 4, 5 and 6, (consuming reactive power during regeneration). Cases 2 and 4 (factory settings during regeneration) have losses about 3-4 kWh higher than case 5 and 6 (reduced loss during regeneration), a reduction of loss during regeneration of 9-12 %.

Chapter 4

Load Sharing between Rotary Converters

In a normal transmission system, the ratio between reactance X and resistance R is about 10. In a power system where impedance is mainly reactance, real power flow will mainly be governed by the voltage angles, while the reactive power flow will mainly be governed by voltage magnitudes.

In the electric traction power system used in Norway, the fundamental frequency is 16 2/3 Hz. Together with the design of the contact line, this gives an X/R ratio about 1. Under such conditions, both real and reactive power flow will depend on both voltage magnitude and angle. A simple example is shown in figure 4.1. The real power flow from source 1 is given in equation 4.1, the reactive power in equation 4.2.

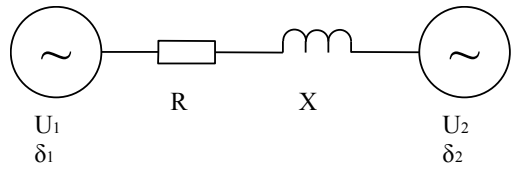

Figure 4.1: A very simple power system.

$$P_{12} = \frac{R(U_1^2 - U_1 \cdot U_2 \cos(\delta_1 - \delta_2)) + X \cdot U_1 \cdot U_2 \sin(\delta_1 - \delta_2)}{R^2 + X^2} \tag{4.1}$$

$$Q_{12} = \frac{X(U_1^2 - U_1 \cdot U_2 \cos(\delta_1 - \delta_2)) - R \cdot U_1 \cdot U_2 \sin(\delta_1 - \delta_2)}{R^2 + X^2} \tag{4.2}$$

The model shown in figure 4.1 may be used to determine the power flow between two converter stations feeding each end of a contact line section. The voltage magnitude can be controlled by the voltage regulators of the generators, either to be kept constant or other characteristics, depending on what is desirable in the system. The voltage angle of each converter's terminal voltage will mostly depend on the real power flow through the converter, and is little influenced by controller settings. According to the Norwegian National Rail Administration [2], the angle of the single phase voltage will lag 36 ° at rated load with respect to the no load angle.

If both converter stations are set to maintain constant 16.5 kV, and a load is placed at the end of the line, close to the first converter station, this converter station's power angle will be lagging compared to its no load angle. This will cause real power to flow from the second converter station through the line, sharing the real power power load between the two converter stations. However, according to equation 4.2, this situation will cause a flow of reactive power from the first converter station to the second through the line. This will increase the current, increasing real and reactive losses, and will cause both converter stations to run at a power factor significantly below unity. To reduce this reactive power flow, the converter stations may be set to decrease their output voltage when loaded. In the Norwegian system, the voltage regulators are set either to a constant voltage, or decreasing voltage when supplying reactive power. This chapter will investigate how the proposed control schemes for reactive power will affect load sharing and losses in a power system fed by rotary converters, by a simulation in steady state by SIMPOW, and a traffic simulation by SIMPOW/TracFeed.

4.1 Load Sharing in Steady State

4.1.1 Model Description

The system topology is shown in figure 4.2. Parameters are typical values given by the Norwegian National Rail Administration [2]. The system consists of two converter stations, each with two converter units with a continuous power of 5.8 MVA. Load flow analysis is done with both one and two converter units in operation in each converter station. Each converter unit has its own transformer both on the 3-phase and single phase side. Converter and transformer data can be found in appendix A.3. The 3-phase grid is represented as a infinite bus of 66 kV, with line impedance giving a short circuit power at the 66 kV input to the converter stations of 250 MVA. The 3-phase lines have a Z/R ratio of 4.

The load sharing is simulated with two different settings of the generators' voltage controllers. One setting is constant 16.5 kV, the second setting is with a decreasing voltage for increasing reactive power. The voltage decrease is set to 8 %, ie. the output voltage should be 0.92 pu = 15.18 kV when the generator supplies its

maximum continuous current to a purely reactive load, see equation 4.3.

$$I_{max,cont} = \frac{5.8MVA}{16.5kV} = 351.5A \tag{4.3}$$

At the single phase side, the converter stations are connected the ends of an 80 km section of contact line, with an impedance of $(0.19 + j0.21)\Omega/km$.

The load is simulated with 6 MW real power. The load is operated either at unity power factor, or according to the characteristic proposed as "minimum loss", section 3.2.1. "Factory settings" give unity power factor at voltage above 14.5 kV, "maximum power transfer" is identical to "minimum loss" above 14.25 kV. The lowest voltage observed at the load is 14.77 kV. 6 MW is chosen, as this is roughly equivalent to the full power of a typical modern electrical locomotive.

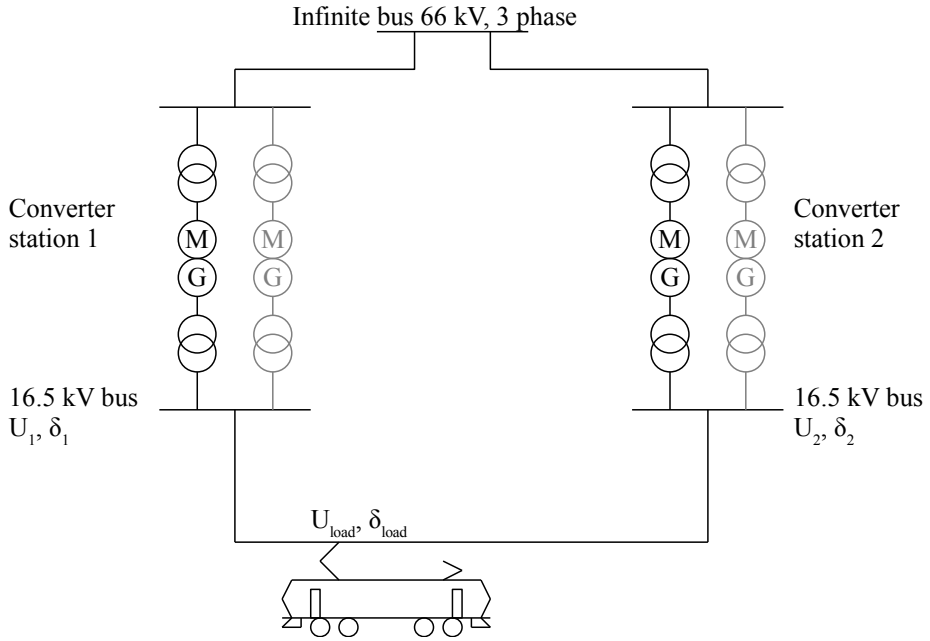

Figure 4.2: System topology for modelling load sharing. Each converter station may have one or two converter units in operation, here the converter stations are shown with one unit out of operation.

Loss Calculation

The losses considered are resistive line loss, resistive loss in transformers and synchronous machines and excitation power in synchronous machines. The line loss is

found as the difference of real power into the contact line and out of the contact line. The resistive loss in transformers and synchronous machines is found as the difference between real power at the 3-phase input and real power at the single phase output of the converter station. The excitation power is found from the excitation current from the simulation $I_{F,pu}$ in pu, the field winding resistance R_F and no-load field current I_{F0}, by equation 4.4.

$$P_F = I_{F,pu}^2 \cdot I_{F0}^2 \cdot R_F \tag{4.4}$$

The loss in the field machines is neglected, as this is in the range of some tens of watts. Iron loss in transformers and synchronous machines is neglected, as these are mostly voltage dependent and the voltage is nearly constant. Mechanical losses, such as friction and fans fixed to the converter shaft, are neglected, as these are speed dependent and the speed is fixed at the synchronous speed. Auxiliary power in the converter stations, such as cooling fans for transformers, is neglected as the load dependency is difficult to estimate. As most no-load losses are neglected, the results cannot be used for comparing the converter losses when running two converter units vs. one. Losses in the 3-phase grid are not considered, as this will mostly depend on the load and operation of the 3-phase grid, which is not included in this model.

4.1.2 Results

Four different configurations of the power supply are simulated, with one and two converter units in each converter station, and with constant 16.5 kV and 8 % decreasing voltage characteristics. As the system is symmetrical around the midpoint, the system is simulated with the load located outside one converter station (0+80 km), and in 10 km steps to the midpoint (40+40 km).

The effect of changing from unity power factor to "minimum loss" is shown in figure 4.3 to 4.6, with respect to sharing of real power load, sharing of current load, loss in the most highly loaded converter station and total loss (both converter stations and single phase line). The location of the load in the graphs is given in km from the closest converter station.

The four cases simulated all show the same basic effects. In the cases with constant 16.5 kV from the converter stations, the "minimum loss" settings has no effect when the vehicle is located at the converter station, as the "minimum loss" settings give unity power factor at 16.5 kV. The effect on load distribution is largest in the area around half way from the end to the midpoint of the line, about 20 km from the nearest converter station. More even load distribution means lower load and lower losses in the converter station nearest to the load, increasing the margin from overloading the converter station. More even load distribution require more power to be transferred from the furthest converter station through the longest line section, which in some cases increase the total line losses.

"Minimum loss" gives equal or higher voltage, with the largest effect on the midpoint of the line, where voltage is increased by 190-290 V depending on number of converter units in operation and the settings of the automatic voltage regulators.

Table 4.1 shows the largest effect of controlling reactive power. The highest reduction of current and real power at the most highly loaded converter station is obtained with the load 20 km from the nearest converter station. Reducing the load at the most highly loaded converter station will increase the margin from overloading the converter station, in other words enable higher power supplied to the load. The "minimum loss" settings are intended to reduce line loss. This effect is most significant at the midpoint of the line, where the line loss is highest.

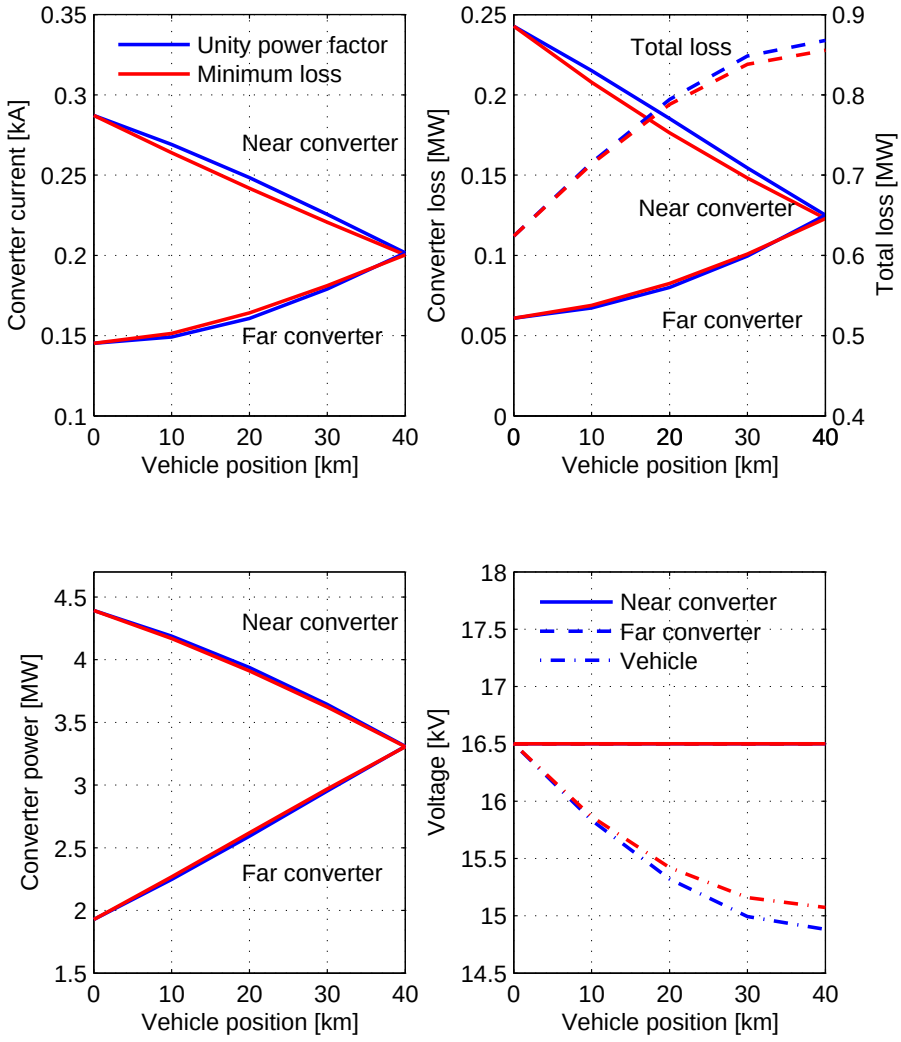

Figure 4.3: Power flow and losses with one converter unit in each station, constant 16.5 kV at the converter stations.

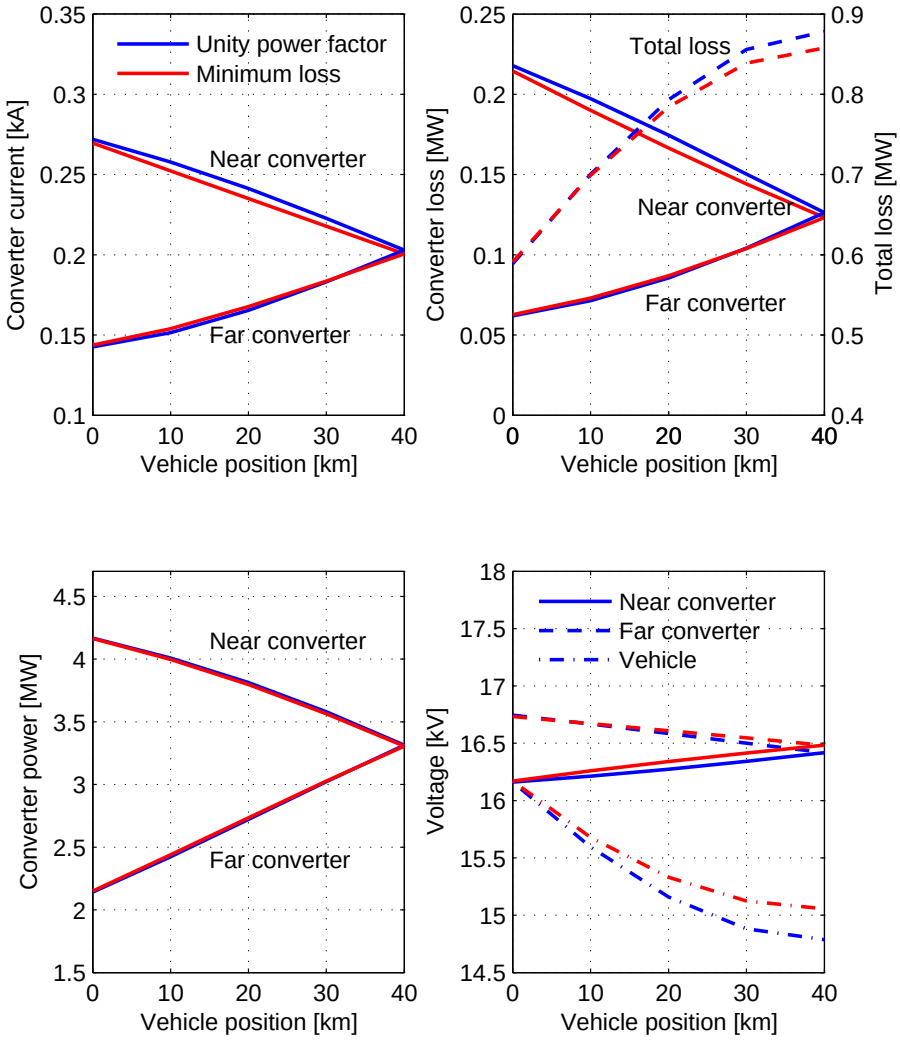

Figure 4.4: Power flow and losses with one converter unit in each station, 8 % decreasing voltage at the converter stations.

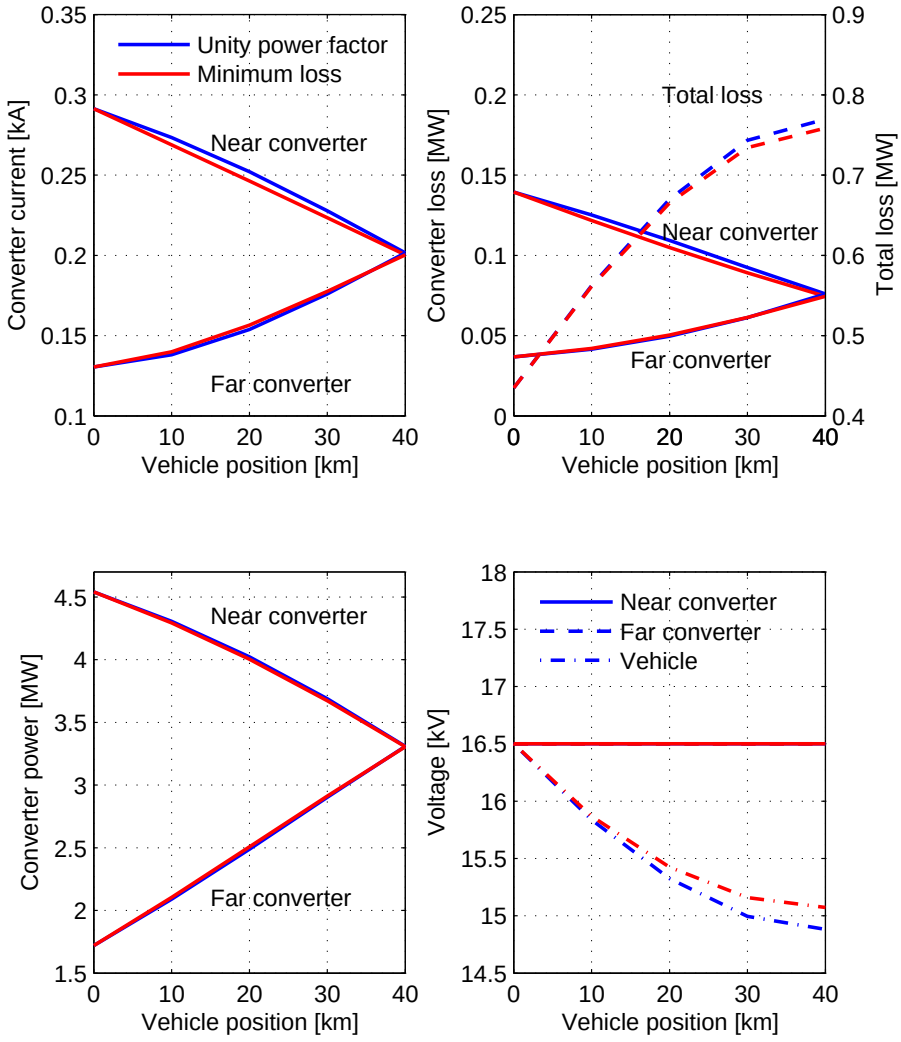

Figure 4.5: Power flow and losses with two converter units in each station, constant 16.5 kV at the converter stations.

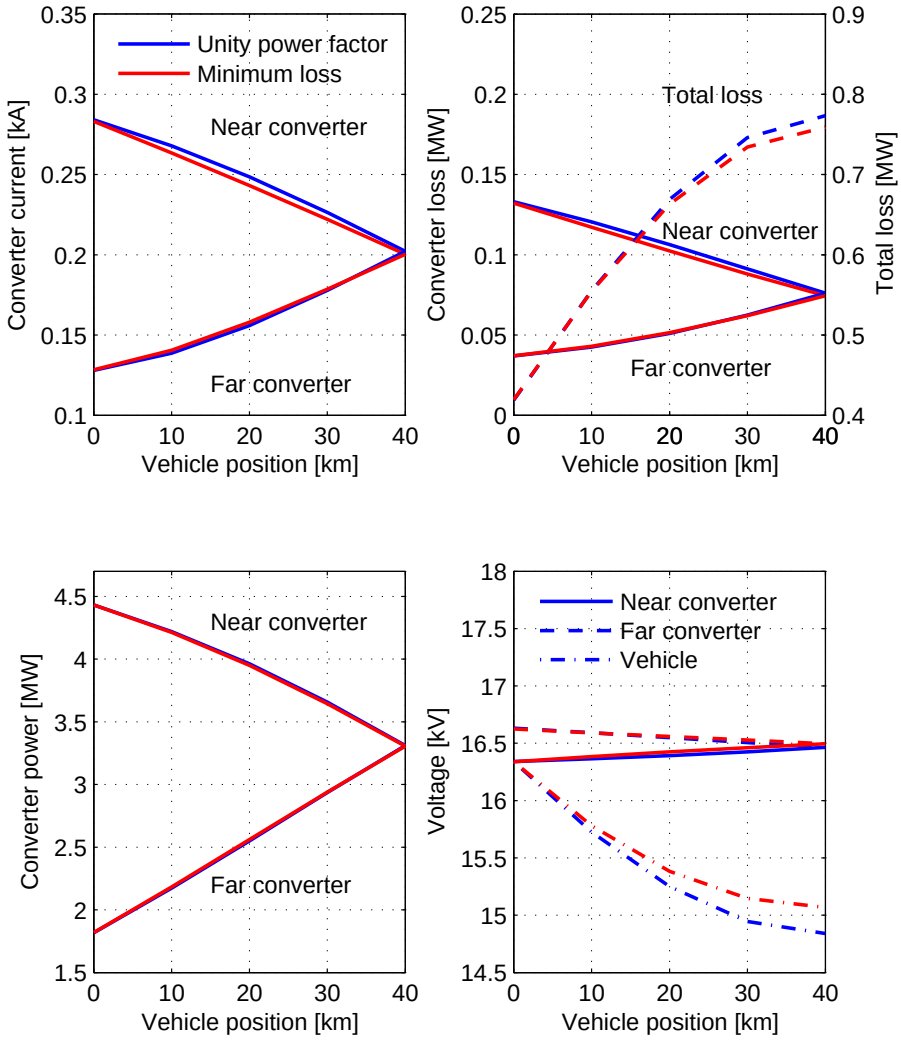

Figure 4.6: Power flow and losses with two converter units in each station, 8 % decreasing voltage at the converter stations.

Table 4.1: Highest reduction of current and loss due to reactive power control. Highest reduction of current and converter loss at the highest loaded converter occurs at 20+60 km line length. Highest reduction of total loss occurs at the midpoint, 40+40 km line length.

Voltage characteristic	Current (20+60 km)		Converter loss (20+60 km)		Total loss (40+40 km)	
	[A]	[%]	[kW]	[%]	[kW]	[%]
One converter unit						
Constant 16.5 kV	6.7	2.7	8.9	4.8	12.3	1.4
8 % decreasing	6.3	2.6	8.0	4.6	20.5	2.3
Two converter units						
Constant 16.5 kV	5.8	2.3	4.3	4.0	10.9	1.4
8 % decreasing	5.4	2.2	4.0	3.7	14.3	1.9

4.2 Traffic Simulation

4.2.1 Description of Simulation Models

Track Model and Route

The track model is based on data for the track between Hønefoss and Nesbyen, a section of Bergensbanen (the Bergen Line) in Norway. The track data is data from the Norwegian National Rail Administration's database, Banedata.

The track model contains information about the adhesion, gradient and tunnels of the track. Curve information might also have been added to include increased friction due to curves, but these data were not available for the section simulated. In this work, adhesion is assumed not to be limiting for the operation of the train. This means that the full tractive effort of the vehicle may be used without risking wheel slip. Tunnels are described by the tunnel factor, the factor by which the aerodynamic resistance is increase. The tunnel factor is set to 2 in this work. All track data are given vs. distance along the track, with stepwise constant values.

All trains simulated start from Hønefoss, driving non-stop until they stop at Nesbyen; a distance of 91.589 km. The speed reference will be the allowed speed for the track, with a maximum speed of 100 km/h . The height profile and speed profile of the track are shown in figure 4.7.

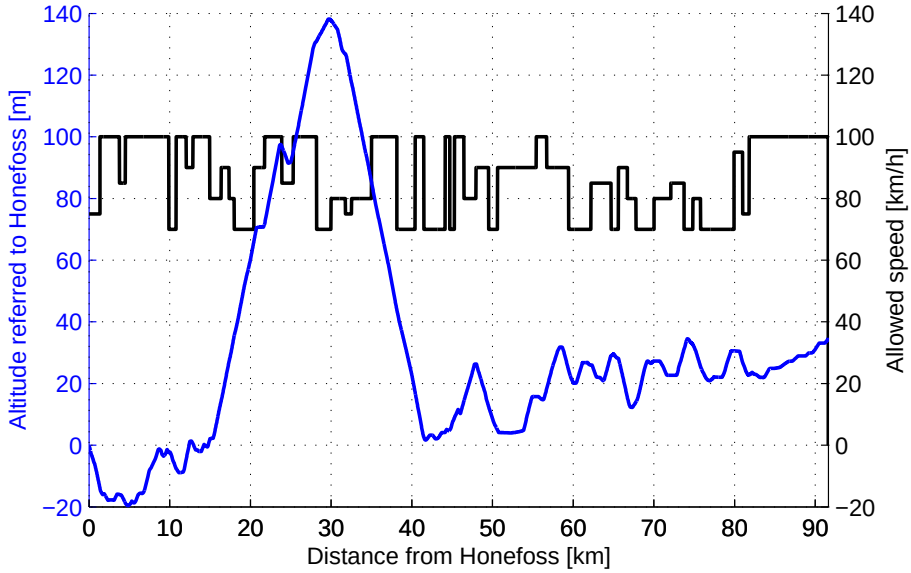

Figure 4.7: Heightprofile and allowed speed between Hønefoss and Nesbyen

Train Model

The train is intended to be a typical freight train in Norway, consisting of a single locomotive of 5.6 MW and 36 two-axle cars, giving a total train mass of 1000 t. The cars are a mix of open and closed cars. A real train would normally consist of a mix of 2, 4 and 6-axle cars, but the total number of axles is realistic. Train data is given in table A.1.

Electrical Model

The electrical infrastructure model used is most aspects the same as described in section 4.1.1, shown in figure 4.2. One converter unit is used in each converter station. The length of contact line is increased to 91.589 km, corresponding to the track model. The simulation is run with both constant 16.5 kV at the converter stations and 8 % decreasing voltage characteristics.

The power limitation of the vehicle by EN50388:2005 is not implemented in the simulation model. Feeding reactive power into the overhead line will increase the line voltage, permitting a higher current and power. The "minimum loss" characteristics is intended to give the minimum loss for a given power, but increased power may though increase the loss. To avoid this effect, the trains are allowed to consume full power, 6.364 MW, over the voltage range occurring in the simu-

lations. Three different train models are used, with different settings for reactive power during traction, see section 3.2.1. All models use factory settings for power limitation and reactive power characteristics during regeneration.

1. Unity power factor during traction, factory settings during regeneration
2. Factory settings
3. "Minimum loss" during traction, factory settings during regeneration

4.2.2 Results

Constant 16.5 kV

The results from the traffic simulations with constant 16.5 kV from the converter stations are shown in table 4.2. The results with unity power factor (case 1) and factory settings (case 2) are very similar. The factory settings give unity power factor above 14.5 kV, and the voltage is above this almost all the time. This can be seen form the reactive production from the vehicle, where case 2 has virtually no reactive production (0.0002 MVArh).

The converter losses at Hønefoss converter are reduced by 1.5 kWh from unity to minimum loss, while the losses at Nesbyen converter station is almost unaffected. This is probably because Hønefoss converter is the most heavily loaded, because of the uphill starting 15 km after departure from Hønefoss. In the load flow analysis, the "minimum loss" settings gave better distribution of load between the converter stations, which would decrease the load on Hønefoss. Lower total converter losses indicate more even distribution of load, which reduces the risk of overloading the converters.

The line loss is increased by the "minimum loss" settings, similar to the load analysis, where both the real and the reactive power of the furthest converter station increased, increasing the line loss.

Table 4.2: Traffic simulation with constant 16.5 kV from converter stations. The last column shows the relative change from case 1 (unity power factor) to case 3 ("minimum loss").

		Simulation case			Change
	Unit	1	2	3	1 to 3 [%]
Vehicle					
Driving time	s	4030	4030	4029	
Traction energy	MWh	2.6593	2.6541	2.6590	-0.01
Energy regenerated	MWh	-0.5041	-0.5040	-0.5054	0.26
Reactive consumption	MVArh	0.1597	0.1616	0.1565	-2.00
Reactive production	MVArh	0.0001	-0.0002	-0.1655	
Hønefoss converter station					
Max current, 2 s	kA	0.3147	0.3159	0.3141	-0.18
Max current, 6 min	kA	0.2231	0.2230	0.2164	-2.99
Max current, 1 hr	kA	0.1340	0.1337	0.1319	-1.55
Loss during traction	MWh	0.0465	0.0464	0.0454	-2.37
Loss during regeneration	MWh	0.0035	0.0034	0.0034	-2.86
Excitation loss	MWh	0.0125	0.0125	0.0122	-2.25
Total converter loss	MWh	0.0625	0.0623	0.0610	-2.37
Nesbyen converter station					
Max current, 2 s	kA	0.3033	0.3034	0.2978	-1.80
Max current, 6 min	kA	0.1613	0.1613	0.1588	-1.55
Max current, 1 hr	kA	0.1163	0.1164	0.1165	0.18
Loss during traction	MWh	0.0354	0.0355	0.0354	0.00
Loss during regeneration	MWh	0.0033	0.0032	0.0033	0.00
Excitation loss	MWh	0.0116	0.0116	0.0114	-1.68
Total converter loss	MWh	0.0503	0.0503	0.0501	-0.39
Contact line					
Loss during traction	MWh	0.1812	0.1815	0.1820	0.44
Loss during regeneration	MWh	0.0366	0.0361	0.0364	-0.55
Total line loss	MWh	0.2178	0.2176	0.2184	0.28
System					
Traction energy	MWh	2.9224	2.9175	2.9218	-0.02
Regeneration	MWh	-0.4607	-0.4613	-0.4623	0.35
Net energy consumption	MWh	2.4821	2.4766	2.4795	-0.11
Total loss	MWh	0.3307	0.3303	0.3296	-0.33

Decreasing Voltage Characteristics

The results from the traffic simulations with 8 % decreasing voltage characteristics from the converter stations are shown in table 4.3. Decreasing voltage characteristics give lower losses than constant 16.5 kV in all components (excitation losses in Nesbyen converter station are unchanged). The effect of reactive power control at the vehicle shows the same tendency as for constant 16.5 kV; slightly lower converter losses, especially for Hønefoss converter station, and higher line losses. Lower total converter losses indicate more even distribution of load, which reduces the risk of overloading the converters.

Table 4.3: Traffic simulation with 8 % decreasing voltage characteristics from converter stations. The last column shows the relative change from case 1 (unity power factor) to case 3 ("minimum loss").

		Simulation case			Change
	Unit	1	2	3	1 to 3 [%]
Vehicle					
Driving time	s	4030	4030	4029	
Traction energy	MWh	2.6503	2.6515	2.6515	0.05
Energy regenerated	MWh	-0.5031	-0.5034	-0.5057	0.52
Reactive consumption	MVArh	0.1355	0.1358	0.1317	-2.80
Reactive production	MVArh	0.0001	-0.0029	-0.1819	
Hønefoss converter station					
Max current, 2 s	kA	0.3024	0.3024	0.2986	-1.23
Max current, 6 min	kA	0.2169	0.2171	0.2122	-2.17
Max current, 1 hr	kA	0.1311	0.1312	0.1296	-1.16
Loss during traction	MWh	0.0446	0.0447	0.0442	-0.90
Loss during regeneration	MWh	0.0032	0.0032	0.0030	-6.25
Excitation loss	MWh	0.0123	0.0123	0.0120	-2.47
Total converter loss	MWh	0.0601	0.0602	0.0592	-1.50
Nesbyen converter station					
Max current, 2 s	kA	0.2929	0.2926	0.2848	-2.77
Max current, 6 min	kA	0.1554	0.1548	0.1516	-2.41
Max current, 1 hr	kA	0.1146	0.1145	0.1139	-0.64
Loss during traction	MWh	0.0348	0.0347	0.0342	-1.72
Loss during regeneration	MWh	0.0031	0.0030	0.0033	6.45
Excitation loss	MWh	0.0116	0.0116	0.0114	-1.61
Total converter loss	MWh	0.0495	0.0493	0.0489	-1.18
Contact line					
Loss during traction	MWh	0.1797	0.1786	0.1840	2.39
Loss during regeneration	MWh	0.0350	0.0362	0.0315	-10.00
Total line loss	MWh	0.2147	0.2148	0.2155	0.37
System					
Traction energy	MWh	2.9094	2.9095	2.9139	0.15
Regeneration	MWh	-0.4618	-0.4610	-0.4679	1.32
Net energy consumption	MWh	2.4678	2.4687	2.4657	-0.08
Total loss	MWh	0.3243	0.3243	0.3236	-0.21

4.3 Discussion and Conclusion

4.3.1 Discussion

When the load is located near one end of the line, the settings "minimum loss" distributes load more evenly, reducing the load and the loss in the nearest converter station. This is, however done at some cost. In a situation with a load close to one end of the line section, reactive power will flow to the converter station furthest from the load. Feeding in more reactive power from the load will increase this flow. When also real power is distributed more evenly between the converter stations, this means both real and reactive power flow will increase between the load and the most remote converter station, causing increased line loss. The "minimum loss" settings tend to reduce the loss of the closest converter station, while increasing the line loss and the loss in the furthest converter station, in total giving a slight reduction of losses.

Sharing the load more evenly between the converter stations will reduce the load on the most heavily loaded converter station, the converter station closest to being overloaded. This will increase the possible loading of the system before a converter station is overloaded.

In a situation where the load is close to the midpoint of the line, load is shared equally between the converter stations regardless of power factor of the load. In this situation, the "minimum loss" settings gives lower loss, without negative side effects.

In the traffic simulation, "minimum loss" gives higher line loss but smaller converter losses, giving a total of slightly lower losses. The converter losses are mainly reduced on the most heavily loaded converter station, Hønefoss. Lower converter losses indicate higher margin from overloading the converters. The overload limit of the converter stations is mainly determined by the allowed temperature in the converters, and lower converter losses mean less heat produced inside the converters.

Martinsen [9] describes how decreasing voltage characteristics depending on reactive power has small effect for modern locomotives, as they have a power factor close to unity. A voltage characteristic with decreasing voltage depending on real power load would probably give a more even load distribution between the converter stations for loads with unity or capacitive power factor. The topic of this thesis is to investigate the consequences of the proposed settings for vehicles when operating at the existing infrastructure, not to find optimal settings of the converter stations, and this topic in not considered any further.

4.3.2 Conclusion

Load Flow Simulation

The settings "minimum loss" tend to reduce the load on the closest, most heavily loaded converter station, increasing the possible load of the system without overloading the converters. However, these settings will in some cases increase the line losses, as more power is to be transferred on a long line section from the furthest converter station.

The minimum loss settings will reduce or keep the total losses unchanged, depending on the position of the load, number of converters in operation and the settings of the automatic voltage regulators. The largest effect is observed at the midpoint of the line, where the total loss is reduced by 10.9 to 20.5 kW for a 6 MW load, a reduction of 1.4 to 2.3 %.

The load of the highest loaded converter station will be reduced or kept unchanged, by distributing the load more evenly between the converter stations. The largest effect is observed with the load 20 km from the nearest converter station. Depending on the number of converters in operation and the settings of the automatic voltage regulators, the current at highest loaded converter station is reduced by 5.4 to 6.7 A for a 6 MW load, or 2.2 to 2.7 %. The loss in the converter station, which is the heat which may cause overload, is reduced by 4 to 8.9 kW, or 3.7 to 4.8 %.

"Minimum loss" gives equal or higher voltage, with the largest effect when the vehicle is at the midpoint of the line, where voltage is increased by 190-290 V depending on number of converter units in operation and the settings of the automatic voltage regulators.

Traffic Simulation

In the traffic simulation, the converter losses in the highest loaded converter was reduced by 1.5 kWh or 2.4 % with constant voltage characteristics, and 0.9 kWh or 1.5 % with 8 % decreasing characteristics, when changing from unity power factor to "minimum loss" settings of the load. The highest current occurring is reduced by 0-3 %.

The total losses are reduced by 1.1 kWh or 0.33 % with constant voltage characteristics, and 0.7 kWh or 0.21 % with 8 % decreasing characteristics, when changing from unity power factor to "minimum loss" settings of the load.

4.3.3 Further Work

The "minimum loss" settings are calculated to give the minimum loss under the assumption that the system is fed by voltage sources with the same voltage angle and magnitude. This assumption is not valid in the real system fed by more than one converter station, where the voltage angles of the converter stations have a large load dependency. It is thereby not given that these are the settings giving the lowest loss in the real system. Thus, further investigation of the following is of interest:

- Finding a control scheme for reactive power reducing the losses and increasing the capacity based on a real system, including the characteristics of a the converter stations. An optimization will probably give different settings depending on the location in the grid (distance to and characteristics of the respective converter stations). When deciding the characteristics to be implemented in a vehicle, this should be taken into consideration giving a good overall performance at any location and grid configuration which is likely to occur.
- Finding optimal settings for the voltage characteristics of the converter stations. These settings will probably give an output voltage depending on both real and reactive power.

Chapter 5

Stability and Effect of Reactive Power

5.1 Simulation Model

The simulation model used is with minor modifications the model developed by Danielsen in [3]. Also methodology, symbols and terminology are to large extent the same as used by Danielsen.

The model represents a universal electrical locomotive, 60 km overhead line, a converter station with one rotary converter unit and an overlying 3-phase grid. The locomotive is a modern electrical rail vehicle, which allows indepedant control of real and reactive power. Such a system is shown in figure 2.2; with the modification that the figure indicates two converter units, for stability analysis only one is used. The system parameters can be found in appendix A.

The model developed by Danielsen gives unity power factor in steady state at the vehicle's current collector. To investigate the effect of reactive power, the model is modified to allow control of reactive power. The model allows two modes of operation, constant and voltage dependant power factor.

5.1.1 Vehicle Control Structure

The main circuit of the vehicle is modelled with the line transformer, one PWM converter and one DC-link. The motor side converter is not modelled, but replaced with a load on the DC-link. Two shunts are present at the DC-link, one capacitor and one RCL series branch. The RCL branch is a filter tuned to 33.4 Hz.

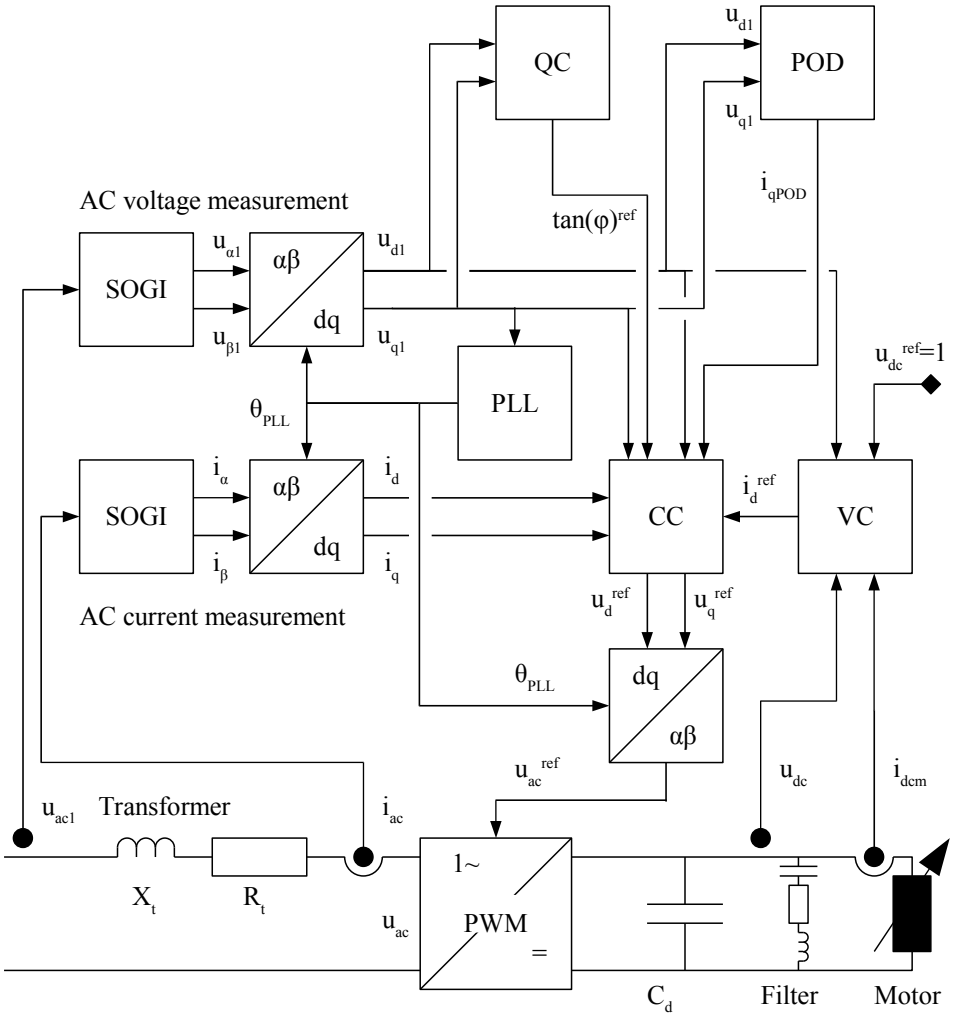

Figure 5.1: The control system of the line side converter.

The control of the line side converter is modelled in a rotating reference frame, also called vector control or dq-control, after the direct and quadrature axis. The signal flow is shown in figure 5.1. Lowercase letters indicate instantaneous values, both for real AC and DC values and when transformed into the d- and q-components. Uppercase letters indicate RMS values.

The d-axis reference is the voltage at the vehicle's current collector. This is the vehicle's interface with the power system, and regulations regarding eg. power factor or current limitation generally consider voltage and current at this point.

Real power is thereby controlled by d-axis current, while reactive power is controlled by q-axis current.

5.1.2 DC-link Voltage Controller - VC

The main control objective of the converter is to keep the DC link voltage constant. The DC-link voltage u_{dc} is measured, and fed into the voltage controller. The voltage controller, figure 5.2, is based in a PI controller, controlling the d-axis current, in other words real power into the vehicle and the vehicle's DC-link. The DC-link voltage reference is set to 1 pu.

The motor current is also measured and fed forward to give a faster response to load changes. Without measuring the motor current, increased motor current would cause a reduced DC-link voltage, which then should be compensated by the voltage controller, but with the feed-forward, this input is sent directly to the current controller.

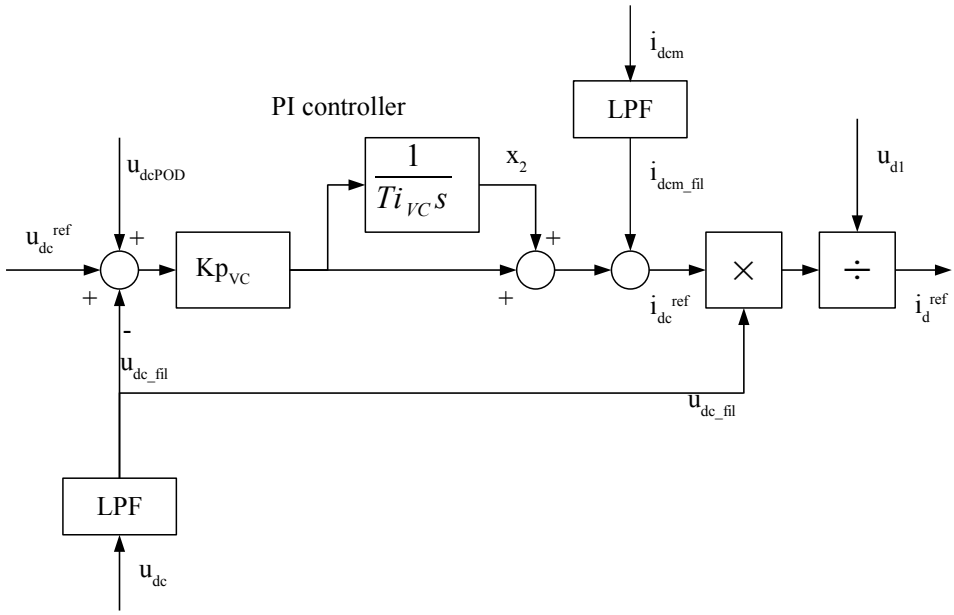

Figure 5.2: Voltage controller (VC).

5.1.3 AC Measurements

The instantaneous values of the line voltage and current are measured. In a 3-phase system, the instantaneous values can easily be converted into two orthogonal

components in a stationary reference frame, commonly called α and β. These components are then transformed into a rotating reference frame (dq-system) by the Park's transform, equation 5.1. In a single phase system, only one component is present. The second, orthogonal component is made artificially, in this case by the second-order generalized integrator (SOGI), figure 5.3. The SOGI is tuned to the synchronous angular speed of the AC system ω_s. The angular speed may be fixed to the nominal value, as in this case, or the actual value may be measured and filtered. The bandwidth of the SOGI is controlled by the gain K_{SOGI}. A higher value gives a higher bandwidth, with faster transient response but lower supression of harmonics.

For the SOGI used for line voltage measurements, $K_{uSOGI} = 0.8$ is chosen in order to filter the large extent of harmonics that can be experienced in railway networks, for example up to 33 % THD is observed [2], [3].

For the SOGI used for line current measurements, an increase of the bandwidth has been necessary and $K_{iSOGI} = 3$ is chosen for better damping of the DC-link second-harmonic resonance [3].

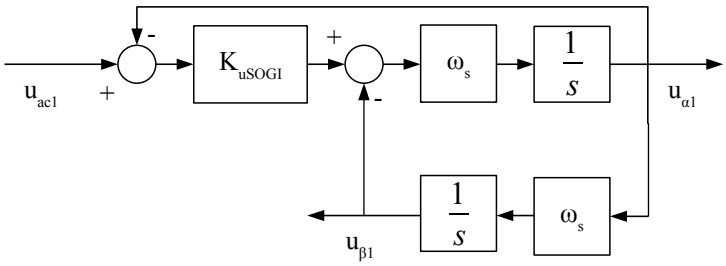

Figure 5.3: A block diagram of second-order generalized integrator (SOGI).

In order to perform the Park's transform, equation 5.1, the angle between the stationary and rotating reference systems θ must be known. The rotational speed and phase of this internal dq-system is determined by use of a phase-locked loop (PLL) that continuously tracks the phase of the line voltage u_{ac1} as shown by the block diagram in figure 5.4. θ_{PLL} is the measured angle used by the vehicle control system. The PLL consist of a PI-controller controlling the q-axis component of the line voltage to be zero, which means the d-axis is in phase with the line voltage u_{ac1}.

$$\begin{bmatrix} u_d \\ u_q \end{bmatrix} = \begin{bmatrix} \cos\theta & \sin\theta \\ -\sin\theta & \cos\theta \end{bmatrix} \cdot \begin{bmatrix} u_\alpha \\ u_\beta \end{bmatrix} \tag{5.1}$$

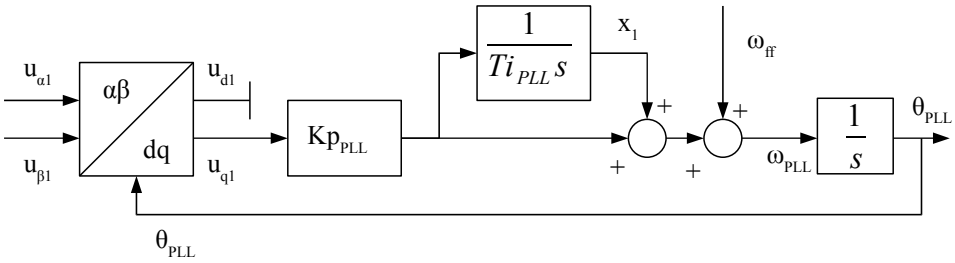

Figure 5.4: Phase locked loop (PLL).

5.1.4 Power Oscillation Damper

The structure of the power oscillation damper is shown in figure 5.5. The design of the POD is discussed by Danielsen in [3]. The first block represents the measurement of the voltage amplitude, which is used by several units in the control system. When plotting the transfer function of the POD, the voltage measurement is modelled as a first order low pass with a time constant $T_1 = 0.02s$. The second block is a high pass filter (wash-out filter), which will ensure that the steady state output of the POD is zero. The third block is a lead-lag block which may be tuned to obtain the desired angle of the output. The gain of the controller may be chosen, as well as limits for the amplitude of the output signal.

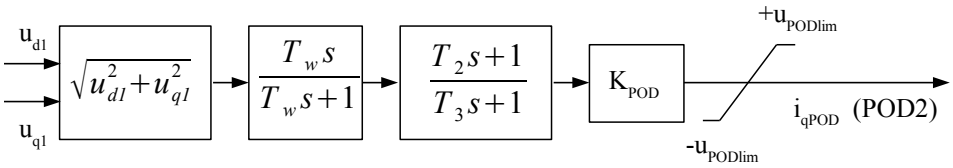

Figure 5.5: Power oscillation damper (POD).

5.1.5 Reactive Power Controller - QC

The reactive power controller is a cornerstone of this thesis and the main modification from the model proposed by Danielsen. In the model proposed by Danielsen, the q-axis current reference is constant equal to zero, giving unity power factor at the current collector in steady state. The reactive current controller, shown in figure 5.6 controls $\tan\phi^{ref}$ as a function of the voltage magnitude at the current

collector. The controller allows $\tan\phi^{ref}$ to be controlled, either according to the settings for minimum loss, as described in section 3.2.1 and in [5], or as a tabular function of voltage, eg. unity power factor at any voltage or the factory settings shown in figure 3.5. U_1 in the minimum loss formula is the voltage at the converter station, in this case assumed to be fixed at 16.5 kV = 1.1 pu.

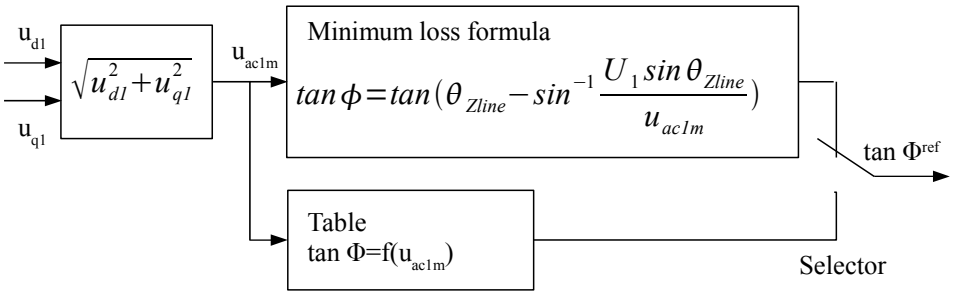

Figure 5.6: Reactive power controller (QC).

5.1.6 Current Controller - CC

The current controller, shown in figure 5.7, comprises two identical PI-controllers, one for d-axis and one for q-axis current. The reference for the d-axis current controller is given by the voltage controller, depending on the motor current and the DC-link voltage. The q-axis current reference is the product of the d-axis reference and $(-\tan\phi^{ref})$, according to the relation in equation 5.2.

$$\tan\phi = \frac{Q}{P} = \frac{-i_q}{i_d} \Big|_{u_q=0} \tag{5.2}$$

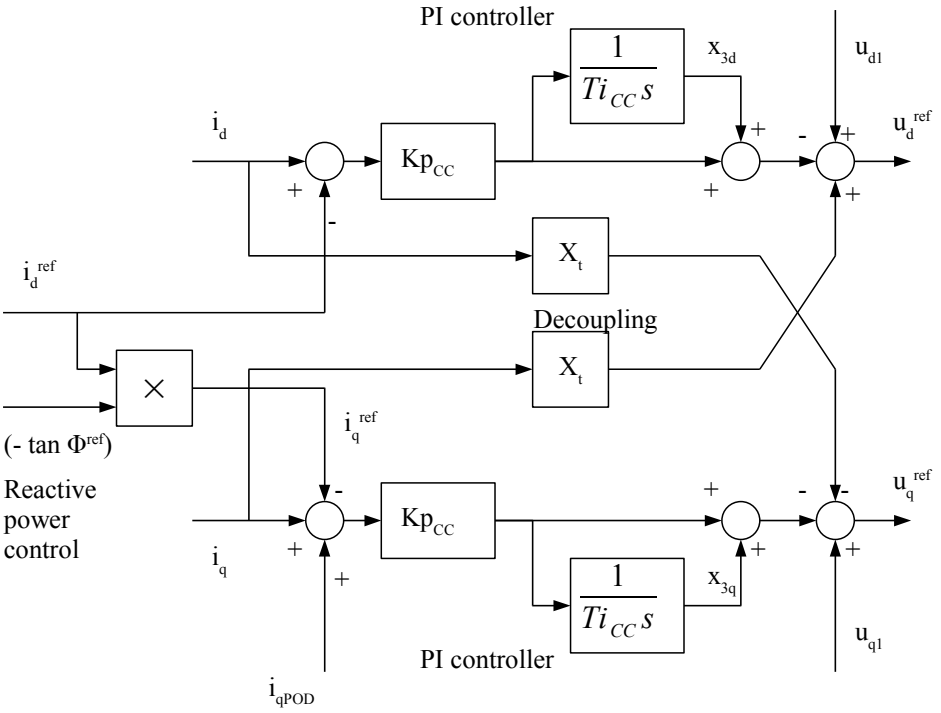

Figure 5.7: Current controller (CC).

5.1.7 Major Simplifications

The simplifications done in this model are the same as by Danielsen. The simplifications are described here, references and discussion regarding the simplifications are given in [3].

PWM Switching

The PWM switching is not modelled, assuming ideal control of the switching $u_{ac}^{ref} = u_{ac}$. It is usual to consider a time delay from u_{ac}^{ref} to u_{ac} of half a switching period. This may be compensated by a modification of the $dq/\alpha\beta$ transformation. The delay and the compensation are both neglected, ie. assuming ideal compensation.

Motor Side

Only a simple representation of the motor side is included in present model. In a quasi-stationary state the motor has to keep its power constant. If not, the torque and further speed reference cannot be fulfilled. However, a motor side acting as a constant power load for all frequencies, i.e., always increase the motor-side current if the DC-link voltage drops, will reduce the stability of the DC-link.

In this work the motor side is described by equations 5.3 and 5.4. The motor is acting as a constant power load at frequencies below the low-pass filter bandwidth. MP is the voltage dependency at frequencies above the filter low-pass bandwidth. In this work $MP = 2$, equal to a constant impedance load.

$$p_{motor}(t) = p_{motor}^{ref} \left(\frac{u_{dc}(t)}{u_{dc\_filt}(t)} \right)^{MP} \tag{5.3}$$

$$u_{dc\_filt}(s) = \frac{u_{dc}(s)}{Tf_{CPL} + 1} \tag{5.4}$$

This motor power consumption is the only load in the vehicle model. Auxiliary power consumption for heating, cooling, battery charging, control system power supply etc. is not included neither from the DC-link nor from a separate transformer winding.

Type of Controllers Used

The control system is implemented with analogue continuous controllers only.

Inverter and DC-link Structure

The structure of an advanced electric rail vehicle in real life may be more detailed than shown in figure 2.3 and 2.4. There may be several DC-links per vehicle and several line- and motor-side inverters in parallel to each DC-link. In this model, all the vehicle's DC-links are aggregated into a large one.

5.2 Impedance- and Admittance-based Representation

5.2.1 Insufficiency of Eigenvalue Calculations

Eigenvalues is a common way of investigating a system's small signal stability, and functions finding eigenvalues are commonly implemented in power system simula-

tion software. Eigenvalue analysis has however two important drawbacks.

Eigenvalues are calculated for a time invariant model, i.e. a rotating reference frame. Rotating machines, transformers and lines are easily represented in a rotating reference frame. Advanced control systems, and thereby the vehicle dynamics may be difficult to represent sufficiently in a rotating reference frame. Real-time simulations may be of value if adequate power supply models can be provided, though they will still not provide explicit information of eigenvalues as they are performed in a stationary reference frame and are hence time variant.

Eigenvalue calculations also require details of the vehicle including the control system to be known. This is often not possible, as the manufacturers' often consider such details as industrial secrets.

Input admittance presented as frequency response characteristics is commonly available for describing the vehicle's behaviour at frequencies above the fundamental, used to determine electric resonance stability. Similar data could be provided by the manufacturers for the low frequency domain; however, this is not known by the author to be praxis.

5.2.2 Impedance and Admittance

The Thevenin equivalent is well known within electrical engineering, where a network of voltage sources, current sources and impedances can, seen from one point of the network, be replaced by a voltage source and an impedance. The voltage source describes the voltage at this point of the network before a change is done, the impedance describes the change of voltage when a current in injected into this point. The Thevenin equivalent is only valid for a network consisting of only constant voltage and current sources, and constant impedances, linear components. A system with non-linear components may also be represented this way, but this representation will only be valid at one operating point.

An AC system may be described by as vectors, e.g. in d- and q-components. In an AC system with rotary machines, power electronics and advanced controllers, the response to d-axis current may be fundamentally different from the response to q-axis current. An example could be the output voltage of a rotary converter with a voltage regulator controlling the voltage magnitude to be kept constant. Assuming the d-axis reference is the voltage, a d-axis current (real power load) will cause the voltage angle to lag compared to the no-load situation. A q-axis current (reactive power) will on the other hand give a very small response, as it will not cause any significant change of voltage phase, and the voltage magnitude is (at least stationary) kept constant by the voltage regulator.

The dynamic properties of the source is represented as impedance, change of voltage per change of current, equation 5.5. Similarly, the load (in this case the vehicle) is represented as an admittance, change of current per change of voltage, equation

5.6. To reflect a dynamic system, the impedance and admittance will normally be frequency dependent.

$$Z_{source} = \frac{\Delta U}{\Delta I} \tag{5.5}$$

$$Y_{load} = \frac{\Delta I_{load}}{\Delta U} \tag{5.6}$$

The source impedance and load admittance can be found by observing the responses from the load and the source to a disturbance current injected, ΔI_s. The load admittance does not describe the inner workings of the load's control system, only the current output for a given voltage input. The impedance and admittance are depending on the operating point, and must thereby be given for a specified operating point.

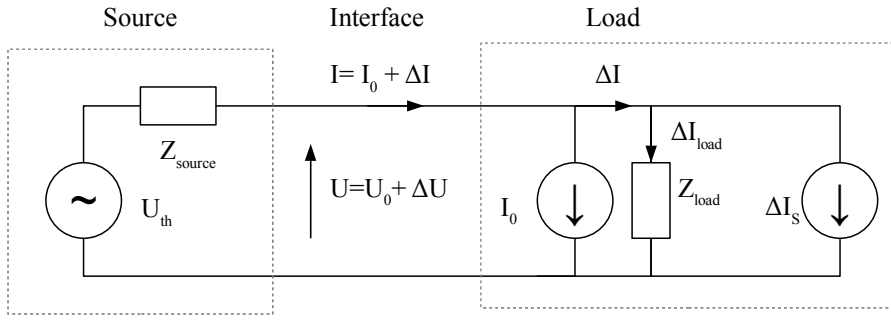

Figure 5.8: Equivalent circuit.

The system can be shown as a control system with feedback, being exposed to a disturbance, as shown in figure 5.9. When the disturbance ΔI_s is known, as well as the system's response ΔI and ΔU; Y_{load} and Z_{source} can be found by solving equations 5.7. This solution is valid for the frequency of the injected disturbance. A frequency sweep of ΔI_s may be performed to obtain Y_{load} and Z_{source} for a range of frequencies.

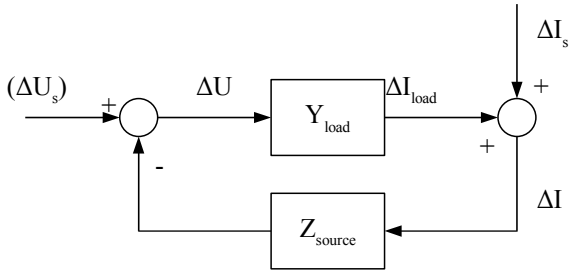

Figure 5.9: Impedance model shown as control system.

$$\begin{aligned} \Delta I_{load} = \Delta I - \Delta I_s = Y_{load} \cdot \Delta U \\ -\Delta U = Z_{source} \cdot \Delta I \end{aligned} \tag{5.7}$$

An AC system may be transformed by the Park's transform into a synchronously rotating reference frame, where AC quantities are transformed into two orthogonal DC components, commonly known as a dq-system. The transformed system is shown as a multiple input - multiple output (MIMO) as shown in figure 5.8.

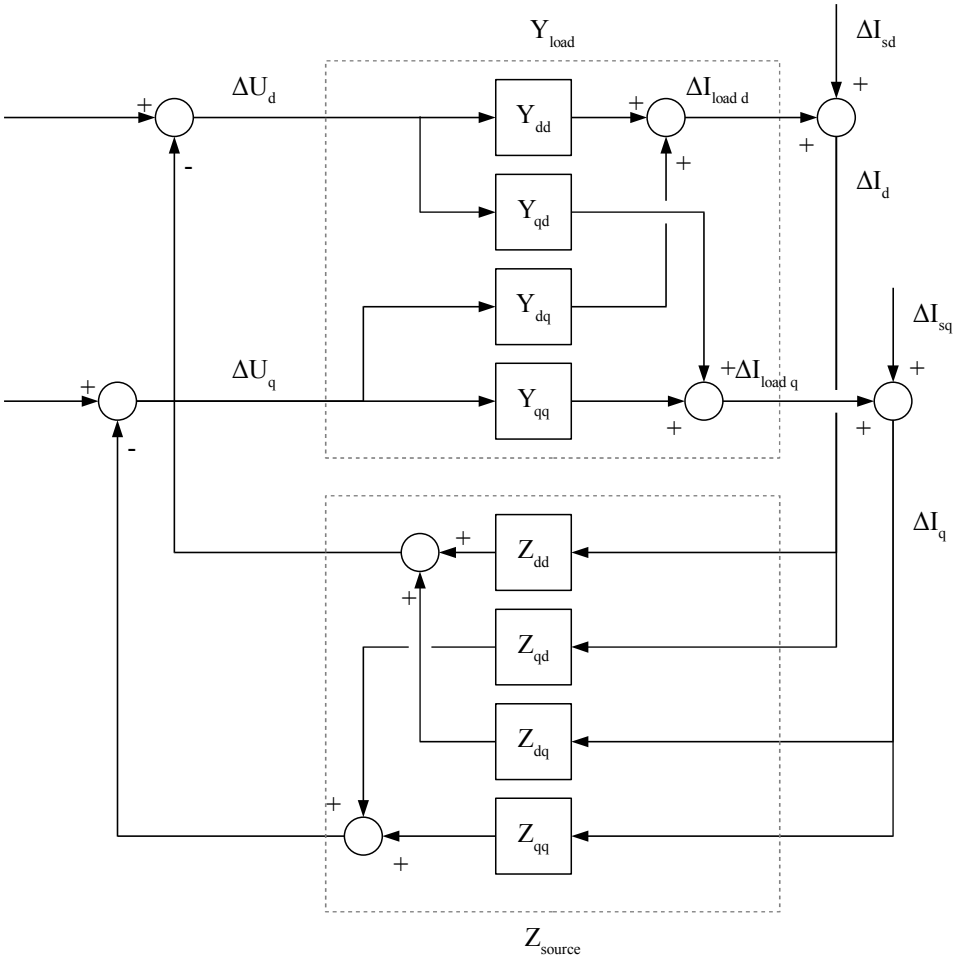

Figure 5.10: Impedance model shown as control system for d- and q-components.

In the MIMO system, the input and output signals may be represented by vectors, and the source impedance and the load admittance as matrices, according to the relations in equation 5.8. The matrices $[Y_{load}]$ and $[Z_{source}]$ can be found by two measurements or simulations, by injecting a pure d-axis, and pure q-axis disturbance current, and solving equation 5.8. The solution of the equations are given in [10].

- One sweep with pure d-axis disturbance current; $\Delta I_{sd1} \neq 0$ and $\Delta I_{sq1} = 0$
- One sweep with pure q-axis disturbance current; $\Delta I_{sd2} = 0$ and $\Delta I_{sq2} \neq 0$

When the d-axis is aligned with the voltage at the interface, the Z_{dd} and Z_{qd} will

represent the power supply's response to real power (d-axis current), while Z_{dq} and Z_{qq} will represent the power supply's response to reactive power.

A change of d-axis voltage ΔU_d represents a change of voltage magnitude, while a change q-axis voltage ΔU_q represents a change of voltage angle. Y_{dd} and Y_{qd} represent the load's response to a change of voltage magnitude, while Y_{dq} and Y_{qq} represent the load's response to a change of voltage angle.

$$\begin{aligned} \begin{bmatrix} \Delta I_{load\ d} \\ \Delta I_{load\ q} \end{bmatrix} = \begin{bmatrix} \Delta I_d - \Delta I_{sd} \\ \Delta I_q - \Delta I_{sq} \end{bmatrix} = \begin{bmatrix} Y_{dd} & Y_{dq} \\ Y_{qd} & Y_{qq} \end{bmatrix} \cdot \begin{bmatrix} \Delta U_d \\ \Delta U_q \end{bmatrix} \\ - \begin{bmatrix} \Delta U_d \\ \Delta U_q \end{bmatrix} = \begin{bmatrix} Z_{dd} & Z_{dq} \\ Z_{qd} & Z_{qq} \end{bmatrix} \cdot \begin{bmatrix} \Delta I_d \\ \Delta I_q \end{bmatrix} \end{aligned} \tag{5.8}$$

5.2.3 Analytical Considerations

To improve understanding of what the load admittance represents, as well as checking the simulation output, the expressions for the steady state admittance of a regulated constant power load are developed.

U and I indicate the voltage and current magnitude at the interface between source and load, while $\bar{U}$ and $\bar{I}$ indicate phasor quantities.

U_1 indicates the voltage magnitude at the terminals of the rotary converter station, which is assumed to be fixed at 16.5 kV = 1.1 pu in the minimum loss formula, equation 3.1. $\theta_{Z\ line}$ is the impedance angle of the overhead line. With the typical value $Z_{line} = (0.19 + j0.21)\Omega/km$, $\theta_{Z\ line} = 47.86°$.

P and Q are the real and reactive power measured at the interface. S is the apparent power magnitude, while the phasor $\bar{S} = P + jQ$.

δ is the voltage angle at the interface. When transforming into d- and q-components, the d-axis reference is the interface voltage, and $\delta \equiv 0$. ϕ is the angle between current and voltage at the interface, where current lagging the voltage gives a positive angle. With $\delta = 0$, $\phi = -\arg \bar{I}$.

For load with constant real and reactive power, the sensitivity to a change of voltage magnitude is given by equation 5.9.

$$\begin{aligned}
\bar{S} &= \bar{U} \cdot \bar{I}^* \\
\bar{I} &= \frac{P - jQ}{U} = \frac{\bar{S}^*}{U} \\
\frac{d\bar{I}}{dU} &= -\frac{P - jQ}{U^2} = -\frac{\bar{S}^*}{U^2} \\
Y = \frac{dI}{dU} &= -\frac{S}{U^2} = -\frac{P}{U^2 \cdot \cos\phi} = -\frac{Q}{U^2 \cdot \sin\phi}
\end{aligned} \tag{5.9}$$

For a load where P and Q are depending on voltage magnitude, the current magnitude I and the load angle ϕ will be voltage dependant. The sensitivities to change of voltage angle and magnitude are given in equation 5.10. For a load where real and reactive power has the same voltage sensitivity, e.g. a constant impedance or constant power load, ϕ will be independent of voltage, i.e. $\frac{d\phi}{dU} = 0$. A limitation of current or power as a function of voltage, e.g. the current limitation according to EN50388:2005 as described in section 3.1.2, will affect $\frac{dI}{dU}$.

$$\begin{aligned}
\bar{I} &= I \cdot e^{j(\delta - \phi)} \\
\bar{U} &= U \cdot e^{j\delta} \\
\frac{d\bar{I}}{dU} &= \frac{dI}{dU} \cdot e^{j(\delta-\phi)} - I \cdot e^{j(\delta-\phi)} \cdot j\frac{d\phi}{dU} \\
\frac{d\bar{I}}{d\delta} &= jI \cdot e^{j(\delta-\phi)} = j\bar{I}
\end{aligned} \tag{5.10}$$

With ϕ as a function of voltage magnitude, $\frac{d\phi}{dU} \neq 0$. The voltage sensitivity of the minimum loss characteristic is shown in equation 5.11.

$$\begin{aligned}
\phi(U) &= \theta_{Z\ line} - \sin^{-1}\frac{U_1 \cdot \sin\theta_{Z\ line}}{U} = \theta_{Z\ line} - \sin^{-1} x \\
\frac{d\phi}{dU} &= -\frac{1}{\sqrt{1-x^2}} \cdot \frac{dx}{dU} = \frac{1}{\sqrt{1 - (\frac{U_1 \cdot \sin\theta_{Z\ line}}{U})^2}} \cdot \frac{U_1 \cdot \sin\theta_{Z\ line}}{U^2} \\
&= \frac{1}{\sqrt{1 - (\frac{U_1 \cdot X_{line}}{U \cdot Z_{line}})^2}} \cdot \frac{U_1 \cdot X_{line}}{U^2 \cdot Z_{line}}
\end{aligned} \tag{5.11}$$

The de-composition into d- and q-components is for a general characteristic (both $P = f(U)$ and $Q = g(U)$) is shown in equation 5.12.

$$
\begin{aligned}
dU_d &= dU \\
Y_{dd} &= \frac{dI_d}{dU_d} = \frac{dI_d}{dU} = Re\frac{d\bar{I}}{dU} = \frac{dI}{dU} \cdot \cos\phi - I\frac{d\phi}{dU} \cdot \sin\phi \\
Y_{qd} &= \frac{dI_d}{dU_d} = \frac{dI_q}{dU} = Im\frac{d\bar{I}}{dU} = -\frac{dI}{dU} \cdot \sin\phi - I\frac{d\phi}{dU} \cdot \cos\phi \\
dU_q &= d\delta_2 \cdot U \\
Y_{dq} &= \frac{dI_d}{dU_q} = \frac{dI_d}{d\delta_2 \cdot U} = \frac{Re(j\bar{I})}{U} = \frac{Re(jI \cdot e^{-j\phi})}{U} = \frac{-I\sin(-\phi)}{U} = \frac{I\sin\phi}{U} \\
Y_{qq} &= \frac{dI_q}{dU_q} = \frac{dI_q}{d\delta_2 \cdot U} = \frac{Im(j\bar{I})}{U} = \frac{Im(jI \cdot e^{-j\phi})}{U} = \frac{I\cos(-\phi)}{U} = \frac{I\cos\phi}{U}
\end{aligned}
\tag{5.12}
$$

To perform a given mechanical work, the real power is to be kept constant when disregarding losses. If reactive power control is implemented under such conditions, the real power P will be constant and $\frac{dP}{dU} = 0$. The sensitivity of the reactive power Q to voltage is shown in equation 5.13, an further used to find the current's sensitivity to voltage in equation 5.14.

$$
\begin{aligned}
Q &= P \cdot \tan\phi \\
\frac{dQ}{dU} &= P \cdot \frac{d(\tan\phi)}{dU} = P \cdot \frac{1}{\cos^2\phi} \cdot \frac{d\phi}{dU}
\end{aligned}
\tag{5.13}
$$

$$
\begin{aligned}
I &= \frac{\sqrt{P^2+Q^2}}{U} = U^{-1} \cdot \sqrt{P^2+Q^2} \\
\frac{dI}{dU} &= U^{-1} \cdot \frac{1}{2\sqrt{P^2+Q^2}} \cdot 2Q \cdot \frac{dQ}{dU} + (-U^{-2}) \cdot \sqrt{P^2+Q^2} \\
&= \frac{1}{U \cdot \sqrt{P^2+Q^2}} \cdot Q \cdot P \cdot \frac{1}{\cos^2\phi} \cdot \frac{d\phi}{dU} - \frac{\sqrt{P^2+Q^2}}{U^2}
\end{aligned}
\tag{5.14}
$$

Current, $\cos\phi$ and $\sin\phi$ can be replaced by powers and voltage, giving the final admittance values shown in equation 5.15. For the minimum loss settings, without limitation of the real power, $\frac{d\phi}{dU}$ is shown in equation 5.11 and $\frac{dI}{dU}$ in equation 5.14.

$$
\begin{aligned}
Y_{dd} &= \frac{dI_d}{dU_d} = \frac{dI}{dU} \cdot \cos\phi - I\frac{d\phi}{dU} \cdot \sin\phi = \frac{dI}{dU} \cdot \cos\phi - \frac{d\phi}{dU} \cdot \frac{Q}{U} \\
Y_{qd} &= \frac{dI_q}{dU_d} = -\frac{dI}{dU} \cdot \sin\phi - I\frac{d\phi}{dU} \cdot \cos\phi = -\frac{dI}{dU} \cdot \sin\phi - \frac{d\phi}{dU} \cdot \frac{P}{U} \\
Y_{dq} &= \frac{dI_d}{dU_q} = \frac{-I\sin(-\phi)}{U} = \frac{I\sin\phi}{U} = \frac{Q}{U^2} \\
Y_{qq} &= \frac{dI_q}{dU_q} = \frac{I\cos(-\phi)}{U} = \frac{P}{U^2}
\end{aligned}
\tag{5.15}
$$

If the source impedance is a line only, the impedance matrice for steady state is shown in equation 5.16. The source impedance of a rotary converter with automatic voltage regulator is not calculated analytically here.

$$
\begin{bmatrix} Z_{dd} & Z_{dq} \\ Z_{qd} & Z_{qq} \end{bmatrix} = \begin{bmatrix} R & -\omega_s \cdot L \\ \omega_s \cdot L & R \end{bmatrix} \tag{5.16}
$$

5.2.4 Stability Criterion

In [11], the control loops shown in figure 5.10 are considered as a MIMO system and the generalized Nyquist stability criterion is applied.

Theorem Generalised Nyquist theorem for a MIMO system[1]**:** *Let P_{ol} denote the number of open-loop unstable poles in $L(s)$. The closed-loop system with loop transfer function $L(s)$ and negative feedback is stable if and only if the Nyquist plot of* $\det([I]+L(s))$ *makes P_{ol} anti-clockwise encirclements of the origin, and does not pass through the origin.*

From this it may be derived ([12]) that the Nyquist contour $\bar{N}(s)$ should make no encirclements of the origin if $[Z_{source}] \cdot [Y_{load}]$ is open-loop stable, and should make P_{ol} anti-clockwise encirclements if $[Z_{source}] \cdot [Y_{load}]$ is unstable. $\bar{N}(s)$ is given in equation 5.17, with the angular speed of oscillation ω_{osc}.

$$
\bar{N}(s) = \det([I] + [Z_{source}] \cdot [Y_{load}])|_{s=j\omega_{osc}} \tag{5.17}
$$

Writing out the elements of the matrices, this criterion may be interpreted as the Nyquist Contour -1 (N-1) in equation 5.18 should not clockwise encircle (-1+j0) as the commonly known Nyquist stability criterion for single-input-single-output

[1] Theorem 4.9 in [12]

(SISO) systems.

$$\begin{aligned}\bar{N}(s) - 1 = &\bar{Y}_{dd}\bar{Y}_{qq}\bar{Z}_{dd}\bar{Z}_{qq} + \bar{Y}_{dq}\bar{Y}_{qd}\bar{Z}_{dq}\bar{Z}_{qd} \\ &- \bar{Y}_{dq}\bar{Y}_{qd}\bar{Z}_{dd}\bar{Z}_{qq} - \bar{Y}_{dd}\bar{Y}_{qq}\bar{Z}_{dq}\bar{Z}_{qd} \\ &+ \bar{Y}_{dd}\bar{Z}_{dd} + \bar{Y}_{qq}\bar{Z}_{qq} + \bar{Y}_{dq}\bar{Z}_{qd}\bar{Y}_{qd}\bar{Z}_{dq}\end{aligned} \tag{5.18}$$

If this interpretation is accepted, the amplitude and phase plot of (N-1) can be presented as well for this MIMO system such as in a SISO system [10].

5.3 Effect of a Passive Control of Reactive Power

The following cases are simulated and compared. The control schemes are described for steady state in section 3.2.1 and in [5]:

1. Unity power factor. This is the reference case, also used as reference case by Danielsen.

2. "Minimum loss", static ϕ. In this case, the operating point is given by the "minimum loss" characteristics. The "minimum loss" characteristics give a voltage dependent load angle ϕ, but this voltage dependency is disregarded in dynamic analyses, keeping ϕ constant at the value from the load flow calculation. This case is chosen to distinguish the effect of changed operating point from the effect of reactive power control. Such a characteristic could be implemented by having a slow response from the reactive power controller, or by having a constant load angle over a voltage range, such as "factory settings" below 13 kV, shown in figure 3.5.

3. "Minimum loss", dynamic ϕ. In this case, the operating point is given by the "minimum loss" characteristics. The reactive power controller controls the q-axis current reference ${i_q}^{ref}$ without intended delay (although some delay is caused by the voltage measurement and the current controller).

The vehicle is operating at half the rated power, 3.67 MW at the DC link, giving approximately 3.8 MW at the current collector. No power oscillation damper (POD) is used. The simulations are run in TRANSTA, using enhanced RMS as described in [3].

The control schemes for reactive power in steady state described in section 3.2.1 all control q-axis current reference by multiplying the d-axis current reference by the output from the reactive power controller. In no-load, the d-axis current reference is zero, so that the reactive power controller has no effect in no-load. Therefore, these control schemes are not compared in no-load.

5.3.1 Operating Points and Steady State Considerations

Operating Points

The operating points for the simulations are shown in table 5.1. Note that the real power is slightly lower for the "minimum loss" cases, due to lower transformer losses.

Table 5.1: Operating points

	Unit	Simulation case		
		Unity power factor	"Minimum loss", static ϕ	"Minimum loss", dynamic ϕ
U_{loco}	kV	12.61	13.71	13.71
P_{loco}	MW	3.811	3.798	3.798
Q_{loco}	MVAr	0.000	-1.039	-1.039
I_{loco}	kA	0.3023	0.2871	0.2871
ϕ	°	0	-15.3	-15.3
ϕ	rad	0	-0.267	-0.267
$^{d\phi}/_{dU_{loco}}$	rad/kV	0	0	0.1441
$^{dI}/_{dU_{loco}}$	kA/kV	-0.0240	-0.0209	-0.0323

Steady State Admittance Matrices

The steady state admittance matrices are calculated according to equation 5.15. There is a small inaccuracy in the values calculated here, as the formula is developed for a constant real power. In this case, the real power is constant 3.67 MW at the DC-link, but will vary slightly at the current collector as the current and thereby the transformer loss is depending on operating voltage, i.e. the vehicle is not a perfect constant power load at the current collector.

Unity power factor:

$$Y = \begin{bmatrix} -0.0240 & 0 \\ 0 & 0.0240 \end{bmatrix} [A/V]$$

"Minimum loss", static ϕ:

$$Y = \begin{bmatrix} -0.0202 & -0.0055 \\ -0.0055 & 0.0202 \end{bmatrix} [A/V]$$

"Minimum loss", dynamic ϕ:

$$Y = \begin{bmatrix} -0.0202 & -0.0055 \\ -0.0484 & 0.0202 \end{bmatrix} [A/V]$$

All the admittances have negative Y_{dd}, i.e. increased voltage magnitude gives reduced d-axis current, which is as expected for a load with constant real power.

Effect of Rotary Converter Voltage Deviation

A constant power load is exactly that, constant power. In this case, the motor side inverter draws a constant power of 3.67 MW from the DC-link. The line side converter in the vehicle is modelled as lossless, ie. the the vehicle is a constant power load at the low voltage side of the vehicle main transformer. Constant power causes reduced voltage to be compensated by increased current. If the constant power load is supplied by a transmission which is not lossless, reduced voltage will cause increased power. This is most likely an effect reducing voltage stability; reduced voltage increases the power consumption, which will cause a further decrease of voltage.

This effect is shown in table 5.2. Load flow calculation is performed in normal operation, the voltage at the converter station U_{con} = 16.5 kV, as well as ± 1 % (± 165 V). Voltage decrease gives a slight increase at the power at the vehicle's current collector P_{loco}, and a larger increase in the line loss $P_{line\ loss}$.

With unity power factor at the vehicle, a voltage deviation at the converter station of 165 V gives a deviation of the vehicle voltage U_{loco} of 266-275 V. For "minimum loss", static ϕ, the voltage deviates 231-235 V, while "minimum loss", dynamic ϕ gives a voltage deviation at the vehicle of 150-152 V.

Table 5.2: Stationary response to voltage deviation at the converter station. Voltage in [kV], real power in [MW] and reactive power in [MVAr].

U_{con}		U_{loco}	ΔU_{loco}	P_{loco}	Q_{loco}	$\tan\phi_{loco}$	$P_{line\ loss}$
Unity power factor							
16.665	(+1 %)	12.874	0.266	3.805	0	0	0.9959
16.500	(ref)	12.608	-	3.811	0	0	1.0417
16.335	(-1 %)	12.333	-0.275	3.818	0	0	1.0927
Minimum loss, static ϕ							
16.665	(+1 %)	13.943	0.231	3.793	-1.037	-0.273	0.9067
16.500	(ref)	13.713	-	3.798	-1.039	-0.273	0.9397
16.335	(-1 %)	13.478	-0.235	3.802	-1.040	-0.273	0.9752
Minimum loss, dynamic ϕ							
16.665	(+1 %)	13.865	0.152	3.793	-0.951	-0.251	0.9068
16.500	(ref)	13.713	-	3.798	-1.039	-0.273	0.9397
16.335	(-1 %)	13.563	-0.150	3.802	-1.132	-0.298	0.9754

5.3.2 Eigenvalue Considerations

For the three cases given, the system's eigenvalues are calculated. Out of a total of 41 eigenvalues (zero-values excluded), the ones having a frequency lower than the fundamental frequency ($\mathrm{Im}(\lambda) < f_s$) and a real part larger than -100 ($\mathrm{Re}(\lambda) >$

-100) are shown in table form in appendix B. The same eigenvalues, except from 13, 14, are shown in figure 5.11.

All the simulated cases have a poorly damped eigenvalue, which will dominate the system's response, the oscillation mode from the rotary converter motor, at about 1.6 Hz. This mode, eigenvalues number 25, 26 for unity power factor and "minimum loss", dynamic ϕ, number 24, 25 in "minimum loss", static ϕ, is shown in table 5.3. The motor mode has negative damping (unstable) with unity power factor. With operating point as for "Minimum loss", but static ϕ, this mode is more damped, but still unstable. "Minimum loss", dynamic ϕ gives a positive damping, though still low (1.13 %).

Table 5.3: Eigenvalues 25,26/ 24,25 (rotary converter mode).

Case	Eigenvalue [1/s ± jHz]	Damping [%]
Unity power factor	0.055± j1.64	-0.53
"Minimum loss", static ϕ	0.0031± j1.61	-0.031
"Minimum loss", dynamic ϕ	-0.11± j1.60	1.12

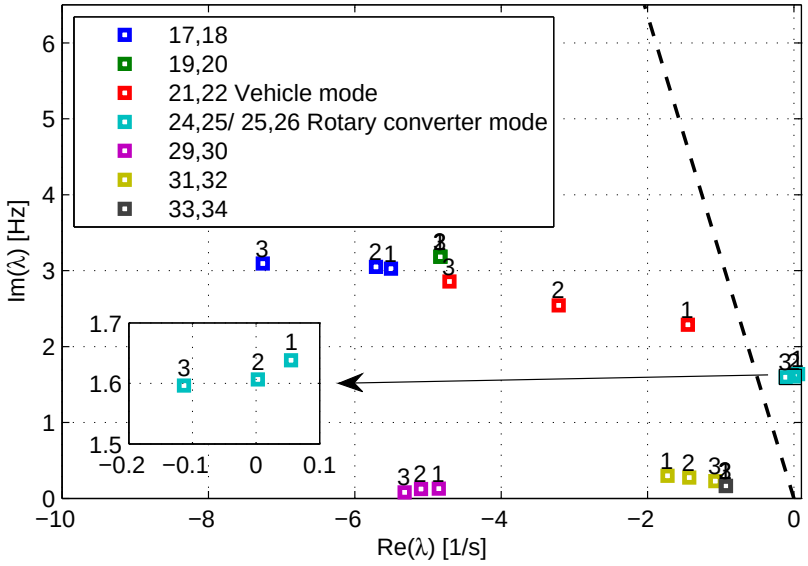

Figure 5.11: Plot of eigenvalues. The dashed line indicates 5 % damping. The numbering refers to the different simulation cases; 1 - unity power factor, 2 - "minimum loss", static ϕ, 3 - "minimum loss", dynamic ϕ.

Eigenvalues 17, 18 are mainly governed by the voltage regulator of the generator. This mode has its damping improved from 27.7 % to 35.3 % when changing from unity power factor to "minimum loss", dynamic ϕ.

The vehicle mode 21, 22, is clearly influenced by the settings for reactive power. When changing from unity power factor to "minimum loss", dynamic ϕ, the eigenvalue is changed from -1.42 [1/s] ± j2.28 [Hz] to -3.29 [1/s] ± j2.85 [Hz], and increase of damping from 9.9 % to 18.1 %. The eigenvalues 31, 32 are dominated by the generator. These are also affected by the settings for reactive power, being changed from -1.42 [1/s] ± j0.35 [Hz] to -0.94 [1/s] ± j0.24 [Hz], but they will have little effect, as their damping in all cases is about 50 %.

Eigenvalues 29, 30 are governed by the vehicle. This mode is somewhat influenced by settings for reactive power, but has in all cases a damping about 99 %.

Eigenvalues 19, 20 and 33, 34 are mainly governed by the voltage regulator, exciter and field winding of the 3-phase motor. Reactive power settings on the single phase side has no significant influence on these modes.

5.3.3 Impedance and Admittance Considerations

Frequncy sweeps are performed to find $[Z_{source}]$ and $[Y_{load}]$ for frequencies from 0.01 to 16 Hz. The impedance and admittance values are shown graphically in attachment C.

The Nyquist contour (N-1) is shown in figure 5.12. The curve for unity power factor encircles the point (-1+j0), which indicates an unstable system. The curve for "minimum loss", static ϕ passes very close to the point (-1+j0), which indicates an unstable or marginally stable system. The curve for "minimum loss", dynamic ϕ does not encircle (-1+j0), which indicates a stable system. Three points of this curve is located far from the others, forming "spikes" out from the rest of the curve. These points are assumed to be caused by an inaccuracy in the simulation, and can probably be neglected when considering the result.

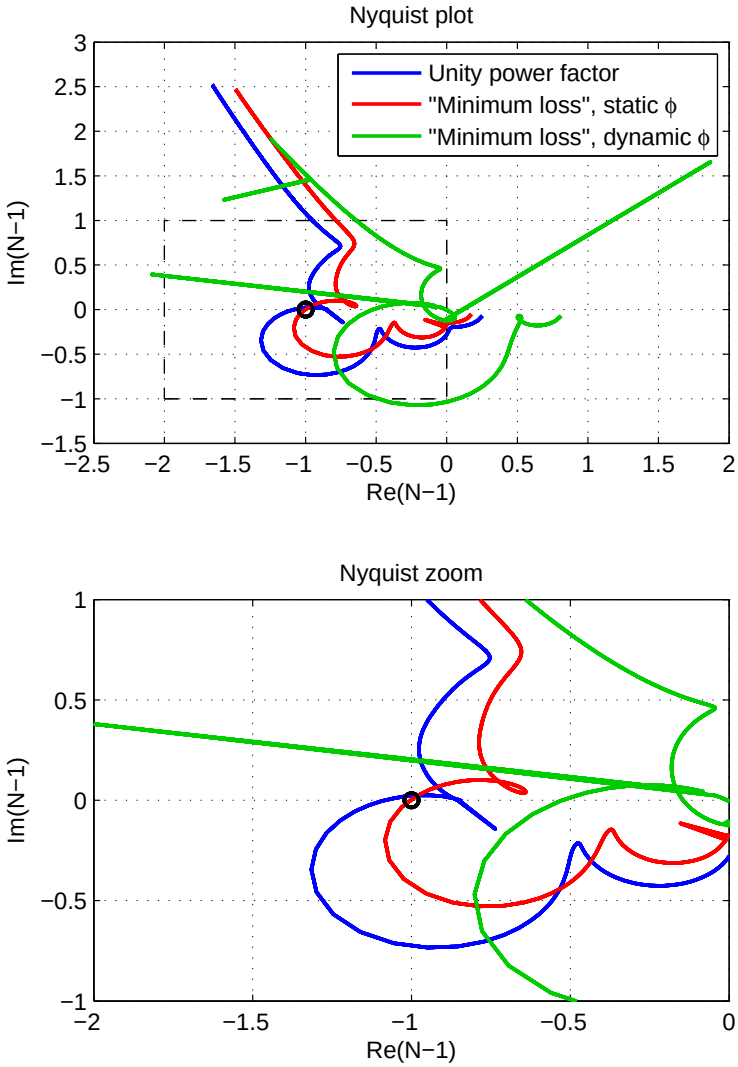

Figure 5.12: Contour of (N-1) for the three simulation cases.

5.3.4 Time Simulations

A 100 kW load is connected at the rotary converter 16.5 kV bus at t=-0.1 s, and disconnected at t=0 s. Rotary converter speed ω_{gen}, voltage U_{loco} and powers (P_{loco} and Q_{loco}) at the vehicle are shown in figure 5.13 and 5.14. Note that there are two different axes for voltage and reactive power due to different operating points.

After about 2 s, the rotary converter mode (1.6 Hz) is dominating the oscillations in all cases.

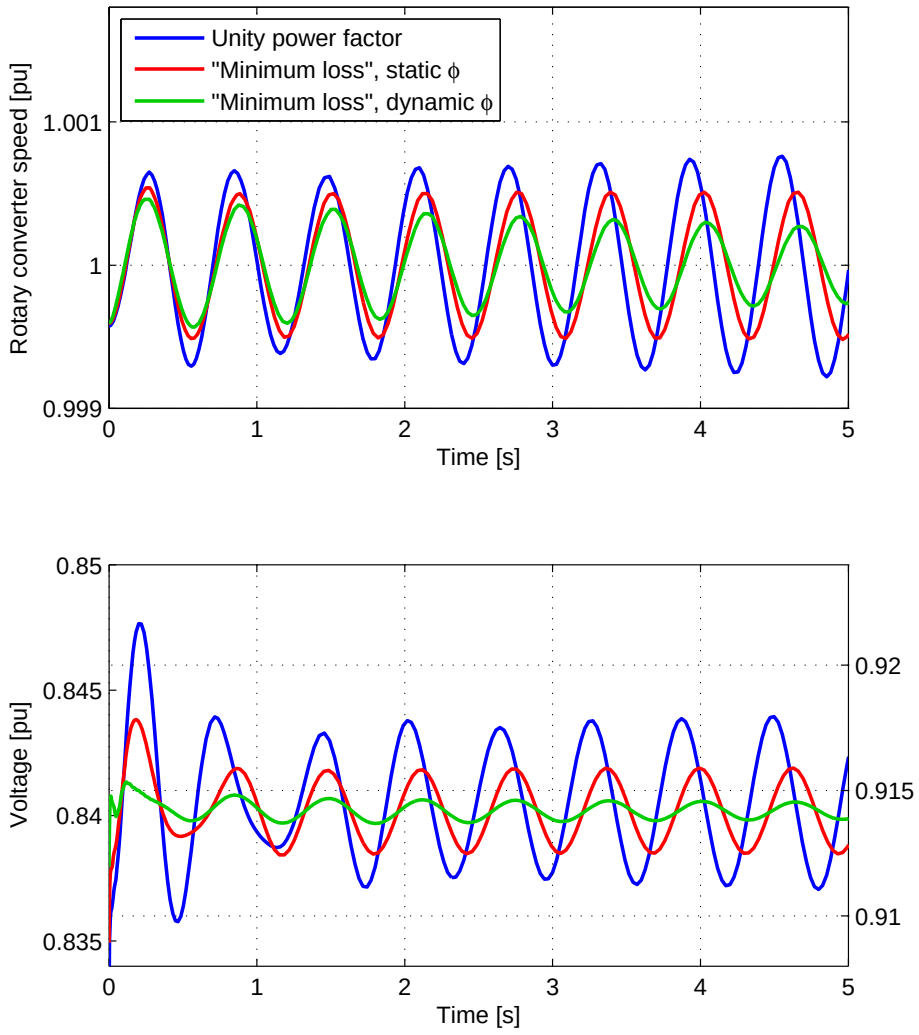

Figure 5.13: Rotary converter speed and voltage at the vehicle. Voltage for unity power factor on left axis, voltage for "minimum loss" on right axis.

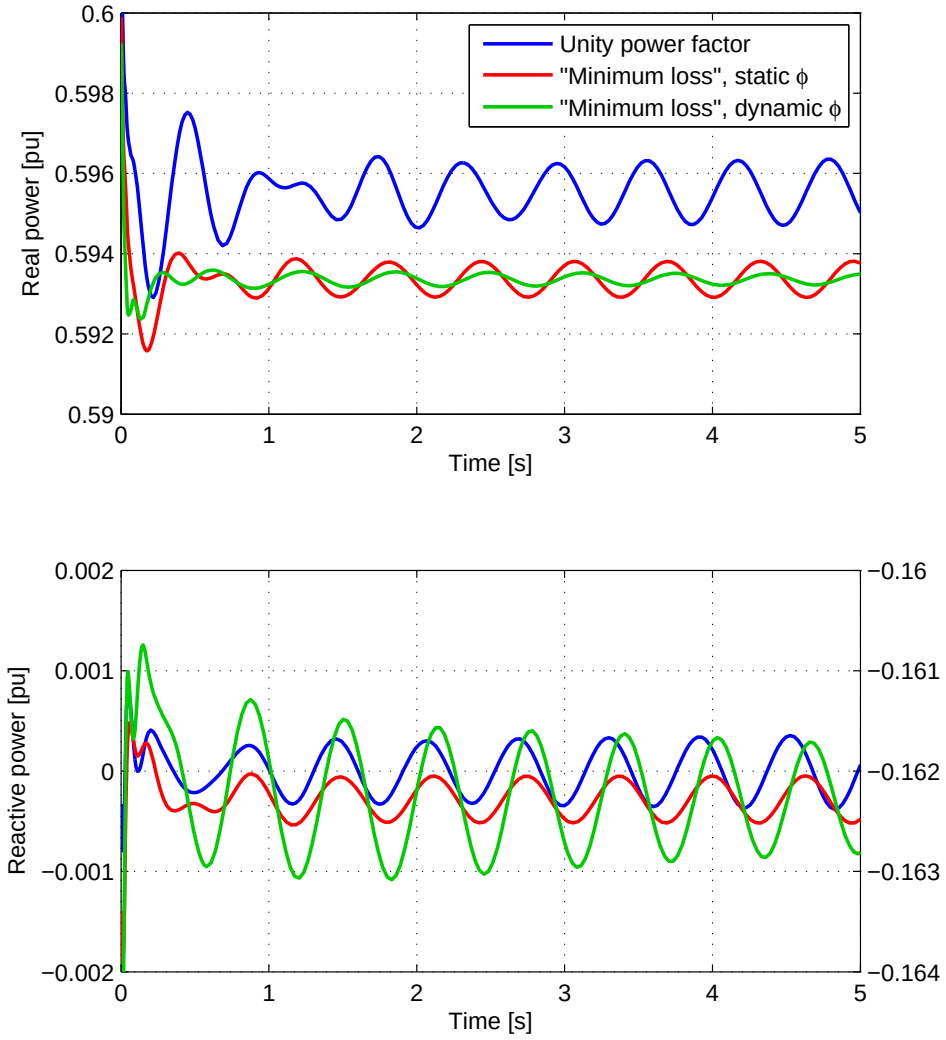

Figure 5.14: Real and reactive power at the vehicle. Reactive power for unity power factor on left axis, reactive power for "minimum loss" on right axis.

The oscillations from figure 5.13 and 5.14 are shown as phasors in figure 5.15 and table 5.4, together with voltage angle at the vehicle δ_{loco}, the real power of rotary converter generator P_{gen}, the electromagnetic torque T_{gen} and the voltage of the converter station's 15 kV busbar U_{con}. The electromagnetic torque is found as the real power of the generator divided by the speed. The phasors are found by fast fourier transform over one fundamental period at t $\approx$ 2.5 s. The phasors are shown in pu relative to the rotary converter speed, ie. what is the system's response to a

given mechanical oscillation.

Damping of mechanical oscillations would be load torque (electromagnetic torque of generator = load torque of mechanical system) oscillating in phase with the speed, increased speed giving increased load torque. In all three cases, the vehicle contributes to destabilizing the the system, as the torque oscillations have a phase > 90 ° from the speed oscillations. In table 5.4, this is shown as negative real part.

The voltage oscillations for "minimum loss", dynamic ϕ are clearly smaller than for "minimum loss", static ϕ and unity power factor, which indicates that the reactive power from the vehicle helps stabilizing the system voltage. "Minimum loss", dynamic ϕ also gives smaller oscillations of the voltage angle at the vehicle. A similar effect is shown in table 5.2, where a 165 V change of the voltage at the rotary converter station gives a change of the vehicle voltage of 266-275 V with unity power factor, but only 150-152 V for "minimum loss", dynamic ϕ.

Smaller oscillations of voltage magnitude and angle at the vehicle give smaller oscillations in the vehicle real power, reducing the vehicle's destabilizing impact on the system.

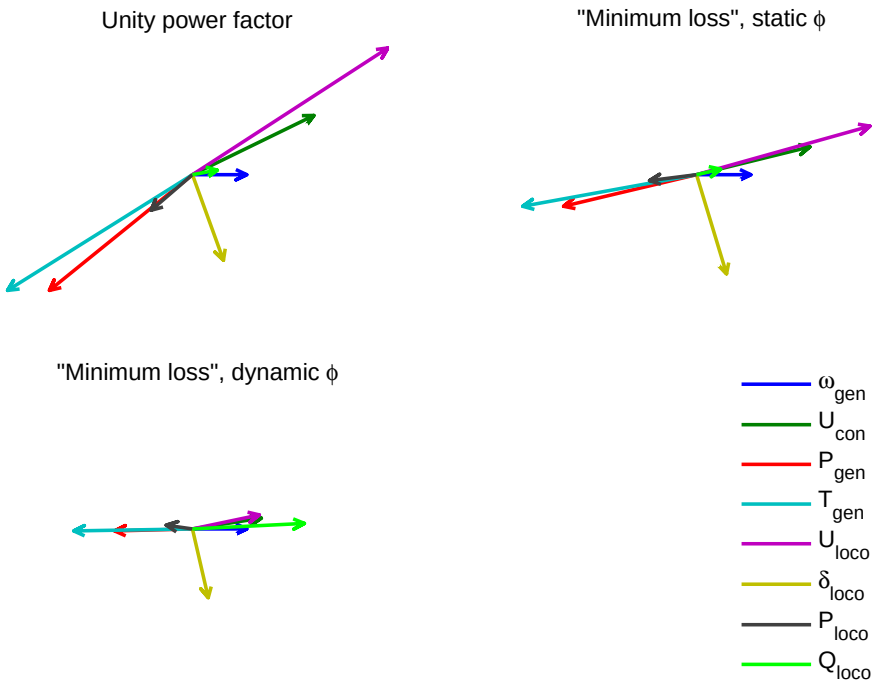

Figure 5.15: Oscillations after disturbance shown as phasors. The speed phasor is set to 1, other phasors scaled accordingly. Positive direction for real and reactive power is from the rotary converter to the vehicle.

Table 5.4: Oscillations after disturbance shown as phasors. The speed phasor is set to 1, other phasors scaled accordingly.

	Unity power factor	"Minimum loss", static ϕ	"Minimum loss", dynamic ϕ
ω_{gen}	1	1	1
U_{con}	2.24+j1.15	2.08+j0.54	1.27+j0.21
P_{gen}	-2.63-j2.26	-2.45-j0.62	-1.43-j0.04
T_{gen}	-3.40-j2.26	-3.20-j0.62	-2.18-j0.04
U_{loco}	3.60+j2.47	3.19+j0.95	1.23+j0.27
δ_{loco}	0.57-j1.67	0.55-j1.93	0.29-j1.34
P_{loco}	-0.76-j0.69	-0.87-j0.12	-0.48+j0.07
Q_{loco}	0.46+j0.09	0.44+j0.11	2.06+j0.11

5.4 Effect of Active Control of Reactive Power - POD

The main purpose of this section is not to find the optimal settings for the PODs, but to investigate the potential of using reactive power for damping oscillations. The dominating oscillation in the system in traction is the rotary converter mode at approximately 1.6 Hz. In no-load, the system will become unstable at long line lengths with an oscillation caused by the vehicle at 4-5 Hz.

The structure of the power oscillation damper (POD) is shown in section 5.1.4. Two different PODs are tested in traction and no-load.

5.4.1 Design of POD

All PODs use the voltage magnitude as input, and send the output signal to the summation point of the q-axis current controller. As negative q-axis current corresponds to positive reactive power, $-i_{q\ POD}$ is shown in graphs and phasor diagrams.

POD2a

POD2a is designed by Danielsen, called POD2 in [3]. POD2 aims to reduce the line voltage oscillations at the rotary converter eigenfrequency by means of reactive power modulation. The pass-band filter created by the measurement block and the wash-out block are chosen to be symmetrical around the rotary converter eigenfrequency. This results in a zero phase of the filter at 1.6 Hz, and no extra lead and lag block is used.

POD2b

POD2b was tuned to damp the vehicle mode which may cause instability in no-load.

A POD with no change of phase except from voltage measurement and $K_{POD} = 0$ was implemented in the model and simulated in no-load, with $K_{POD} = 0$. The sensitivity of the vehicle mode (0.111 1/s ± j4.324 Hz) to K_{POD} was found to 2.560 1/s/pu ± j1.617 Hz/pu, giving an angle of -75 ° from moving the eigenvalue straight to the left. During parameter scanning POD2a in no-load (figure 5.21), scanning of T_w indicated a minimum of Re(λ) with $T_w = 0.03s$. The lead-lag block was tuned so that the wash-out and the lead-lag totally increased the phase by 75 ° at 4.32 Hz. The gain was first set to 1. At this setting, the vehicle mode decayed too fast to perform Fourier analysis over a complete cycle, and the gain was reduced to 0.5.

The POD parameters are shown in figure 5.5, and resulting bode plots are shown in figure 5.16.

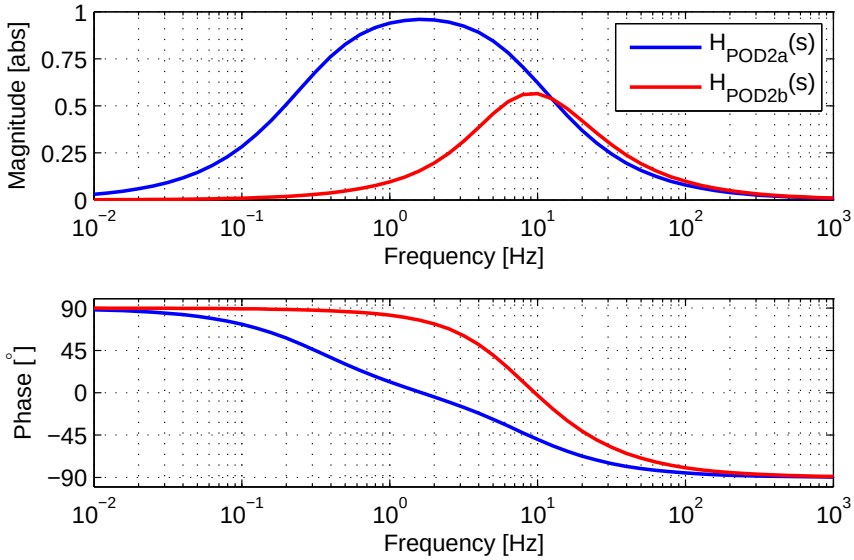

Figure 5.16: Bodeplots of POD transfer functions.

Table 5.5: POD parameters.

Parameter	Unit	POD2a	POD2b
T_1	[s]	0.02	0.02
T_w	[s]	0.47	0.03
T_2	[s]	0	0.05
$T_3 (= T_{POD})$	[s]	0	0.02
K_{POD}	[pu]	1	0.5
u_{PODlim}	[pu]	0.01	0.01

5.4.2 Traction - Damping of Rotary Converter mode

The vehicle is investigated in traction, at the operating point "minimum loss", dynamic ϕ in table 5.1. The settings used for reactive power is "minimum loss", dynamic ϕ, without POD, as well as with POD2a and POD2b. Unity power factor is already investigated by Danielsen, "minimum loss", static ϕ is primarily made as a reference case to distinguish the effect of dynamic control of reactive power from the effect of operating point. "Minimum loss", dynamic ϕ also yielded the best damping of the rotary converter mode.

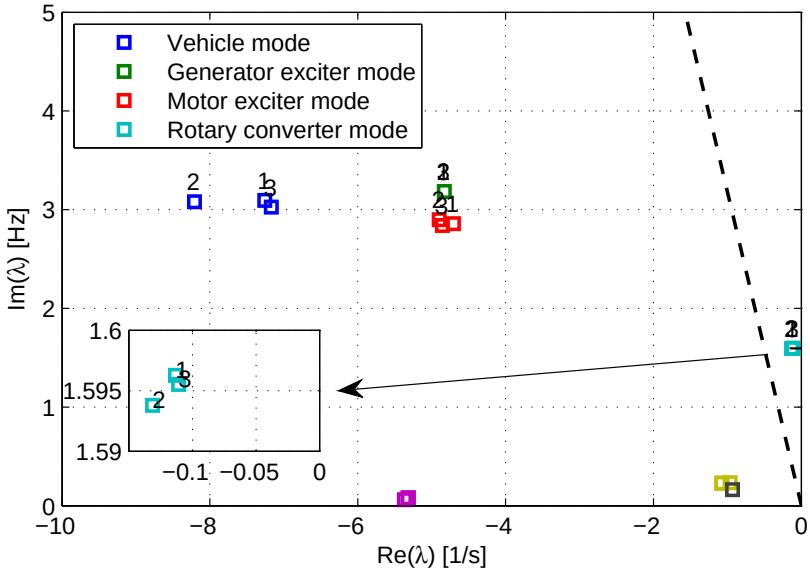

Figure 5.17: Plot of eigenvalues without POD (1) and with POD2a (2) and POD2b (3). The dashed line indicates 5 % damping.

The eigenvalues are shown i figure 5.17. The least damped eigenvalue is the rotary converter mode at 1.6 Hz. POD2a is designed to work on this mode, and improves damping somewhat; real part is changed from -0.1133 1/s to -0.1313 1/s. POD2b is designed to damp oscillations at higher frequency, and at 1.6 Hz, its effect is mainly to reduce the oscillation frequency, while the damping is slightly poorer.

The eigenvalue is scanned for the parameters of POD2a, see figure 5.18. The scanning for gain K_{POD} indicates a movement mainly left-right (notice the axes), which indicates that the angle is tuned relatively well. However, as gain is increased, the effect of further increase is reduced, and POD2a cannot affect the eigenvalue much. The reason for this is probably that the reactive power reduces the voltage oscillation, while the voltage is used as input for the POD. Stabilizing the voltage reduces the mode's observability.

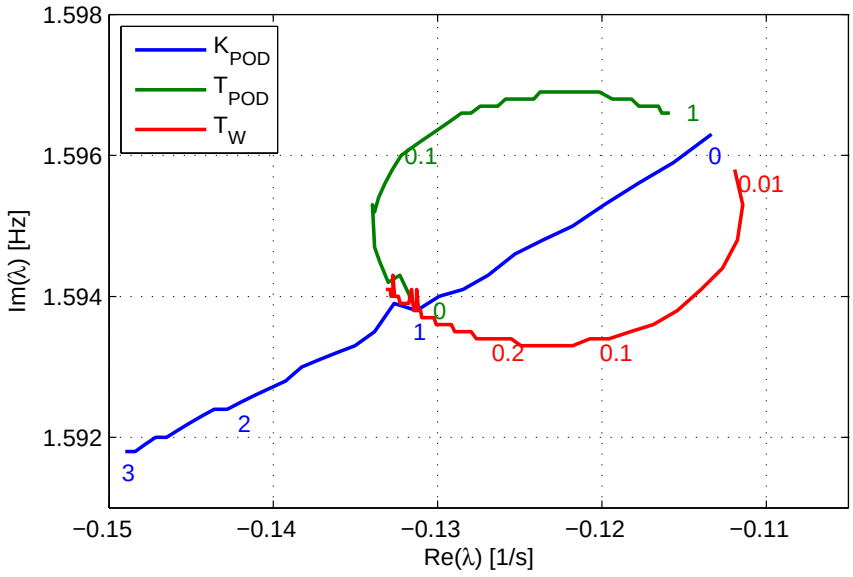

Figure 5.18: Data scanning of the eigenvalue 25 (rotary converter mode) with respect to the parameters of POD2a. K_{POD} is scanned 0-3, T_{POD} is scanned 0-1 s, T_W 0.01-1 s.

The oscillation of the rotary converter mode is shown as phasors in figure 5.19 and table 5.6. POD2a reduces the voltage oscillation at the vehicle U_{loco} for a given speed oscillation by about 27 %, which gives reduced power and torque oscillations. POD2b has only small effect.

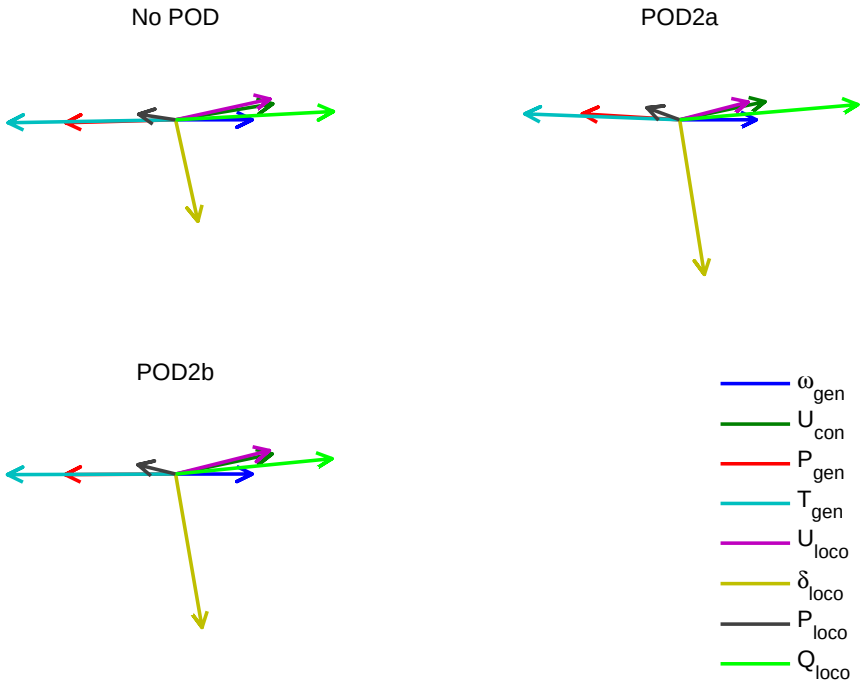

Figure 5.19: The 1.6 Hz oscillation (rotary converter mode) as phasors.

Table 5.6: The 1.6 Hz oscillation (rotary converter mode) as phasors.

	No POD	POD2a	POD2b
ω_{gen}	1	1	1
U_{con}	1.27+j0.21	1.12+j0.24	1.26+j0.27
P_{gen}	-1.43-j0.04	-1.27+j0.08	-1.44-j0.01
T_{gen}	-2.18-j0.04	-2.02+j0.08	-2.19-j0.01
U_{loco}	1.23+j0.27	0.89+j0.23	1.23+j0.31
δ_{loco}	0.29-j1.34	0.32-j2.04	0.35-j2.03
P_{loco}	-0.48+j0.07	-0.43+j0.16	-0.49+j0.12
Q_{loco}	2.06+j0.11	2.33+j0.20	2.04+j0.20

5.4.3 No-load - Damping of Vehicle Mode

Eigenvalues and Stability Limit

The vehicle is tested in no-load with 200 km line length. Eigenvalues for this case are shown in figure 5.20. 200 km is chosen as a round number close to the stability limit in no-load without POD. The rotary converter mode is stable but poorly damped in no-load, and this mode will not cause instability at any line length. The rotary converter mode is very little affected by the reactive power settings in no-load. Its value is found to be -0.32 1/s ± j1.58 Hz as without as well with both PODs, very close to the values found by Danielsen without a vehicle; simulated to -0.34 1/s ± j1.59 Hz, measured to -0.33 1/s ± j1.57 Hz (table 3-2 in [3]).

The control schemes for reactive power in steady state described in section 3.2.1 all control q-axis current reference by multiplying the d-axis current reference by the output from the reactive power controller. In no-load, the d-axis current reference is zero, so that the reactive power controller has no effect in no-load. Therefore, these control schemes are not compared in no-load.

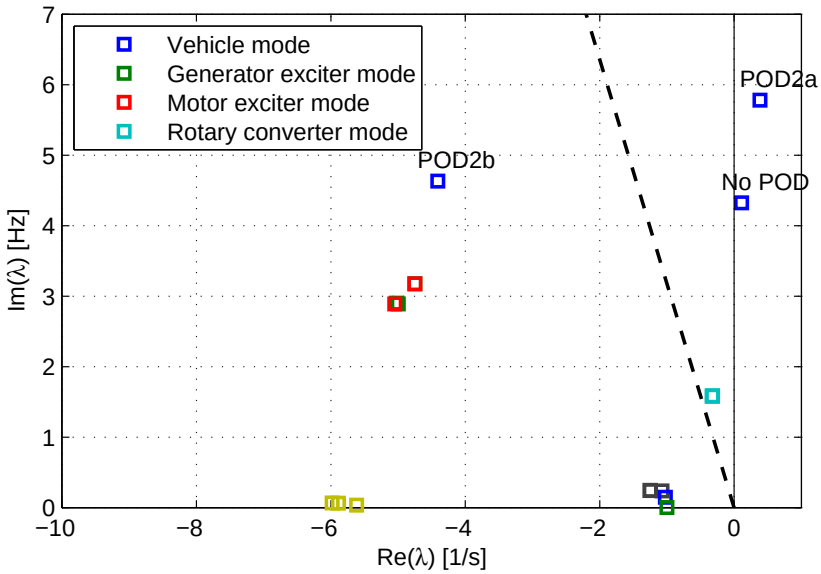

Figure 5.20: Plot of eigenvalues in no-load. The dashed line indicates 5 % damping.

The mode causing instability is an oscillation caused by the dynamics of the vehicle. This mode will also appear in a system fed from a stiff voltage source, not only a rotary converter. This mode is clearly affected by the reactive power from the vehicle. POD2a is tuned for oscillations at a lower frequency than the vehicle mode at 4.32 Hz. For this oscillation, POD2a makes the mode more unstable and

increases its frequency.

POD2b is tuned for damping the vehicle mode, and damps the mode well with only a minor change of frequency. Similar effects can be seen on the stability limits shown in table 5.7. POD2a increases frequency and decreases stability limit. POD2b has less effect on frequency, while the stability limit is nearly doubled, see table 5.7.

Table 5.7: The stability limit with and without POD.

Model	Stability limit [km]	Oscillation frequency [Hz]
No POD	197	4.35
POD2a	193	5.84
POD2b	341	4.06

Parameter Scanning

Parameter scanning of K_{POD} at POD2a shows clearly how it increases frequency with little effect on the damping, figure 5.21. Scanning of T_w indicates a possibility for tuning POD2a to give a far better performance, by setting T_w to 0.02-0.03 s.

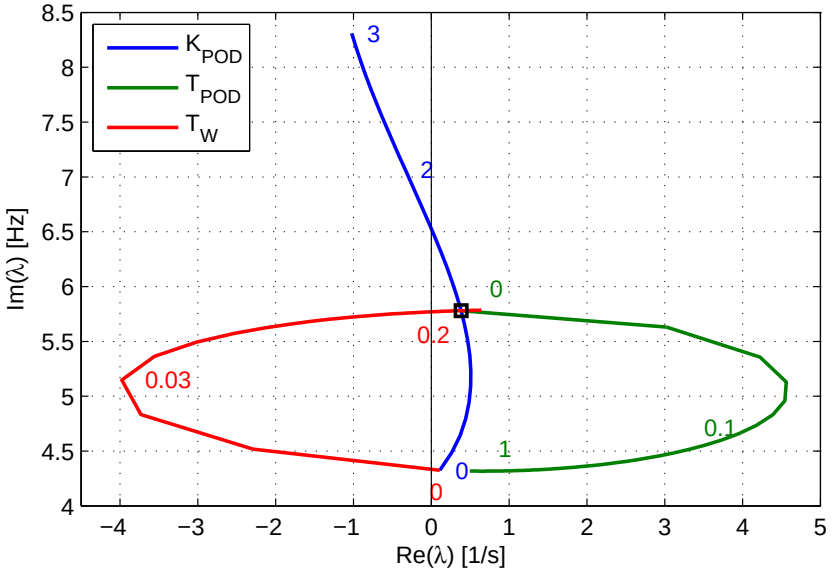

Figure 5.21: Data scanning of the eigenvalue 25 (rotary converter mode) with respect to the parameters of POD2a. K_{POD} is scanned 0-3, T_{POD} is scanned 0-1 s, T_W 0.01-1 s.

Time Simulations

The system is excited by the same disturbance as used in section 5.3.4; a 100 kW resistor is connected to the rotary converter 16.5 kV bus at t=-0.1 s, and disconnected at t=0 s.

The response without POD is shown in figure 5.22. The rotary converter speed oscillates with about 1.6 Hz, slowly decaying as predicted from the eigenvalues. The voltage at the converter station shows significant influence from both 1.6 and 4.32 Hz oscillations. At the vehicle, the oscillation is little affected by the 1.6 Hz from the rotary converter, the response is dominated by an increasing oscillation at 4.32 Hz.

The response with POD2a is shown in figure 5.23. The rotary converter oscillates similarly as without POD. The vehicle mode shows clearly higher frequency than without POD, and the magnitude of the oscillations increase faster than without POD.

The response with POD2b is shown in figure 5.24. The rotary converter oscillates similarly as without POD. The vehicle mode gives an oscillation at 4.63 Hz, which decays within a few cycles.

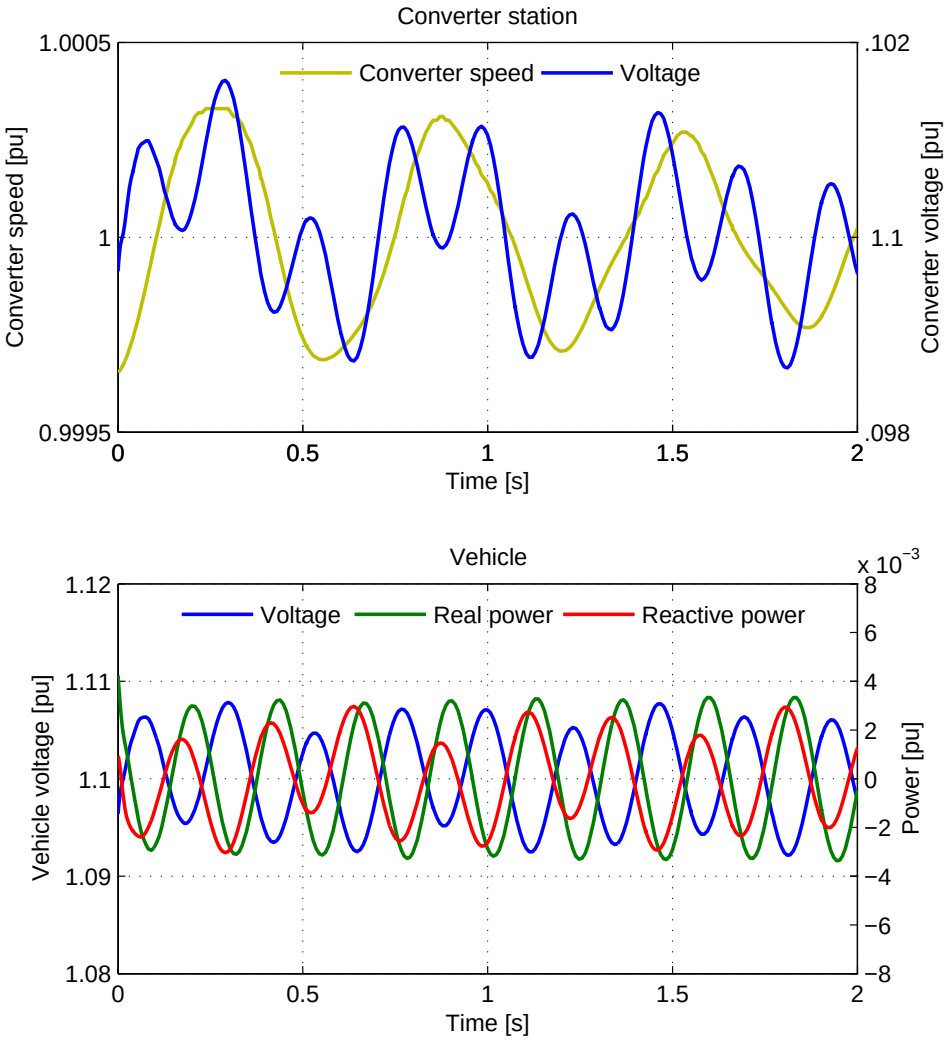

Figure 5.22: Oscillation in no-load after disturbance without POD.

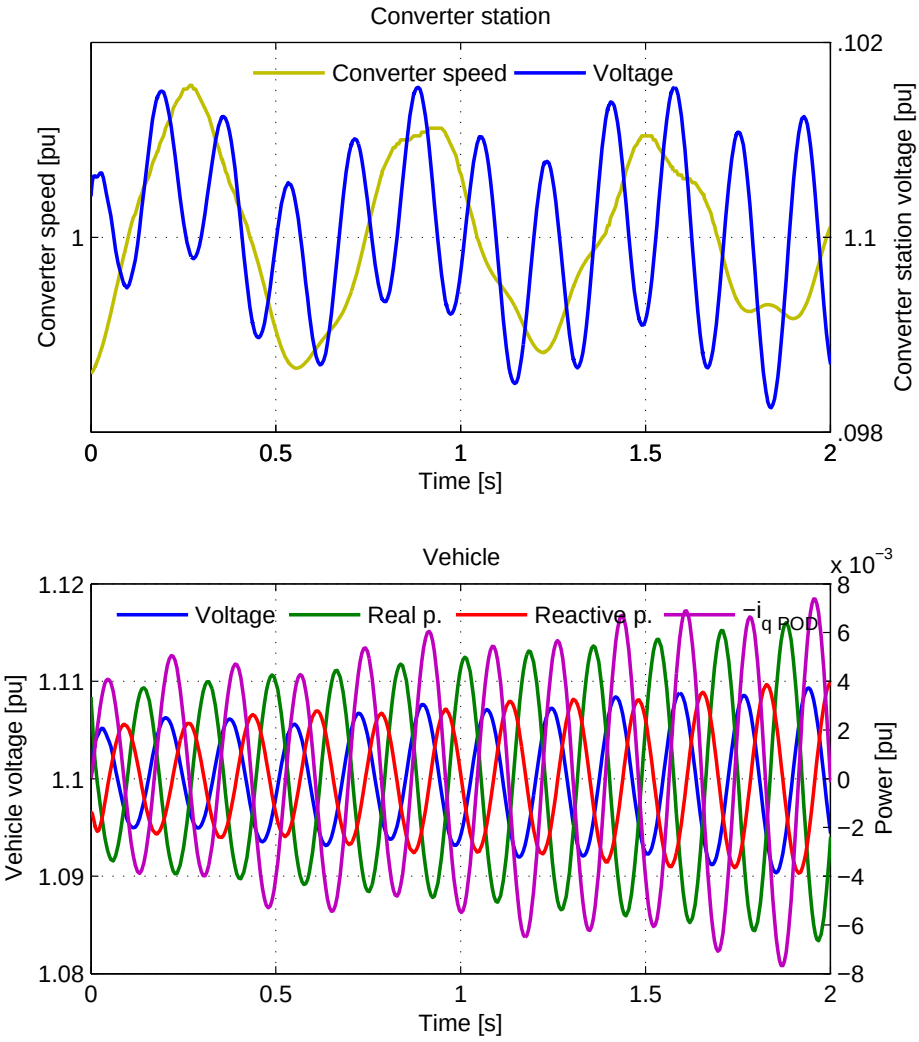

Figure 5.23: Oscillation in no-load after disturbance with POD2a.

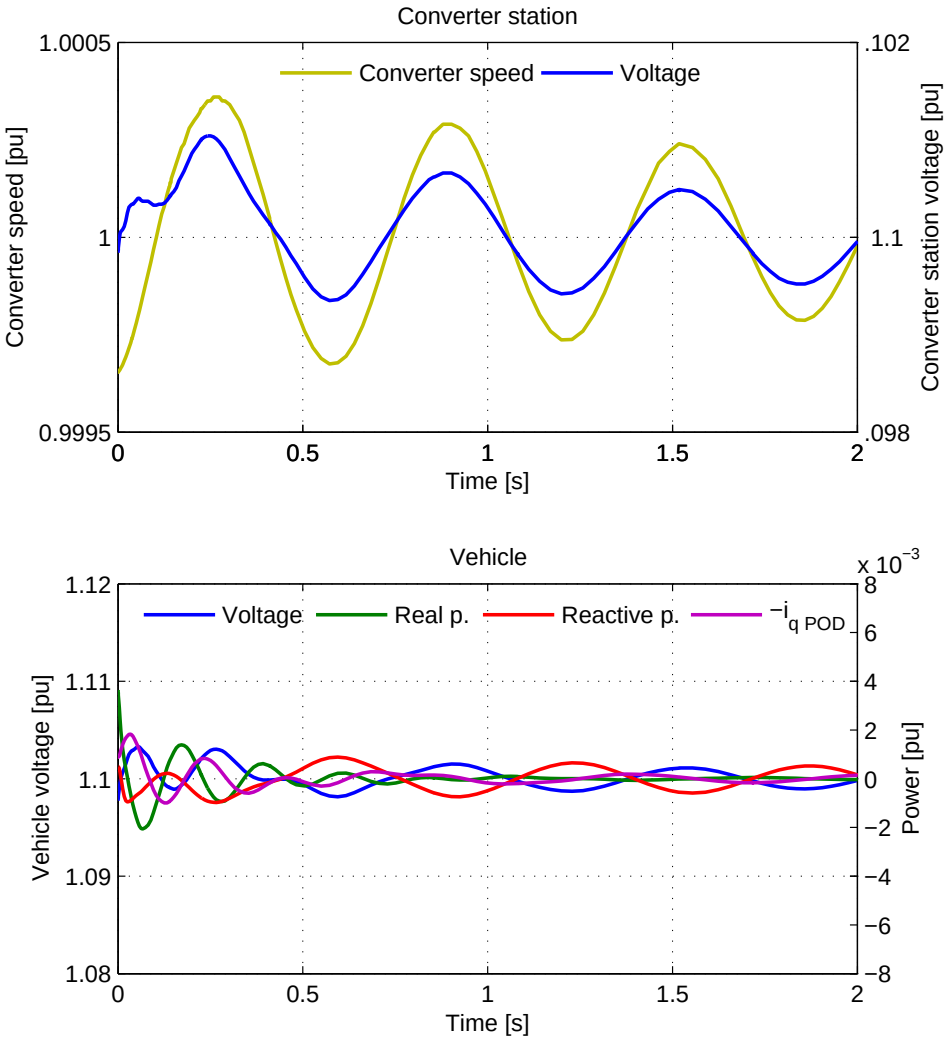

Figure 5.24: Oscillation in no-load after disturbance with POD2b.

The oscillations from the vehicle mode (4-6 Hz) in figure 5.22 to 5.24 are found by Fourier analysis and shown as phasors in figure 5.25 and numerically in table 5.8. The voltage oscillation at the vehicle is set to 1, i.e. the phasors show the response to a given voltage oscillation.

Without any POD, the reactive power at the vehicle Q_{loco} is oscillating almost in 180 ° out of phase with the voltage U_{loco}; lower voltage ⇒ higher reactive power ⇒ even lower voltage; the reactive power destabilizes the system.

With POD2a, the reactive power is lagging the voltage oscillation by 125 °. Consuming reactive power will decrease the line. Reactive power oscillating more than ± 90 ° out of phase with the voltage will have a destabilizing contribution, as lower voltage will occur together with increased reactive power, reducing the voltage further.

Reactive power lagging the voltage will contribute to increasing the frequency of the oscillation. When the voltage is high, the reactive power will increase shortly after, decreasing the voltage again, i.e. the voltage is decreased earlier than without the increased reactive power, contributing to an increased oscillation frequency.

With POD2b, the reactive power has about the same phase as without the POD, but the amplitude is smaller. When comparing figure 5.22 and 5.24, it can be seen that both voltage and reactive power oscillations are reduced significantly, so that the reactive power oscillation compared to the voltage is only slightly reduced.

Table 5.8: The 4-6 Hz oscillation (vehicle mode) shown as phasors.

	No POD	POD2a	POD2b
U_{loco}	1	1	1
U_{con}	0.12+0.04j	0.15+0.06j	0.14+0.09j
P_{loco}	-0.42+0.26j	-0.38+0.56j	-0.46+0.34j
Q_{loco}	-0.37-0.09j	-0.24-0.32j	-0.29-0.07j
$-i_{q\ POD}$	-0.00-0.00j	0.66-0.44j	0.32+0.29j

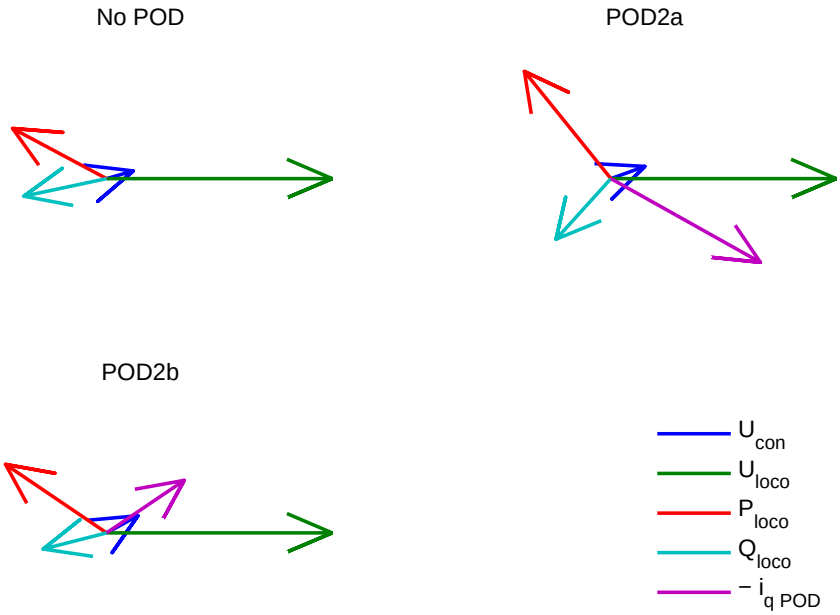

Figure 5.25: The 4-6 Hz oscillation (vehicle mode) shown as phasors. The frequency can be found from the eigenvalues in figure 5.20.

5.5 Discussion and Conclusion

5.5.1 Discussion

Admittance Values

Steady state admittances correspond quite closely to the simulated values. The magnitude of the simulated values are within 1 % lower to 11 % higher than the values from the analytic calculation. Higher admittance magnitude means that current changes more than for an ideal constant power load. Decreased voltage gives increased transformer losses, and thereby increased power at the vehicle's current collector, which corresponds well to the values from the simulation.

Reasons for Increased Damping with Passive Control of Reactive Power

The vehicle gives a negative contribution to damping in a cases simulated, most for unity power factor, least for "minimum loss", dynamic ϕ.

The change of operating point from unity power factor to "minimum loss", static ϕ gives a reduced voltage drop in the transmission, and thereby reduced voltage oscillations at both the converter station terminals and at the vehicle. But the voltage oscillation at the vehicle is in both cases about 1.5 times the voltage oscillation at the converter station.

In the cases simulated here, the vehicle increases its real power when voltage decreases, despite its constant real power control objective. This effect is also observed and commented by Danielsen [3], p. 120. Increasing vehicle power at decreasing voltage causes increased transmission losses, as more power is to be transferred at a lower voltage, both causing increased current. Reduced voltage oscillations at the vehicle gives reduced oscillation in the vehicle real power, which reduces the line loss oscillations, which again reduces oscillations in generator power and torque.

With "minimum loss" dynamic ϕ, reactive power is used in a way stabilizing the voltage at the vehicle, where more reactive power is fed into the grid at lower voltages, less at higher voltages. This reduces the voltage oscillations at the vehicle, such that the voltage oscillation is slightly smaller at the vehicle than at the converter station. The voltage oscillations for a given speed oscillation are decreased clearly from the other cases, both at the converter station and at the vehicle. A more stable vehicle voltage reduces the vehicle real power oscillations, which reduces the oscillations in generator power and torque.

Effect of Power Oscillation Damper - Traction

POD2a has some stabilizing effect on the rotary converter mode. The effect is very similar to the effect obtain when changing from "minimum loss", static ϕ to "minimum loss", dynamic ϕ. Increasing the gain reveals that the potential of further stability improvement is limited, probably because the reactive power is stabilizing the voltage, and at the same time using the voltage magnitude as input. Keeping the voltage perfectly constant would require a finite output, while the voltage oscillation at the input would be zero, i.e. an infinite gain.

Danielsen describes in [3], p. 141, how a power oscillation damper (POD) can control the vehicle to produce or consume reactive power to keep the vehicle's current magnitude, and thereby the transmission losses, constant during changing voltage at the converter station terminals. This would give a constant real power load at the converter station, eliminating the destabilizing impact of the vehicle. This control scheme is however not possible with the minimum loss settings, neither with passive ("minimum loss", dynamic ϕ) nor active control (POD) of reactive

power. Reactive power is already used to keep losses at its minimum, and a minor change of power factor will not influence the power loss. This can easily be shown by the criterion for finding the minimum of a function, the point where its derivative equals 0 ($\frac{dP_{loss}}{d\phi} = 0$).

An illustration is shown in table 5.2. The simulations with "minimum loss", static ϕ and "minimum loss", dynamic ϕ give virtually the same loss for a given voltage at the converter station, even though the reactive power differs approximately 9 % between "minimum loss", static ϕ and "minimum loss", dynamic ϕ when the converter station voltage is running at 16.665 kV or 16.335 kV.

It is observed that the POD2a yields better results for a vehicle operating at unity power factor than at capacitive power factor. Danielsen obtains an eigenvalue of 0.15 1/s ± j1.6 Hz at unity power factor, while at "minimum loss", dynamic ϕ, the eigenvalue is 0.13 1/s ± j1.6 Hz.

In addition to the POD2a, Danielsen describes two PODs acting on the real power of the vehicle, called POD1a and POD1b. With unity power factor in steady state, these PODs give eigenvalues of -0.38 1/s ± j1.6 Hz and -0.43 1/s ± j1.6 Hz, which is better damping than the rotary converter in no-load (-0.34 1/s ± j1.59 Hz) [3].

POD2b is not tuned to damp the rotary converter mode, and has very limited effect on this.

Effect of Power Oscillation Damper - No-load

POD2b has good effect on stabilizing the vehicle mode in no-load. The vehicle mode is fundamentally different from the rotary converter mode. The rotary converter mode is a mechanical oscillation, which can be influenced through the electromechanical torque of the generator, which is closely connected to real power, but only indirectly connected to reactive power. The vehicle mode is caused by the vehicle dynamics and its response to the line voltage, and could also cause instability in a system fed by a stiff voltage source, with no rotary converter at all. The line voltage is clearly affected by reactive power, and applied correctly, reactive power can stabilize the line voltage, damping the oscillation.

The purpose of this chapter is not tuning the POD optimally, but describing the effects of reactive power and its potential to improve stability. The oscillation frequency, and then the frequency the POD should be tuned for, is depending on the line length. The optimal tuning of a POD for no-load is probably not tuning it to give maximum damping at 200 km, where a very good damping may be obtained, but to tune it to increase the limit at which an acceptable stability in no-load may be obtained to a maximum. A real vehicle should be tuned for stable operation at any power and line voltage likely to occur, which will probably require a more sophisticated tuning procedure than shown here.

5.5.2 Conclusion

Traction - Damping of Rotary Converter Mode

The vehicle is found to destabilize the system in traction in all cases simulated, as the electromagnetical load torque of the rotary converter oscillates more than 90 ° out of phase with the speed oscillations. The vehicle power increases slightly at a lower voltage; this effect is amplified by a long line as higher power transfer at lower line voltage increases the line loss.

Speed oscillations of a rotary converter is a mechanical oscillation, which is influenced by the electromagnetic torque of the rotary converters generator. Reactive power is only indirectly coupled to electromagnetic torque, and can only in limited degree be used to stabilize speed oscillations of a rotary converter:

- Reactive power can be controlled to stabilize the voltage at the vehicle, reducing the real power oscillations at the vehicle in traction. This is however only reducing the destabilizing impact, not creating a stabilizing impact. When voltage magnitude is used as input for the reactive power controller, the observability of the oscillations is reduced. This limits the possible stabilizing effect of a reactive power controller.
- When operating at capacitive power factor to obtain minimum loss, the line loss cannot be modulated to damp speed oscillations of a rotary converter. This reduces the potential for stabilizing such an oscillation by reactive power.

No-load - Damping of Vehicle Mode

In no-load, the vehicle control system and its response to the line voltage is found to cause instability at long line lengths. Reactive power can be used to control the line voltage and thereby stabilize the system.

5.5.3 Further Work

Stability during regenerative braking is not investigated here. During regeneration, the vehicle is only allowed to operate at unity or inductive power factor to prevent an unacceptable voltage increase. This is not the operation giving minimum loss, and could thereby enable active damping through modulating the line loss by reactive power.

The control system structure and parameters of the vehicle in this thesis are copied from Danielsen. The structure and most of the parameters are considered as fixed, and not discussed here. Better performance could probably be achieved by tuning

parameters of the vehicle, together with the application of some kind of POD. Parameters should be tuned for stable operation over the entire operating range. A modification of the control structure could also be considered.

Stability analyses are in this thesis done on a system consisting of one vehicle and one rotary converter. To ensure stable operation in a real system, also more complex systems should be considered, consisting of several types of vehicles and static and rotary converters.

Chapter 6

Equivalent Admittance-based Dynamic Load Model

Assuming the manufacturer of a vehicle provided the input admittances as functions of frequency and the steady state characteristics of the vehicle, a simulation of small signal stability should be possible. This chapter describes the modelling of a dynamic load to be equivalent to the complete vehicle model, based on the operating point and the vehicle admittance seen from the power system. The dynamic behaviour of the equivalent model is compared to the behaviour of the complete model as found in chapter 5.

The equivalent load model will only be valid for the operating point (line voltage and vehicle power) at which the admittances are found.

The term "admittance-based" is used as the load model is defined by a response (a change of current) to a disturbance (change of voltage), and admittance is defined as current per voltage. The term "equivalent load model" is also used in this chapter as a shorter form of "equivalent admittance-based dynamic load model".

6.1 Modelling an Equivalent Admittance-based Dynamic Load

The input admittances as functions of frequency of the vehicle model are found, as described in section 5.2.2. The admittances are found for the operating points in table 5.1. The resulting admittances are shown in appendix C, figure C.2, C.4 and C.6. The admittances are found for the frequencies 0.01 Hz to 16 Hz. A load model is to be implemented in DSL (Dynamic Simulation Language), being equivalent to

the vehicle at the given operating point regarding small signals at frequencies well below the fundamental, 16 2/3 Hz.

6.1.1 Finding Transfer Function for Admittances

Curve Fitting by MatLab

The admittances of the equivalent load model are to be found on the form shown in equation 6.1, 6.2, 6.3 and 6.4. The factors $b_{1..}$, $b_{2..}$, $b_{3..}$ and $a_{1..}$, $a_{2..}$, $a_{3..}$ are found by the MatLab function `invfreqs`. The numerical values are shown in appendix D.1. The `invfreqs` function solves the direct problem of minimizing the weighted sum of the squared error between the actual and the desired frequency response points.

$$Y_{dd} = \frac{\Delta I_d(s)}{\Delta U_d(s)} = \frac{b_{1dd} \cdot s^2 + b_{2dd} \cdot s + b_{3dd}}{a_{1dd} \cdot s^2 + a_{2dd} \cdot s + a_{3dd}} \tag{6.1}$$

$$Y_{qd} = \frac{\Delta I_q(s)}{\Delta U_d(s)} = \frac{b_{1qd} \cdot s^2 + b_{2qd} \cdot s + b_{3qd}}{a_{1qd} \cdot s^2 + a_{2qd} \cdot s + a_{3qd}} \tag{6.2}$$

$$Y_{dq} = \frac{\Delta I_d(s)}{\Delta U_q(s)} = \frac{b_{1dq} \cdot s^2 + b_{2dq} \cdot s + b_{3dq}}{a_{1dq} \cdot s^2 + a_{2dq} \cdot s + a_{3dq}} \tag{6.3}$$

$$Y_{qq} = \frac{\Delta I_q(s)}{\Delta U_q(s)} = \frac{b_{1qq} \cdot s^2 + b_{2qq} \cdot s + b_{3qq}}{a_{1qq} \cdot s^2 + a_{2qq} \cdot s + a_{3qq}} \tag{6.4}$$

Frequency Weighting and Frequency Range

The admittances are found for frequency steps of 0.01 Hz (0.01 Hz, 0.02 Hz ... 16 Hz). As a change from 0.01 Hz to 0.02 Hz is relatively a far larger change than from 7.99 Hz to 8.00 Hz, the admittance for a given frequency is given a weight inversely proportional to its frequency, e.g. the weight at 0.02 Hz is set to 50 while the weight for 1 Hz is set to 1. The weight is used for minimizing the weighted sum of the squared error between the actual and the desired frequency response points. For the models of loaded vehicle starting curve fitting at 0.01 Hz, the weight for 0.01 Hz is set to 1000000, to obtain a correct steady state value.

As the voltages and currents in the power system are modelled as phasors with fundamental frequency 16 2/3 Hz, the model is not valid above the fundamental frequency. The model is expected not to be fully valid at frequencies slightly below the fundamental; in most cases are therefore only frequencies below 8 Hz considered. The only exception is done for unity power factor, loaded vehicle. In this case curve fitting from 0.01 to 8 Hz gave a model with an obviously incorrect response, while curve fitting from 0.01 to 16 Hz gave a response fairly close to the complete vehicle model.

To obtain better fit around the frequencies of interest (eigenvalues at 1-5 Hz), it is chosen to simulate a set of models where the bandwidth for curve fitting is reduced. It is chosen to run curve fitting from 0.5 Hz to 6 Hz. The admittance for a given frequency is given a weight inversely proportional to its frequency. No frequency is given weight of 1000000, as a steady state error is accepted for the bandwidth-reduced models. The frequency responses of the equivalent load models are shown together with the complete model responses in appendix D.2 and D.3.

Suppression of Erroneous Data

The admittances at some frequencies are found to be far from the admittances of neighbouring frequencies, forming "spikes" from an otherwise smooth curve. These spikes are assumed to be caused by numerical errors, and are given weight 0 when finding weighted least square error.

6.1.2 Implementation in SIMPOW

The load flow simulation (OPTPOW) is performed as for simulations with the complete vehicle model, as in chapter 5. When performing the dynamic simulation (DYNPOW), the dynamic vehicle model is replaced by an equivalent load model. The initial current $\bar{I}_0$ is taken from the OPTPOW (load flow) model of the vehicle, while the change of current $\Delta\bar{I}$ due to voltage change $\Delta\bar{U}$ is described by equations 6.1 to 6.4, see figure 6.1. The 3-phase grid, the rotary converter station and the overhead line is simulated by the same model as in chapter 5.

The equivalent load model is implemented as a load in SIMPOW written as a DSL-file. The source code can be found in appendix D.4.

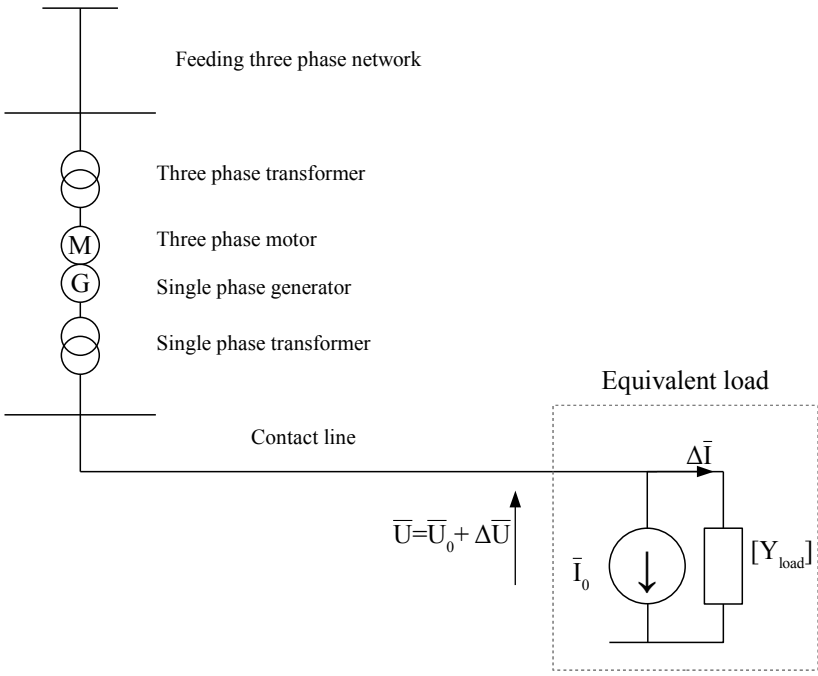

Figure 6.1: Circuit for simulation with the equivalent load model. The infrastructure model is the complete model used in this thesis, while the vehicle model is replaced by the equivalent load model. I_0 is found from load flow, while ΔI is controlled by the admittances described by equation 6.1 to 6.4.

6.2 Complete Model vs. Equivalent Load Model

6.2.1 Eigenvalue Considerations

The eigenvalues of the system are shown in figure 6.2 (unity power factor), figure 6.3 ("Minimum loss", static ϕ) and figure 6.4 ("Minimum loss", dynamic ϕ), comparing the eigenvalues found with the complete vehicle model to the equivalent load models. The four pairs of eigenvalues having the lowest damping are shown in table 6.1, 6.2 and 6.3.

The four pairs of eigenvalues having the lowest damping show similar results for the complete model and the equivalent load model, shown in table 6.3.

Both equivalent load models give eigenvalues relatively close to the complete vehicle model, though the bandwidth-reduced model (0.5-6 Hz) is in all cases clearly closer than the model based on curve fitting at 0.01-8 Hz or 0.01-16 Hz. The rotary converter mode at 1.6 Hz is the least damped mode, and will dominate the response in all cases. Particularly for unity power factor, there is a significant difference between the complete model and equivalent load model 0.01-16 Hz. The complete model has a real part of 0.06 1/s which gives a damping of -0.53 %, while the equivalent load model 0.01-16 Hz has a real part of 0.43, which gives a damping of -4.2 %.

Unity power factor

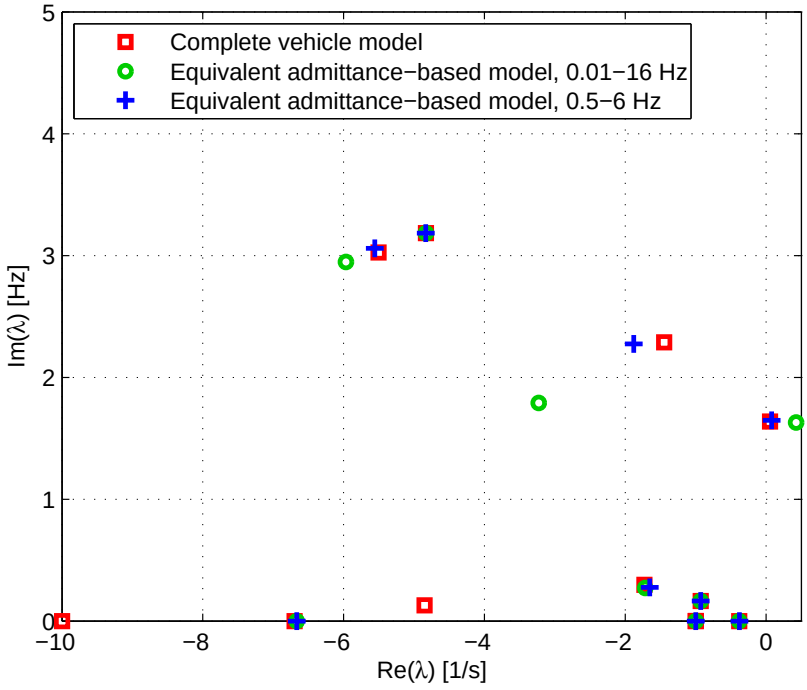

Figure 6.2: Eigenvalues with unity power factor for the complete model and the equivalent load models.

Table 6.1: Eigenvalues with unity power factor for the complete model and the equivalent load models. Eigenvalue numbers refer to the complete model, as in table B.1.

	Eigenvalue [1/s], [Hz]			
Eigenvalue number	Complete model	Equivalent load model 0.01-16 Hz	Equivalent load model 0.5-6 Hz	Main participant
17, 18	-5.49 ± j3.03	-5.92 ± j2.95	-5.55 ± j3.06	Vehicle
19, 20	-4.83 ± j3.19	-4.83 ± j3.19	-4.83 ± j3.19	Motor exciter
21, 22	-1.42 ± j2.28	-2.66 ± j1.72	-1.83 ± j2.26	Generator exciter
25, 26	0.06 ± j1.64	0.43 ± j1.63	0.078± j1.65	Rotary converter

"Minimum Loss", Static ϕ

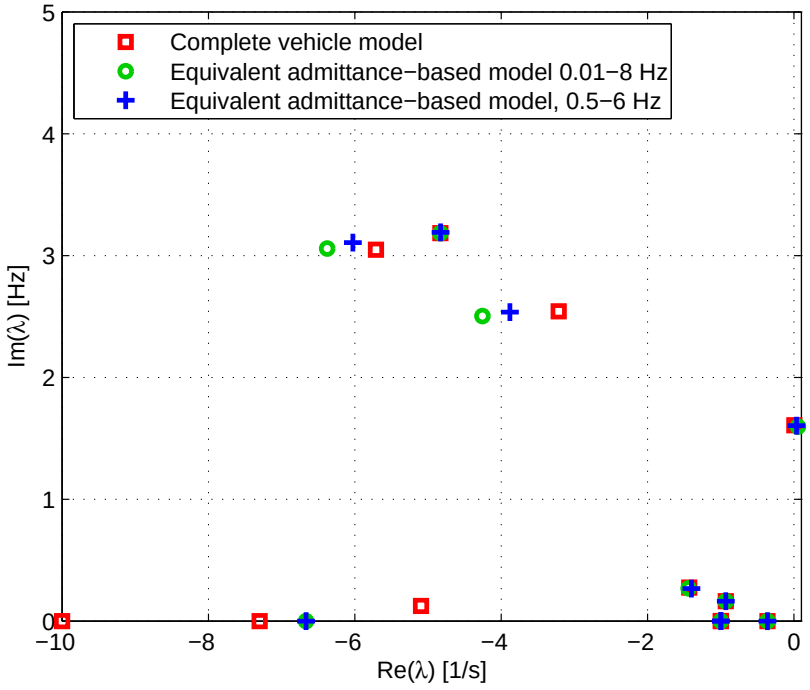

Figure 6.3: Eigenvalues with "minimum loss", static ϕ for the complete model and the equivalent load models.

Table 6.2: Eigenvalues with "minimum loss", static ϕ for the complete model and the equivalent load models. Eigenvalue numbers refer to the complete model, as in table B.2.

	Eigenvalue [1/s], [Hz]			
Eigenvalue number	Complete model	Equivalent load model 0.01-8 Hz	Equivalent load model 0.5-6 Hz	Main participant
17, 18	-5.72 ± j3.05	-6.40 ± j3.05	-6.03 ± j3.11	Vehicle
19, 20	-4.83 ± j3.18	-4.83 ± j3.19	-4.83 ± j3.19	Motor exciter
21, 22	-3.21 ± j2.54	-4.38 ± j2.48	-3.88 ± j2.54	Generator exciter
25, 26	0.003 ± j1.61	0.053 ± j1.59	0.003 ± j1.60	Rotary converter

"Minimum Loss", Dynamic ϕ

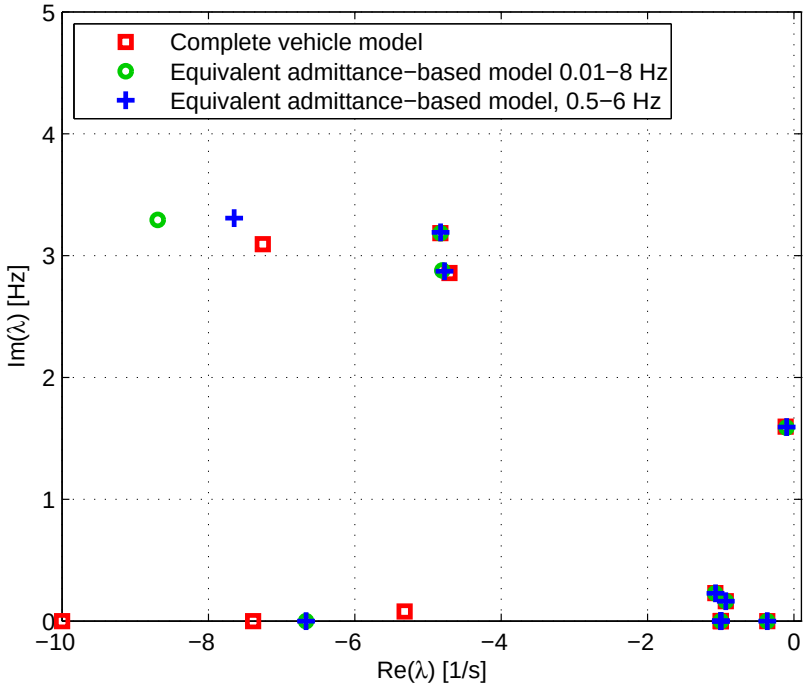

Figure 6.4: Eigenvalues with "minimum loss", dynamic ϕ for the complete model and the equivalent load models.

Table 6.3: Eigenvalues with "minimum loss", dynamic ϕ for the complete model and the equivalent load models. Eigenvalue numbers refer to the complete model, as in table B.3.

	Eigenvalue [1/s], [Hz]			
Eigenvalue number	Complete model	Equivalent load model 0.01-8 Hz	Equivalent load model 0.5-6 Hz	Main participant
17, 18	-7.34 ± j3.10	-8.69 ± j3.29	-7.65 ± j3.31	Vehicle
19, 20	-4.83 ± j3.19	-4.83 ± j3.18	-4.83 ± j3.19	Motor exciter
21, 22	-4.75 ± j2.85	-4.80 ± j2.88	-4.78 ± j2.87	Generator exciter
25, 26	-0.11 ± j1.60	-0.10 ± j1.59	-0.10 ± j1.59	Rotary converter

6.2.2 Time Domain Results

With "minimum loss", dynamic ϕ, the three least damped eigenvalues are very similar for the the equivalent load models and the full vehicle model. A time domain simulation is performed to compare their response to a disturbance.

The system is excited with the same disturbance as in section 5.3.4, a 100 kW load

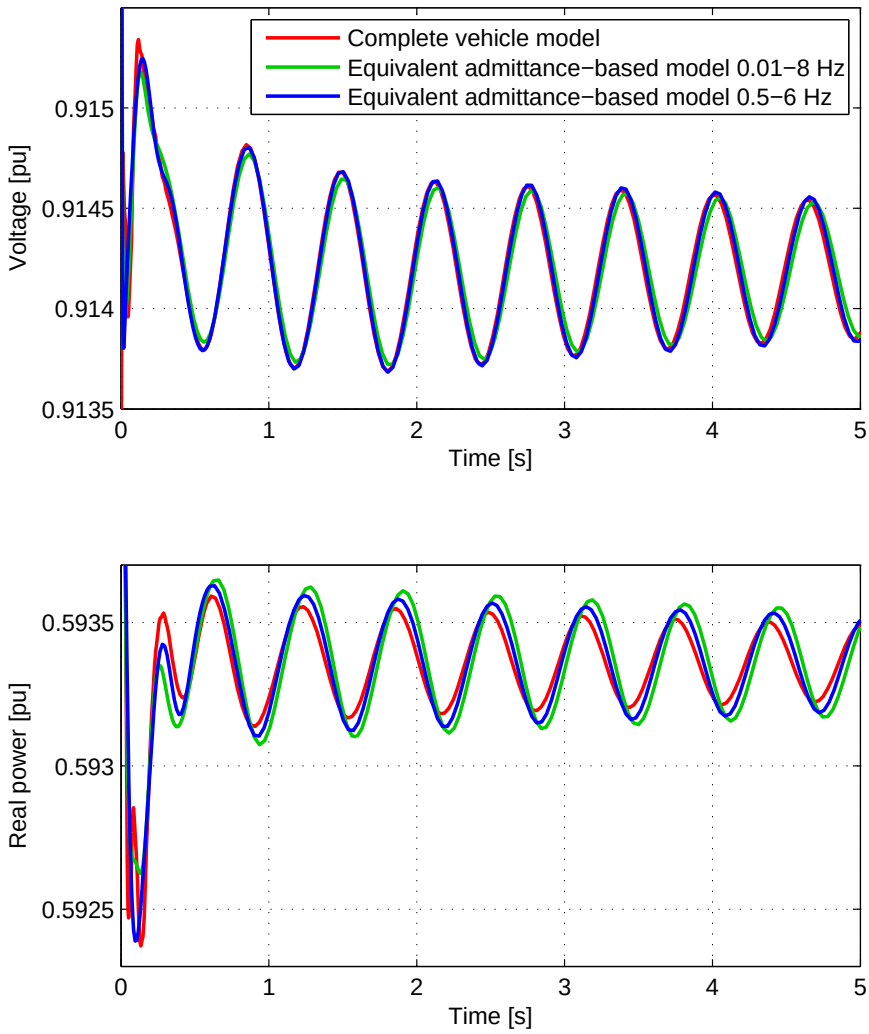

Figure 6.5: Voltage and real power at the vehicle, with "minimum loss", dynamic ϕ for the complete model and the equivalent load models.

is connected at the rotary converter 16.5 kV bus at t=-0.1 s, and disconnected at t=0 s. The resulting voltage and real power at the vehicle's current collector are shown in figure 6.5, together with the corresponding data from the simulation using the complete vehicle model.

The deviation between the models are most easily observed in the real power consumed by the vehicle, particularly in the first second. The equivalent admittance based model 0.5-6 Hz follows the complete vehicle model closely at the first oscillation down to 0.5924 pu, while the equivalent load model 0.01-8 Hz has a minimum value 0.5927 pu.

6.3 Long Line Stability Test - No-Load

The long line stability test is performed in no-load, i.e. the vehicle motor current $i_{dcm} = 0$ to avoid a voltage collapse due to a high voltage drop. Depending on the control structure of the vehicle, the input admittance will in most cases depend on the operating point of the vehicle (power and line voltage). When operating the vehicle in no-load, the operating point and thereby the input admittance is independent of the line length. In order to simplify finding the stability limit from the load admittance and source impedance, the vehicle is supplied by a stiff voltage source of 16.5 kV and a line with $(0.19 + j0.21)\Omega/km$.

The different control schemes for reactive power described in section 3.2.1 and [5] all give unity power factor at 16.5 kV, and the choice of control scheme will have no effect. Therefore, only the scheme for unity power factor is used in no-load.

6.3.1 Stability Limit by Simulation, Complete Model and Equivalent Load Models

The admittances of the vehicle in no-load are found as described in section 5.2.2, shown in figure C.8. Equivalent load models are made, based on curve fitting at 0.01-8 Hz and 0.5-6 Hz. The admittances of the equivalent load models and the complete vehicle model are shown in figure D.7 and D.8.

The eigenvalues for the complete vehicle model and and the equivalent load models are shown in figure 6.6, for 200 km line length. The eigenvalues that are closest to cause instability are eigenvalues 9,10, -1.63 1/s ± j4.51 Hz in the complete vehicle model. For the equivalent load model, 0.5-6 Hz, two extra pairs of eigenvalues appear at about -5.5 1/s ± j4.8 Hz.

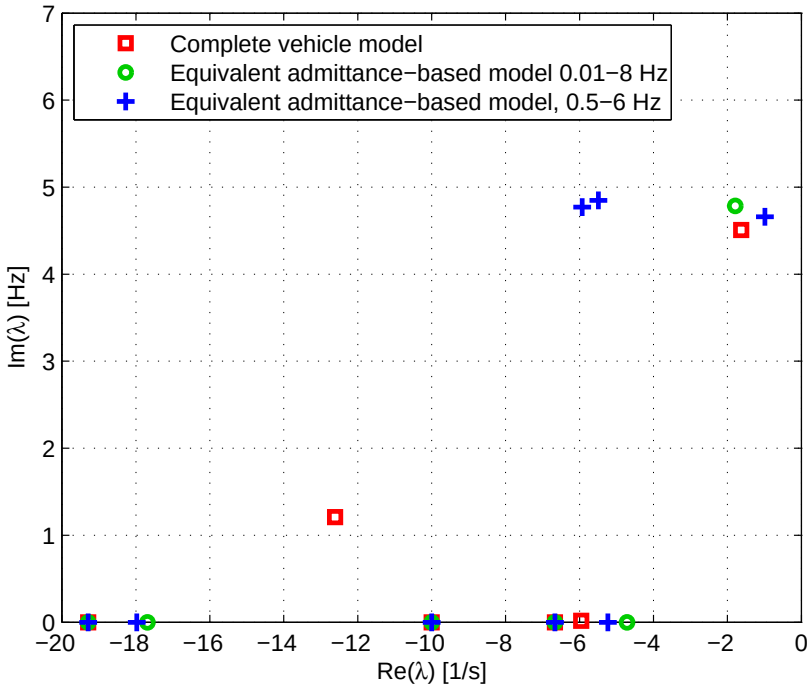

Figure 6.6: Eigenvalues for the complete vehicle model and equivalent load models, found for frequencies 0.01-8 Hz and 0.5-6 Hz. The eigenvalues are found for 200 km line length at no-load.

A data scanning of the eigenvalues 9,10 for the line length is performed for both the complete model and the equivalent load models, shown in figure 6.7. The stability limit and the oscillation frequencies are shown in table 6.4. Both equivalent load models indicate a stability limit 6-7 km different from the complete model, and an oscillation frequency about 0.2 Hz higher.

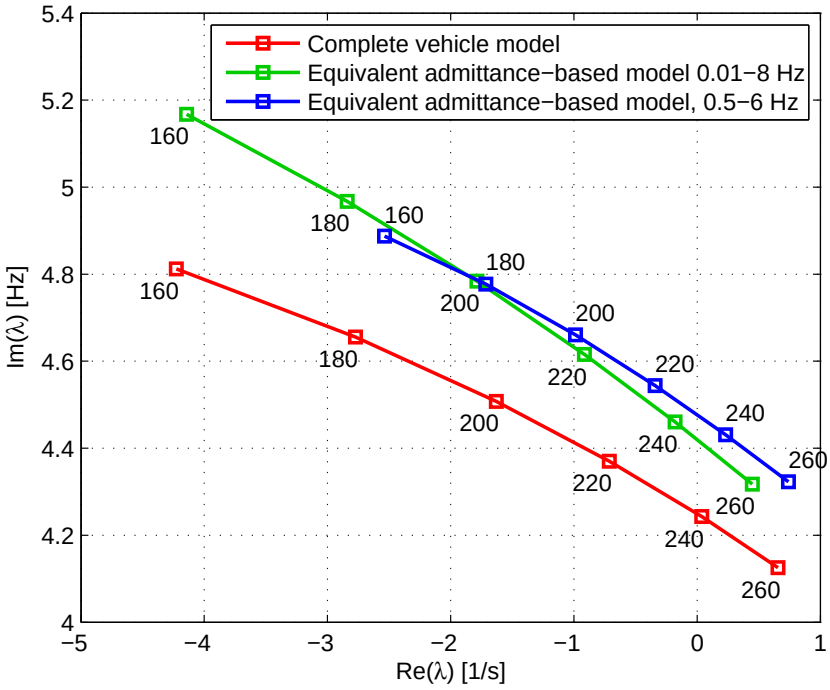

Figure 6.7: Data scanning for line length of the dominant eigenvalue for the complete vehicle model and equivalent load models, found for frequencies 0.01-8 Hz and 0.5-6 Hz.

Table 6.4: The stability limit for the complete vehicle model and equivalent load models.

Model	Stability limit [km]	Oscillation frequency [Hz]
Complete vehicle model	239	4.25
Equivalent load model, 0.01-8 Hz	245	4.42
Equivalent load model, 0.5-6 Hz	232	4.48

6.3.2 Stability Limit from Impedance-based Modelling

The source impedance, which consist of only line impedance, and the load admittance are found for 200 km line length, shown in figure C.7 and C.8. The Nyquist contour (N-1), equation 5.17, is found for line lengths from 200 to 300 km. When calculating N-1, the load admittance is constant, while the source impedance found in the simulation for 200 km is increased proportionally with the line length. The

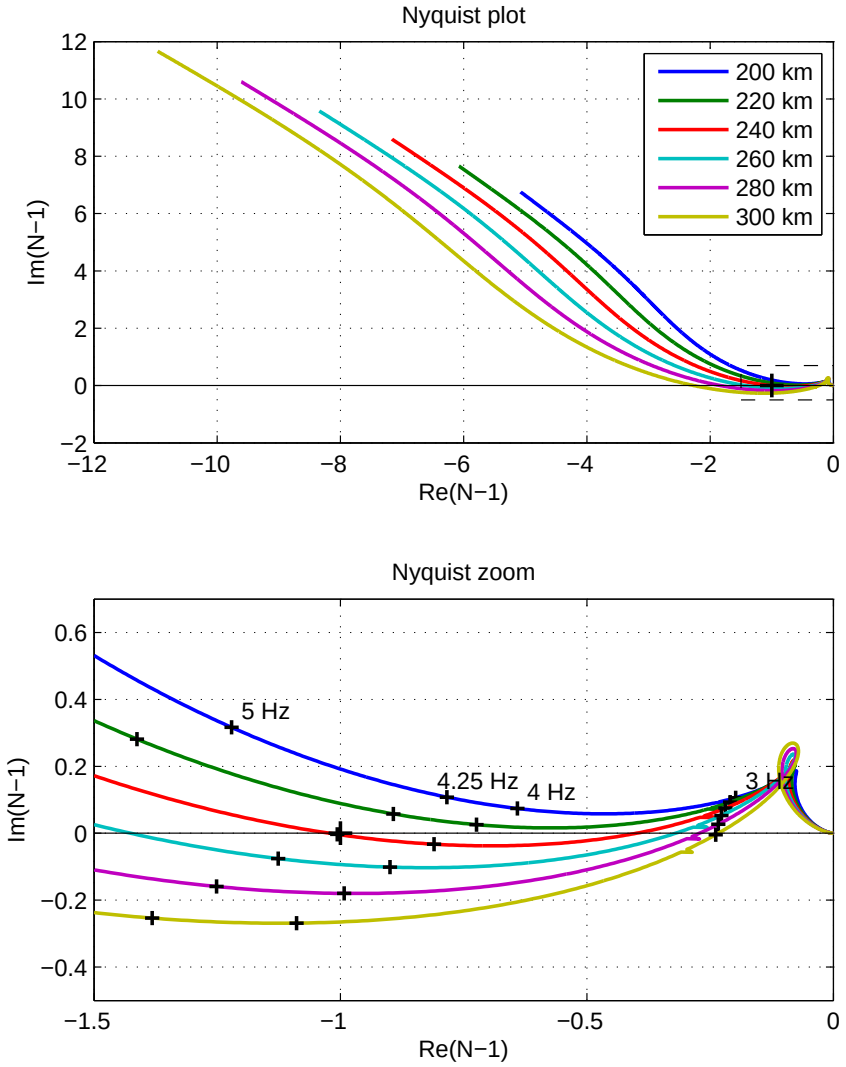

Figure 6.8: Nyquist plot for line lengths from 200 to 300 km.

Nyquist contours are shown in figure 6.8. The curves for 200 and 220 km do not encircle (-1+j0) (stable system), while the curves for 240 km and above do (unstable system). The curve for 239 km is not shown here but this would pass through (-1+j0) indicating a a marginally stable system at 239 km, the stability limit. The marker for 240 km, 4.25 Hz is located very close to (-1+j0). This method for finding the stability limit is further described and investigated in [11].

6.4 Discussion and Conclusion

6.4.1 Discussion

Equivalent Admittance-Based Dynamic Load Models vs. Complete Vehicle Model

The four least damped pairs of eigenvalues were found to be relatively similar with the equivalent admittance-based dynamic load models (also called "equivalent load model") compared to the complete vehicle model. One of these modes, 19,20, is mainly caused by the exciter of the rotary converter motor, and is earlier found very little affected by reactive power characteristics. Keeping this mode unchanged gives thereby little information regarding the vehicle behaviour. The two other modes are found two be clearly affected by the reactive power settings; that these modes are nearly unchanged indicate that the equivalent load model behaves similar to the complete vehicle model.

The time domain simulations also show similar behaviour between the complete model and the equivalent load models.

In all cases with loaded vehicle, the bandwidth-reduced models (0.5-6 Hz) have smaller deviation from the complete model than the models based on curve fitting at 0.01-8 Hz or 0.01-16 Hz. For the long line stability test, performed in no-load, the two equivalent load models have about the same magnitude of deviation from the complete vehicle model.

Finding Stability Limit Directly from Load Admittance

The stability limit is found by the Nyquist contour from $[Y_{load}]$ and $[Z_{source}]$ to 239 km, the same value as found by scanning of eigenvalues. Also the oscillation frequency is close to the value from eigenvalue scanning, 4.25 Hz.

6.4.2 Conclusion

Equivalent load models can be made from the steady state characteristics of the vehicle, determining the operating point; and the admittance for the operating point of interest, describing the dynamic behaviour. The equivalent load model is an approximation, and does not behave exactly like the original vehicle. Curve fitting only in the frequency range where oscillations are expected to occur gives a dynamic response which is more similar to the original vehicle than a model based on curve fitting over a larger range. This is, however, assumed to reduce the accuracy outside this frequency range, e.g. steady state characteristics.

To find whether a system is stable or not, finding the Nyquist contour from the original admittance gives higher accuracy than a simulation the equivalent load model, as the equivalent load model represents an approximation. On the other hand, the Nyquist plot gives less information about damping and details about dynamic behaviour than a simulation of the equivalent load model, finding eigenvalues and time response.

6.4.3 Further Work

The equivalent load model is an approximation. Assuming a complete vehicle model is not available, only the admittance as function of frequency, a deeper understanding of the equivalent load modelling would be of interest in order to determine and improve the accuracy of this approximation. Improving the accuracy is assumed to include higher order transfer functions and modified weighting of frequencies.

The equivalent load model is only valid at a specified operating point, i.e. line voltage and vehicle power. By finding the admittances for several operating points, it should be possible to make an equivalent load model for any point within this range by interpolation.

Chapter 7

Conclusion

This thesis investigates the settings for reactive power during traction proposed in the project done by the author fall 2010. In a system fed by rotary converters, the settings are found to give a reduction of converter station loading and total loss of a few percent in the best case, no significant change in the worst case.

The effect of reactive power on the system stability is investigate. During traction, the challenging issue regarding stability is speed oscillations of the rotary converter. Controlling reactive power, both through the steady state characteristics (passive control) and through a power oscillation damper (POD) has a limited effect on these oscillations. In no-load, the challenging issue regarding stability is oscillations caused by the vehicle control system and its response to the line voltage. In this case, the steady state characteristics have no effect, but the POD improves damping and stability limit significantly.

For simulation of a real vehicle, a complete simulation model of the vehicle and its control system might not be available. In such a case, an equivalent load model can be made, based on the steady state characteristics and the input admittance of the vehicle.

7.1 Loadflow - Capacity and Losses

In traffic simulation, the "minimum loss" settings reduced the converter losses at the highest loaded converter station by 1.5 - 2.4 % compared to unity power factor. The highest current occurring is reduced by 0-3 %.

The total losses are reduced by 0.33 % with constant voltage characteristics, and 0.21 % with 8 % decreasing characteristics, when changing from unity power factor

to "minimum loss" settings of the load.

7.2 Stability

7.2.1 Rotary Converter Speed Oscillations in Traction

Speed oscillations of a rotary converter can only to a limited extent be influenced by controlling reactive power at the vehicle.

Danielsen implemented and tested power oscillation dampers (PODs) acting on either real or reactive power. In this thesis only PODs acting on reactive power is used. PODs acting on real power damp rotary converter speed oscillations clearly better than PODs acting on reactive power.

The vehicle may be operated at capacitive power factor keeping the line loss at a minimum, but this mode of operation reduces the stabilizing effect of controlling reactive power. When the line loss is already at a minimum, it cannot be modulated to damp oscillations by controlling reactive power.

7.2.2 Oscillations from Vehicle Control System in No-load

In no-load, the vehicle control system and its response to the line voltage is found to cause instability at long line lengths. Reactive power can be used to control the line voltage and thereby stabilize the system.

7.3 Equivalent Load Modelling

An equivalent admittance-based load model can be made from the steady state characteristics of the vehicle, determining the operating point; and the admittance for the operating point of interest, describing the dynamic behaviour. The equivalent admittance-based load model is an approximation, and does not behave exactly like the original vehicle. Curve fitting only in the frequency range where oscillations are expected to occur gives a dynamic response which is more similar to the original vehicle than a model based on curve fitting over a larger range. This is, however, assumed to reduce the accuracy outside this frequency range, e.g. steady state characteristics.

To find whether a system is stable or not, finding the Nyquist contour from the original admittance gives higher accuracy than a simulation with the equivalent admittance-based load model, as the equivalent admittance-based load model represents an approximation. On the other hand, the Nyquist plot gives less informa-

tion about damping and details about dynamic behaviour than a simulation of the equivalent load model, finding eigenvalues and time response.

7.4 Further Work

The settings for reactive power proposed in the fall project are calculated for a system fed by one or more stiff voltage sources with the same voltage angle and magnitude. A real optimization of the system should be a lot more complex, as it should consider both reactive power control at the vehicles and settings of the automatic voltage regulators at the converter stations in a system consisting of several vehicles and converter stations.

Stability is not analysed during regenerative braking. Capacitive power factor is not allowed during regeneration, meaning that the transmission line will not be operated at minimum loss. As loss is not at its minimum, it will vary with the power factor of the vehicle, and reactive power may be used for modulating the line loss to damp oscillations.

The settings for power factor during regenerative braking described in section 3.2.2 include ramps where the power factor should be changed as a function of voltage. It would be of interest how such ramps affect stability, and if there is a maximum slope of the ramps to ensure stability is not violated.

Equivalent load models may be modelled from the vehicle steady state characteristics and input admittance. Such a load model may be used in a time domain simulation or eigenvalue calculation, without revealing the inner workings of the vehicle and its control system. It would be of interest to improve the accuracy of the equivalent admittance-based load modelling, and to estimate the accuracy of such a model assuming the complete model is not available for comparison.

References

[1] Steimel, A. (2008). *Electric Traction - Motive Power and Energy Supply, Basics and Practical Experience*. Oldenbourg Industriverlag, Munich.

[2] The Swedish Rail Administration/The Norwegian National Rail Administration (2007). *Requirements on rolling stock in Norway and Sweden regarding EMC with the electrical infrastructure and coordination with the power supply and other vehicles (BVS 543.19300/JD 590)*. Retrieved 18 August 2010 from http://www.jernbaneverket.no/Documents/Marked/Infrastrukturens%20egenskaper/590/Vedlegg/T9004d00.pdf

[3] Danielsen, S (April 2010). *Electric Traction Power System Stability - Low-frequency interaction between advanced rail vehicles and a rotary frequency converter*, (Doctoral theses No. 2010:56, NTNU), NTNU Norwegian University of Science and Technology, Trondheim, Norway.

[4] Biedermann, N. (January 2010). *Criteria for the voltage in railway power supply systems*, (Thesis No. XR-EE-EME 2010:002, KTH, 2010) KTH Royal Institute of Technology, Stockholm, Sweden. Retrieved 9 September 2010 from https://eeweb01.ee.kth.se/upload/publications/reports/2010/XR-EE-EME_2010_002.pdf

[5] Toreid, E. (November 2010). *Active Control of Reactive Power in a Modern Electrical Rail Vehicle*, (Special study). School of Environment, Resources and Development, Asian Institute of Technology, Thailand.

[6] Performance description ... (Restricted). Document number 3EGM015763D0045.

[7] CENELEC. (November 2004). *European standard EN50163 - Railway Applications - Supply voltages of traction systems.*

[8] CENELEC. (August 2005). *European standard EN50388 - Railway applications - Power supply and rolling stock - Technical Criteria for the coordination between power supply (substation) and rolling stock to achieve interoperability.*

[9] Martinsen, F. (October 2009). *Spenningsregulatorinnstilling i roterende omformerstasjoner* (Settings of Voltage Regulators in Rotary Converter Stations). The Norwegian National Rail Administration, Oslo, Norway.

[10] Danielsen, S. (13 September 2010) *Impedance-based study of low-frequency interaction between a rotary converter and an electric vehicle.* The Norwegian National Rail Administration, Oslo, Norway.

[11] Pika, S. (August 2010) *Understanding of the Stability Criterion for a Double-Feedback Loop System*, Master thesis, Narvik University College, Narvik, Norway.

[12] Skogestad, S. and Postlethwaite, I. (2005) *Multivariable Feedback Control - Analysis and Design* John Wiley & Sons Ltd, West Sussex, England.

[13] Stensby, Ø. (14 January 2011) Email: "SV: Magnetiseringstap omformer" ("RE: Excitation losses converter")

[14] IEEE Std 421.5 - 2005 IEEE Recommended Practice for Excitation System Models for Power System Stability Studies, *IEEE Std 421.5-2005 (Revision of IEEE Std 421.5-1992).* pp. 0_1-85, 2006.

Appendix A

Simulation Model Parameters

A.1 Train Model Parameters for Traffic Simulation

Table A.1: Train data used in simulation. Locomotive data from [6].

Parameter	Unit	Value
Train mass	t	1000
Dynamic mass[1]	t	1054.2
Total length	m	500
A[2]	kN	12.07
B[2]	kN/(km/h)	$7.722 \cdot 10^{-2}$
C[2]	kN/(km/h)^2	$3.735 \cdot 10^{-3}$
Locomotive mass (adhesion mass)	t	84
Rated mechanical power	MW	5.6
Rated electrical power for traction	MW	6.364
Efficiency[3] (lower at speed below 40 km/h)	1	0.88
Auxillary electrical power and no-load losses	kW	123.5
Max tractive effort	kN	300
Max electric braking effort	kN	240

[1] Dynamic mass is locomotive mass · 1.1 + cars' mass · 1.05.

[2] A, B and C are constants describing the train's driving resistance, $F_R = A + B \cdot v + C \cdot v^2$. F_R is driving resistance in kN, v is speed in km/h.

[3] Efficiency does not include auxiliary power

A.2 Power System Topology and Parameters

The dynamic simulation model is with a few exceptions the same model and parameters as used by Danielsen [3].

A transportable synchronous-synchronous rotary frequency converter type ASEA Q38, having a rated power of 4 MVA, is feeding a single-track railway and one single rail vehicle. A single-line diagram in figure A.1 shows the steady-state power flow for the reference case without reactive power control. The rotary converter

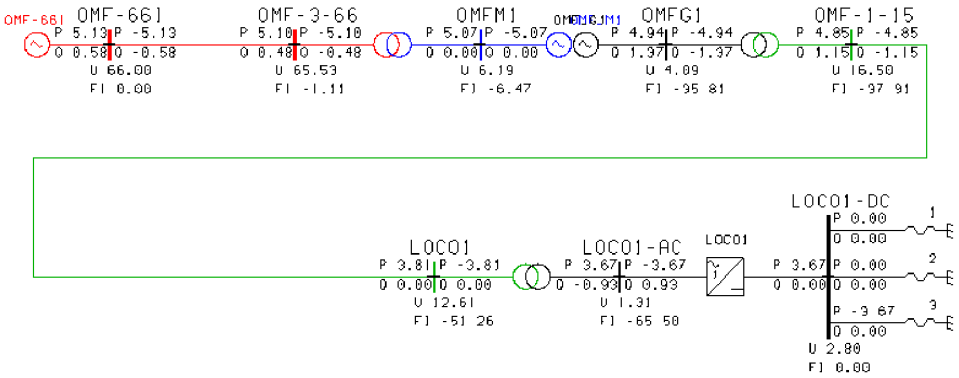

Figure A.1: Power system topology. The power flow shown is for the vehicle operating at unity power factor.

is fed from a 66 kV 3-phase grid, having a short circuit power of 250 MVA at the transformer upside, which are typical values in the Norwegian electrical traction power system [2]. The 3-phase grid is assumed to have a Z/R ratio of 4. Both the motor and generator include exciters and automatic voltage controllers (AVR). The motor excitation adjusted so the reactive power at its terminal equals zero, which gives the reference voltage for the AVR. Furthermore, if necessary (here it was not) the three-phase transformer tap-changer may be adjusted (in increments of 300 V) in order to keep the motor voltage as close as possible to 6.3 kV. The line voltage at the single-phase transformer 15-kV side is controlled to be 16.5 kV with a zero load-depending slope by use of the AVR. Data for the converter, the transformers and the regulators are given in appendix A.3.

Between the rotary converter and the rail vehicle, there is 60 km of overhead contact line. This length was chosen since it is the length of line for which a vehicle is required to operate stably in order to be accepted for operation in Norway and Sweden [2]. The line impedance is $(0.19 + j0.21)\Omega/km$.

The rail vehicle is based on exercise 17.8 by Steimel [1] and is further introduced and explained by Danielsen in [3]. It represents a 6.4 MW universal locomotive measured on wheel. This results in an electrical rating of 7.35 MW. The vehicle

is operated on half of the rated power, i.e., 3.67 MW. The power and voltage at the vehicle's current collector vary slightly between the simulation cases, as the vehicle's transformer loss and the line's voltage drop depend on the vehicle's settings for reactive power. Further details about the vehicle are shown in appendix A.4.

A.3 Rotary Converter Parameters

A.3.1 Synchronous Machines

The rotary converter synchronous-machine parameters used in this thesis are given in Table A.2. They have all been received from the former manufacturer of these machines, but the following changes, as described by Danielsen [3], apply:

- The inertia constant is increased by 5 % to take the exciters into account.
- The motor q-axis sub-transient reactance is increased by 42 % in order to adapt to the poor damping observed in reality.

Table A.2: Rotary converter synchronous machine parameters.

	Parameter	Unit	Motor	Generator
S_N	Rated power	MVA	4.4	4.0
U_N	Rated voltage	kV	6.3	4.0
X_a	Stator leakage reactance	pu	0.11	0.096
R_a	Stator resistance	pu	0.0033	0.00175
X_d	D-axis synchronous reactance	pu	0.90	1.02
X'_d	D-axis transient reactance	pu	0.24	0.12
X''_d	D-axis sub-transient reactance	pu	0.165	0.10
X_q	Q-axis synchronous reactance	pu	0.40	0.47
X'_q	Q-axis transient reactance	pu	0.40	0.47
X''_q	Q-axis sub-transient reactance	pu	0.34	0.11
T'_{d0}	D-axis transient time constant	s	4.0	8.6
T''_{d0}	D-axis sub-transient time constant	s	0.04	0.08
T''_{q0}	Q-axis sub-transient time constant	s	0.10	3.4
H	Inertia constant	MWs/MVA	1.70	1.87
R_F	Field winding resistance[1]	Ω	0.345	0.208
I_{F0}	No-load field current[1] (= 1 pu)	A	110	148

The reactances are unsaturated and saturation in is not included in the model. The converter was originally designed for a continuous power of 4.0 MVA, but it

[1] From [13].

is later found to be dimesioned sufficiently for a continuous power of 5.8 MVA [9]. Generator data are given for a pu base power of 4.0 MVA.

A.3.2 Transformers

The parameters for the transformers connecting the rotary converter to the respective grids used in this thesis are given in Table A.3. The data are found in test protocols.

Table A.3: Rotary-converter transformer parameters.

	Parameter	Unit	Motor	Generator
S_N	Rated power	MVA	4.4	4.0
U_{N1}	Rated voltage first winding	kV	66	4.0
U_{N2}	Rated voltage second winding	kV	6.3	16.6
ER_{12}	Short-circuit resistance	pu	0.0054	0.014
EX_{12}	Short-circuit reactance	pu	0.079	0.034

A.3.3 Automatic Voltage Regulator Parameters

The parameters for the exciters and ASEA YGUA automatic voltage regulators used in this thesis are given in Table A.4. The standard excitation system model IEEE Type DC1A 'Excitation system with DC commutator exciter' [14] is used. The background for the different parameter values are:

- T_R is assumed to be half of the rectifier diode-bridge switching frequency equal to a quarter of a fundamental period.
- K_A is calculated by Stensby based on measurements from Landström.
- T_A and T_F are measured in Landström.
- K_E is according to Högberg, zero due to rheostat adjustment.
- T_E, VR_{MIN} and VR_{MAX} are found for the motor exciter by Stensby. Similar measurements and calculations are performed for generator exciter.
- K_F is assumed to be equal to typical values as given by Andersson and Fouad.

Table A.4: Automatic voltage regulator parameters

	Parameter	Unit	Motor	Generator
T_R	Regulator input filter time constant	s	0.005	0.015
K_A	Regulator amplifier gain	pu	382	382
T_A	Regulator amplifier time constant	s	0.11	0.11
K_E	Exciter constant related to self-excited field	pu	0.0	0.0
T_E	Exciter time constant	s	0.46	0.53
K_F	Regulator stabiliser circuit gain	pu	0.04	0.04
T_F	Regulator stabiliser circuit time constant	s	0.7	0.7
VR_{MIN}	Min value of regulator output	pu	-2.9	-3.5
VR_{MAX}	Max value of regulator output	pu	2.9	3.5

No current (power) dependent voltage charateristic is used by Danielsen ($R_C = X_C = 0$ %), and this characteristic are used in the stability section of this thesis. In the load sharing section, there are used both a constant voltage characteristic ($R_C = X_C = 0$ %), and a characteristic with decreasing voltage for reactive power ($R_C = 0$, $X_C = 8$ %, with 16.5 kV, 5.8 MVA as pu base).

A.4 Vehicle Model Parameters

A.4.1 Electrical Component Values

The vehicle's nominal power is 6.4 MW measured on wheel, which is used as the base power for the per unit system. Taking losses and 5 % overload into account as shown by Steimel [1], the rated power is 7.35 MVA. The line-side converter's switching frequency is 250 Hz.

The vehicle transformer and DC-link parameters are listed in Table A.5 and Table A.6, respectively.

Table A.5: Vehicle transformer parameters.

	Parameter	Unit	Value
S_N	Rated power	MVA	7.35
U_{N1}	Rated voltage first winding	kV	15
U_{N2}	Rated voltage second winding	kV	1.568
ER_{12}	Short-circuit resistance	pu	0.05
EX_{12}	Short-circuit reactance	pu	0.333

Table A.6: Vehicle DC-link parameters.

Parameter		Unit	Value
U_{dcN}	Rated voltage	kV	2.8
C_d	DC-link capacitor	mF	24.4
C_2	Second-harmonic filter capacitor	mF	16.52
L_2	Second-harmonic filter inductor	mH	1.375
R_2	Second-harmonic filter resistor	mΩ	30

A.4.2 Control System Parameters

The vehicle control-system parameters used in the original model in this thesis are listed in Table A.7. The per unit values are related to $S_{Base} = 6.4$ MW and the transformer secondary side voltage $U_{Base} = 1.568$ kV.

Table A.7: Vehicle control system parameters.

Parameter		Unit	Value
Ku_{SOGI}	Voltage measurement SOGI gain	pu	0.8
Ki_{SOGI}	Current measurement SOGI gain	pu	3
Kp_{PLL}	Phase-locked loop gain	pu	51
Ti_{PLL}	Phase-locked loop integration time	s	0.079
Kp_{VC}	DC-link voltage controller gain	pu	1.67
Ti_{VC}	DC-link voltage controller integration time	s	0.06
Kp_{CC}	AC current controller gain	pu	0.87
Ti_{CC}	AC current controller integration time	s	180
Tu_{DC}	DC-link voltage measurement filter bandwidth	Hz	100
Ti_{DC}	Motor current measurement filter bandwidth	Hz	100
Tf_{CPL}	Motor damping filter time constant	s	0.15

Appendix B

Eigenvalue Tables

Table B.1: Eigenvalues for unity power factor

No.	Eigenvalue [1/s], [Hz]	Damping [%]	Main participation	
13, 14	-21.01 ± 6.15	47.7	Vehicle AC voltage measurement	0.25
			Vehicle AC voltage measurement	0.51
			Vehicle PLL angle	0.52
			Vehicle PLL loop filter	0.17
			Vehicle voltage controller	0.10
			Vehicle AC current measurement	0.12
17, 18	-5.49 ± 3.03	27.7	Vehicle voltage controller	0.13
			Generator exciter field voltage	0.72
19, 20	-4.83 ± 3.19	23.4	Motor exciter field voltage	0.98
21, 22	-1.42 ± 2.28	9.9	Vehicle DC-link	0.16
			Vehicle DC-link	0.11
			Vehicle DC-link	0.13
			Generator d-axis damper winding flux	0.10
			Generator field winding flux	0.10
			Vehicle AC voltage measurement	0.38
			Vehicle voltage controller	0.44
			Vehicle d-axis current controller	0.11
			Generator exciter field voltage	0.16
25, 26	0.06 ± 1.64	-0.5	Motor power angle	0.52
			Motor speed	0.27
			Generator speed	0.27
29, 30	-4.56 ± 0.11	99.0	Vehicle DC-link	0.23
			Vehicle AC voltage measurement	0.10
			Vehicle AC voltage measurement	0.15
			Vehicle voltage controller	0.11
			Vehicle d-axis current controller	0.43
			Vehicle q-axis current controller	0.61
31, 32	-1.42 ± 0.35	53.8	Generator d-axis damper winding flux	0.28
			Generator speed	0.17
			Generator field winding flux	0.59
			Generator exciter field voltage	0.66
33, 34	-0.93 ± 0.16	66.9	Motor field winding flux	0.70
			Motor exciter regulator voltage	0.69

Table B.2: Eigenvalues for "minimum loss", static ϕ

No.	Eigenvalue [1/s], [Hz]	Damping [%]	Main participation	
13, 14	-25.49 ± 6.37	53.7	Vehicle AC voltage measurement	0.33
			Vehicle AC voltage measurement	0.47
			Vehicle PLL angle	0.49
			Vehicle PLL loop filter	0.15
			Vehicle AC current measurement	0.13
17, 18	-5.72 ± 3.05	28.6	Vehicle AC voltage measurement	0.12
			Vehicle voltage controller	0.20
			Generator exciter field voltage	0.53
19, 20	-4.83 ± 3.18	23.5	Motor exciter field voltage	0.98
21, 22	-3.21 ± 2.54	19.7	Vehicle DC-link	0.16
			Vehicle DC-link	0.11
			Vehicle DC-link	0.10
			Vehicle AC voltage measurement	0.27
			Vehicle PLL angle	0.10
			Vehicle voltage controller	0.40
			Generator exciter field voltage	0.26
25, 26	3.10E-003 ± 1.61	0.0	Motor power angle	0.50
			Motor speed	0.25
			Generator speed	0.25
29, 30	-4.82 ± 0.13	98.6	Vehicle DC-link	0.21
			Vehicle AC voltage measurement	0.11
			Vehicle d-axis current controller	0.40
			Vehicle q-axis current controller	0.45
31, 32	-1.25 ± 0.31	54.6	Generator d-axis damper winding flux	0.25
			Generator speed	0.10
			Generator field winding flux	0.56
			Generator exciter field voltage	0.68
33, 34	-0.93 ± 0.16	67.2	Motor field winding flux	0.70
			Motor exciter regulator voltage	0.70

Table B.3: Eigenvalues for "minimum loss", dynamic ϕ

No.	Eigenvalue [1/s], [Hz]	Damping [%]	Main participation	
12, 13	-25.95 ± 9.13	41.2	Overhead line	
			Vehicle transformer	0.13
			Vehicle AC voltage measurement	0.55
			Vehicle AC voltage measurement	0.38
			Vehicle PLL angle	0.27
			Vehicle AC current measurement	0.27
			Vehicle AC current measurement	0.13
17, 18	-7.34 ± 3.10	35.3	Vehicle DC-link	0.21
			Vehicle DC-link	0.14
			Vehicle AC voltage measurement	0.18
			Vehicle PLL angle	0.18
			Vehicle PLL loop filter	0.11
			Vehicle voltage controller	0.43
			Vehicle AC current measurement	0.10
19, 20	-4.83 ± 3.19	23.4	Motor exciter field voltage	0.98
21, 22	-4.75 ± 2.85	25.6	Vehicle voltage controller	0.13
			Generator exciter field voltage	0.86
25, 26	-0.11 ± 1.60	1.1	Motor power angle	0.51
			Motor speed	0.25
			Generator speed	0.25
29, 30	-5.16 ± 0.10	99.2	Vehicle DC-link	0.19
			Vehicle d-axis current controller	0.40
			Vehicle q-axis current controller	0.43
31, 32	-0.94 ± 0.24	52.4	Generator d-axis damper winding flux	0.21
			Generator field winding flux	0.51
			Generator exciter field voltage	0.65
33, 34	-0.93 ± 0.16	67.2	Motor field winding flux	0.70
			Motor exciter regulator voltage	0.70

Appendix C

Impedance and Admittance Plots

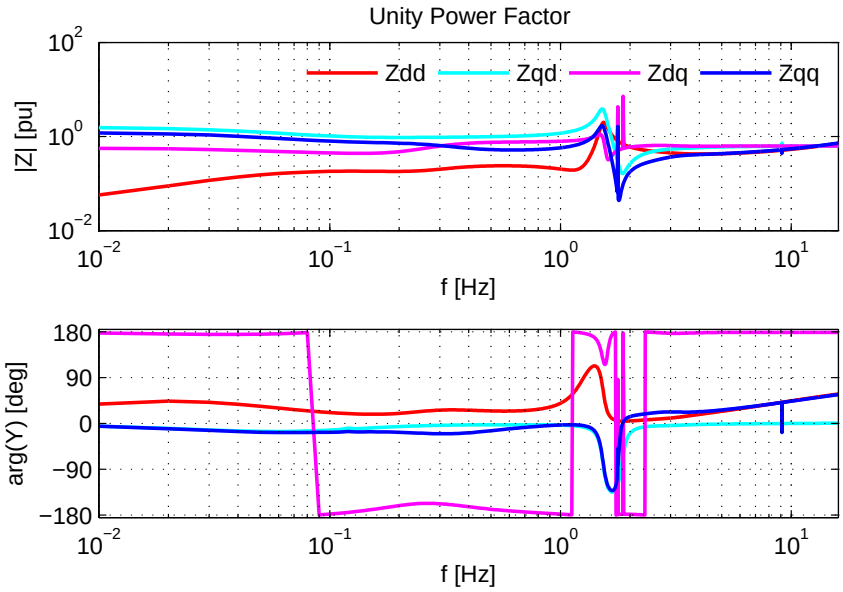

Figure C.1: Power supply impedance from case "Unity power factor".

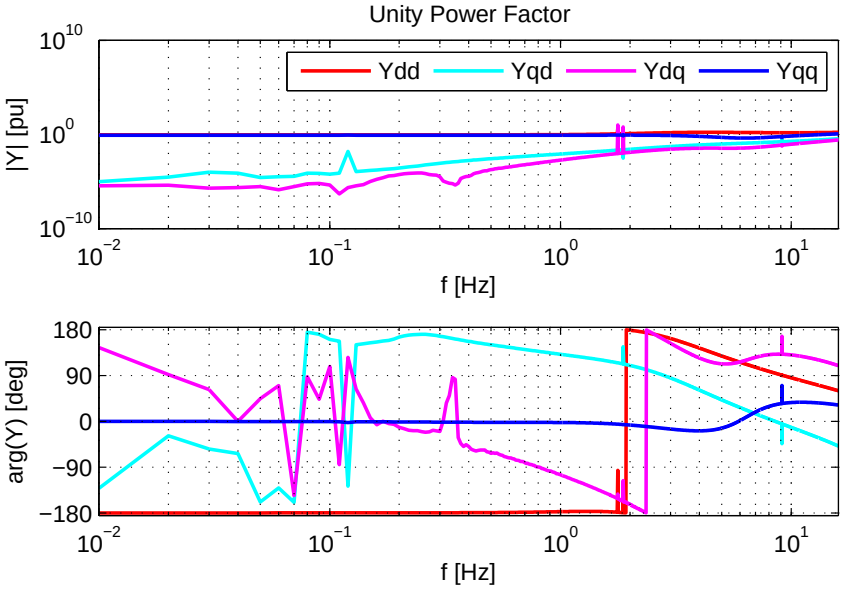

Figure C.2: Load admittance from case "Unity power factor".

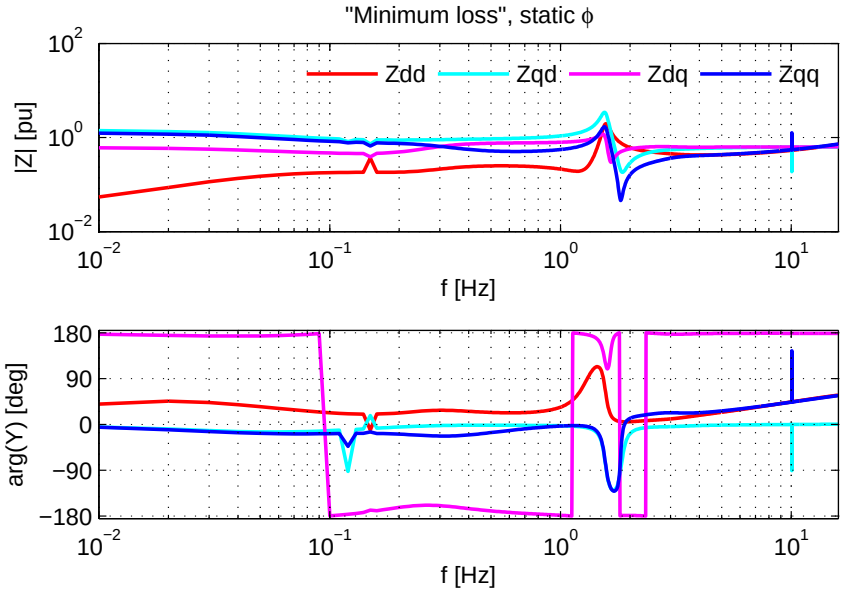

Figure C.3: Power supply impedance from case "Minimum loss", static ϕ.

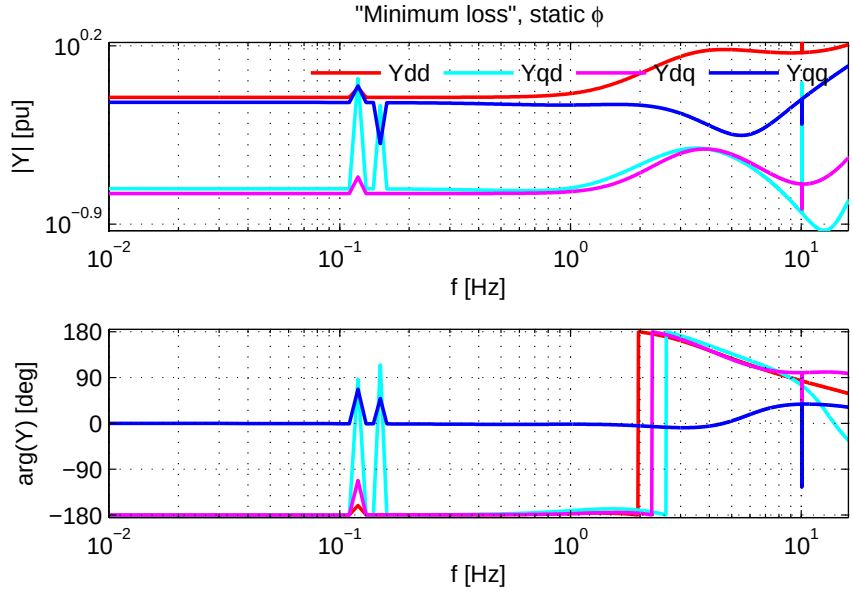

Figure C.4: Load admittance from case "Minimum loss", static ϕ.

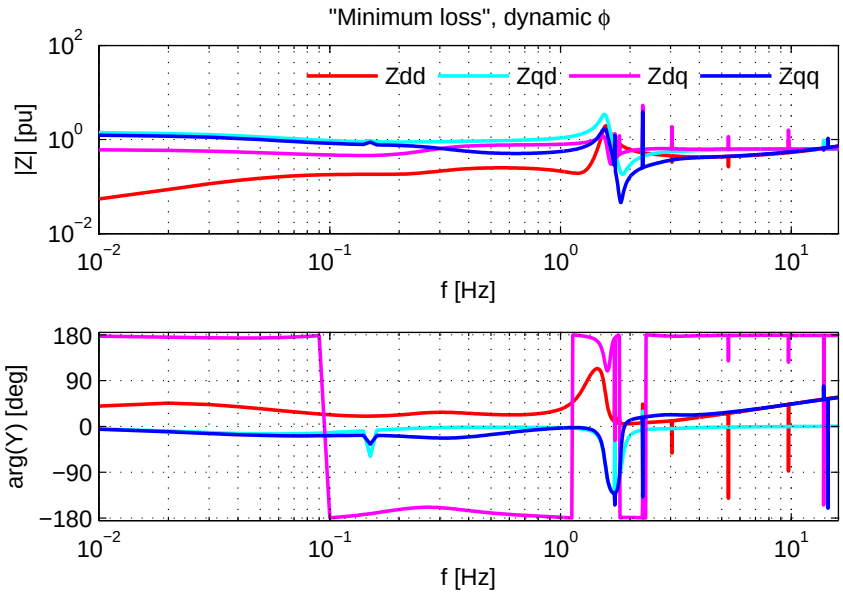

Figure C.5: Power supply impedance from case "Minimum loss", dynamic ϕ.

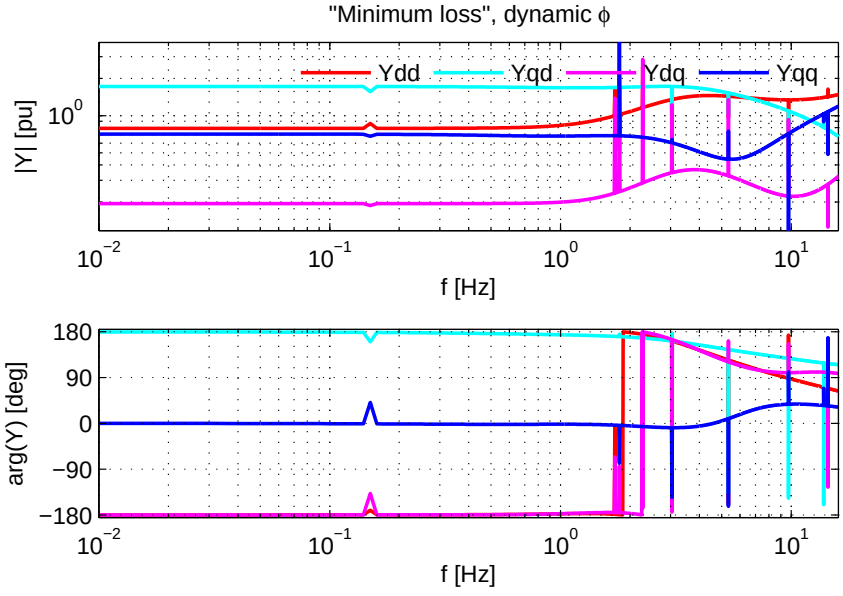

Figure C.6: Load admittance from case "Minimum loss", dynamic ϕ.

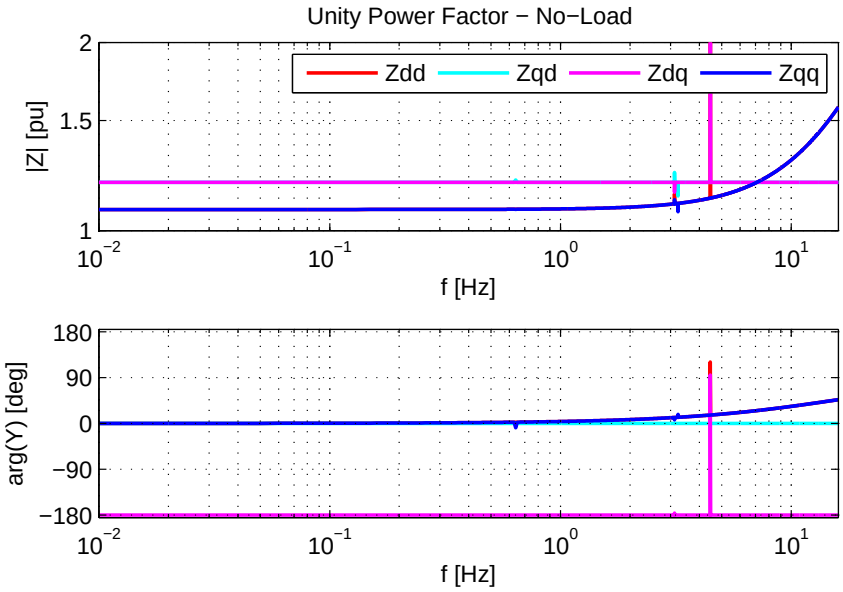

Figure C.7: Power supply impedance in no-load, stiff voltage source, 200 km line.

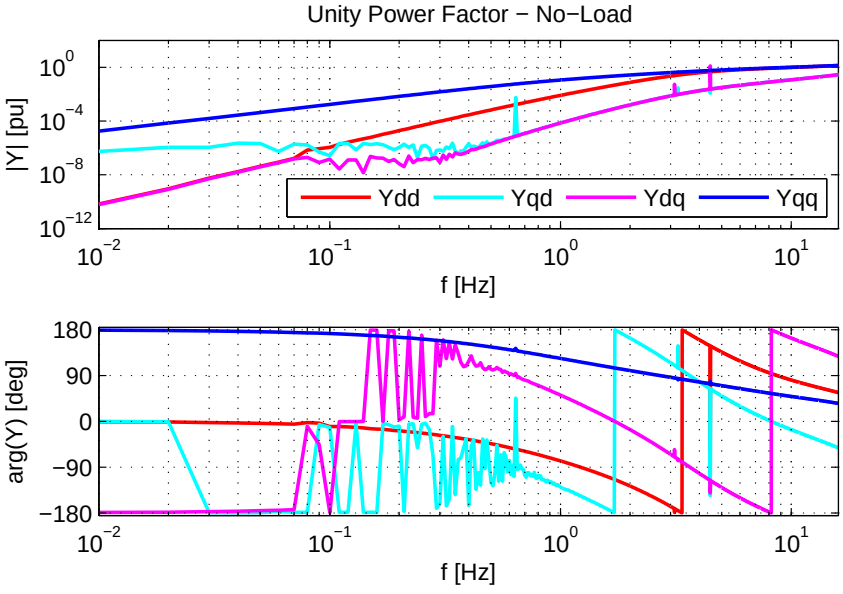

Figure C.8: Load admittance in no-load, unity power factor.

Appendix D

Equivalent Load

D.1 Equivalent Load Parameters

Table D.1: Parameters for transfer functions describing the equivalent load, for operating points from table 5.1 and at no-load at 16.5 kV.

Parameter	Simulation case			
	Unity power factor, 0.01-16 Hz	"Minimum loss", static ϕ, 0.01-8 Hz	"Minimum loss", dynamic ϕ, 0.01-8 Hz	No-load, 0.01-8 Hz
b_{1dd}	1.59485	1.05291	0.946526	0.823758
b_{2dd}	-77.2403	-50.2389	-51.0383	-12.2242
b_{3dd}	-628.033	-687.341	-697.44	11.64
b_{1qd}	-0.244924	0.00497904	-0.0432643	0.00939448
b_{2qd}	20.2574	-8.75212	-84.0027	0.627388
b_{3qd}	-0.0657475	-150.133	-1055.65	0.395931
b_{1dq}	0.163352	0.0802644	0.0803873	-0.00983501
b_{2dq}	4.78589	-9.1714	-9.17628	-0.62376
b_{3dq}	-0.0525647	-140.742	-140.691	-0.421945
b_{1qq}	1.34009	0.941673	0.941606	1.35809
b_{2qq}	34.0905	20.7327	20.7344	-0.81361
b_{3qq}	2632.12	1242.81	1242.34	0.601939
a_{1dd}	1	1	1	1
a_{2dd}	65.2998	49.5733	50.3289	49.8551
a_{3dd}	689.856	903.112	884.288	1737.99
a_{1qd}	1	1	1	1
a_{2qd}	105.026	28.06	56.9394	11.9967
a_{3qd}	8448.02	721.289	612.462	1706.82
a_{1dq}	1	1	1	1
a_{2dq}	53.509	33.2391	33.2585	12.0383
a_{3dq}	11978.7	724.824	724.564	1691.59
a_{1qq}	1	1	1	1
a_{2qq}	77.2624	46.7774	46.7939	63.6794
a_{3qq}	3122.74	1750.5	1749.85	239.965

Table D.2: Parameters for transfer functions describing the bandwidth-reduced equivalent load, for operating points from table 5.1 and at no-load at 16.5 kV.

Parameter	Simulation case			
	Unity power factor, 0.5-6 Hz	"Minimum loss", static ϕ, 0.5-6 Hz	"Minimum loss", dynamic ϕ, 0.5-6 Hz	No-load, 0.5-6 Hz
b_{1dd}	0.923636	0.919521	0.822807	0.498749
b_{2dd}	-52.6472	-45.8278	-46.2618	-7.74997
b_{3dd}	-710.338	-601.305	-623.877	20.0456
b_{1qd}	0.0658099	0.000641705	-0.144582	0.0119592
b_{2qd}	1.04935	-9.511	-74.3714	0.168518
b_{3qd}	-0.496844	-115.077	-1747.45	0.817123
b_{1dq}	0.0157188	0.0811354	0.0811758	-0.0124268
b_{2dq}	-0.58692	-8.47684	-8.47771	-0.163302
b_{3dq}	-1.05112	-129.852	-129.893	-0.874087
b_{1qq}	0.697737	0.751806	0.75199	1.32268
b_{2qq}	9.18958	10.102	10.1109	-0.82489
b_{3qq}	675.387	783.103	783.49	1.85008
a_{1dd}	1	1	1	1
a_{2dd}	43.2238	43.7786	44.5145	29.3209
a_{3dd}	818.187	834.674	826.749	1310.14
a_{1qd}	1	1	1	1
a_{2qd}	22.1258	28.5163	57.598	10.8976
a_{3qd}	725.282	611.743	1042.11	954.488
a_{1dq}	1	1	1	1
a_{2dq}	21.8746	30.5964	30.6038	11.0702
a_{3dq}	579.383	706.403	706.449	938.646
a_{1qq}	1	1	1	1
a_{2qq}	18.378	22.3447	22.3619	61.6969
a_{3qq}	819.086	1134.42	1134.99	248.658

D.2 Admittance of Equivalent Load - Loaded Vehicle

Admittance as function of frequency for the complete vehicle model, shown with dots, and the admittance-based equivalent load shown as lines. The control scheme for reactive power and frequency range are given in the caption for each figure.

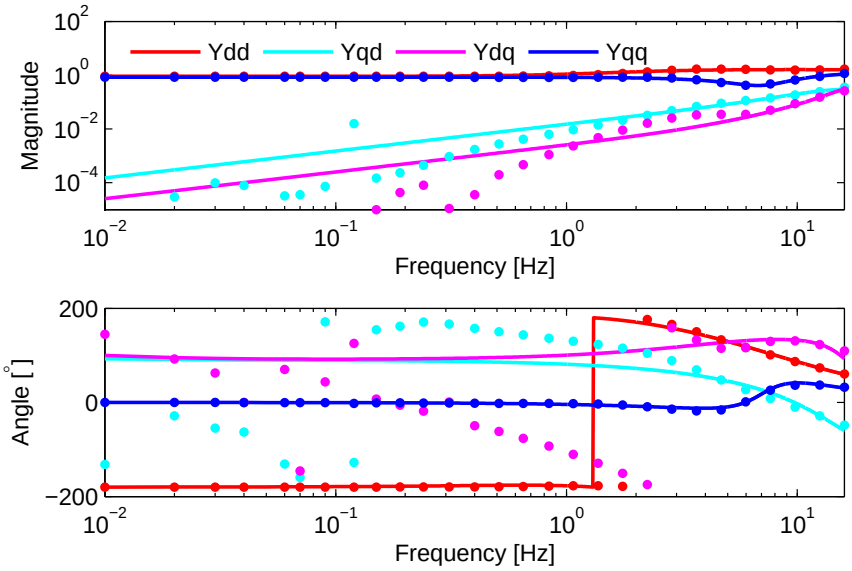

Figure D.1: Unity power factor, curve fitting performed from 0.01 to 16 Hz.

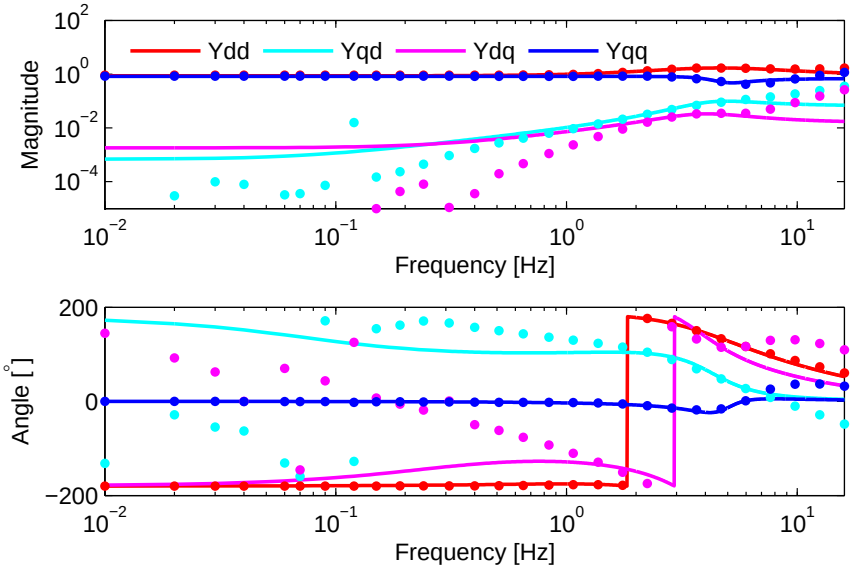

Figure D.2: Unity power factor, curve fitting performed from 0.5 to 6 Hz.

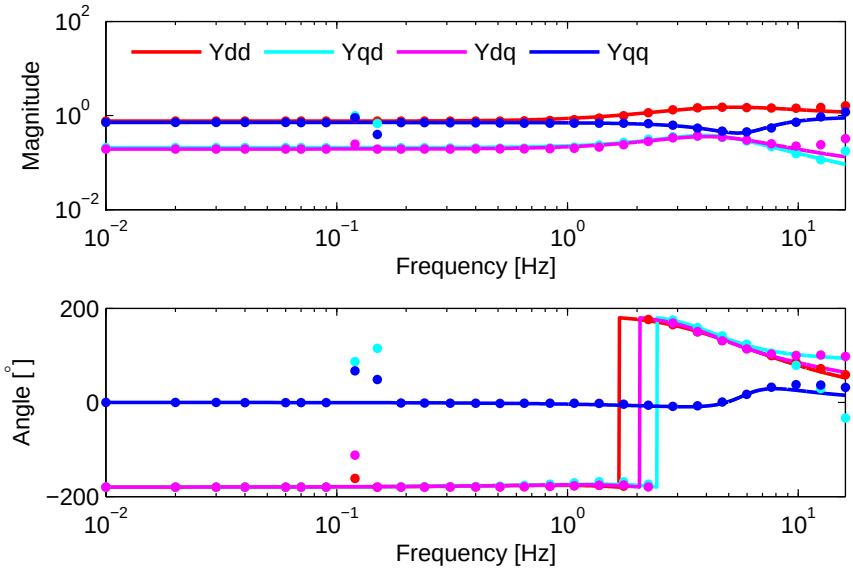

Figure D.3: "Minimum loss", static ϕ, curve fitting performed from 0.01 to 8 Hz.

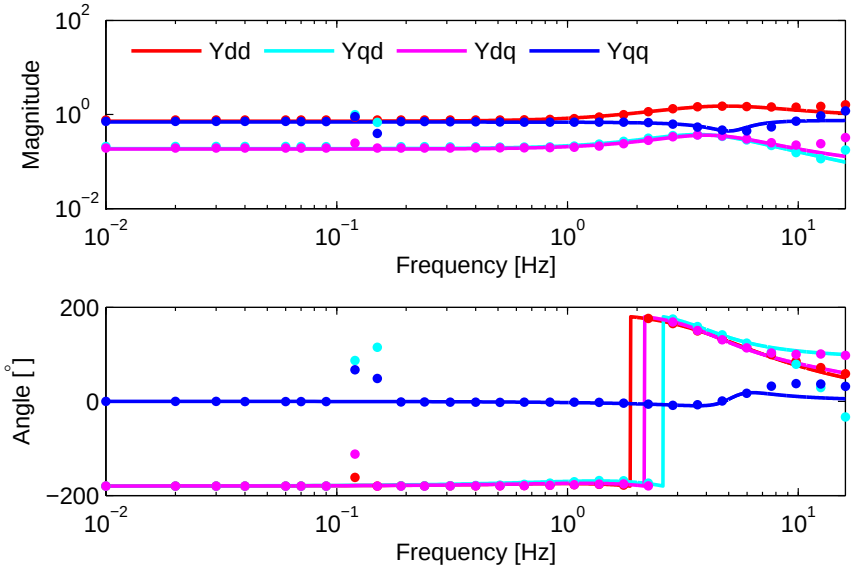

Figure D.4: "Minimum loss", static ϕ, curve fitting performed from 0.5 to 6 Hz.

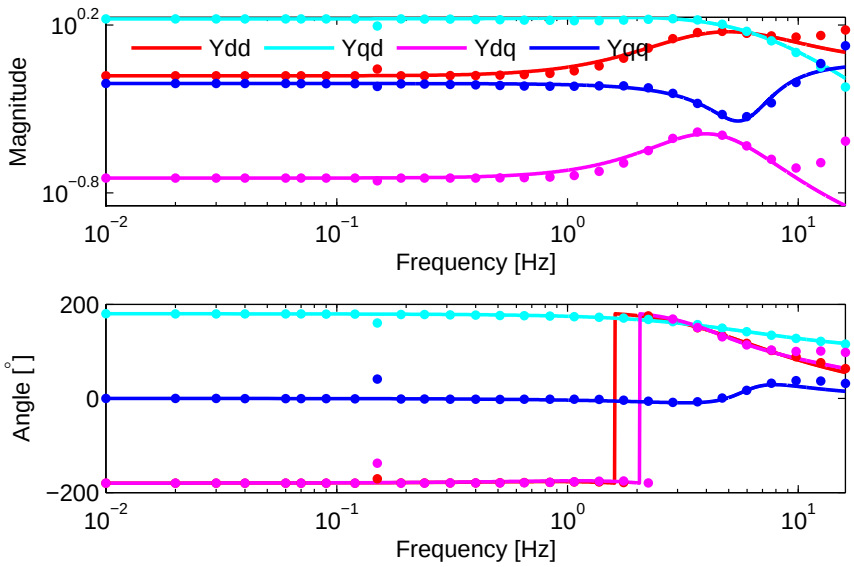

Figure D.5: "Minimum loss", dynamic ϕ, curve fitting performed from 0.01 to 8 Hz.

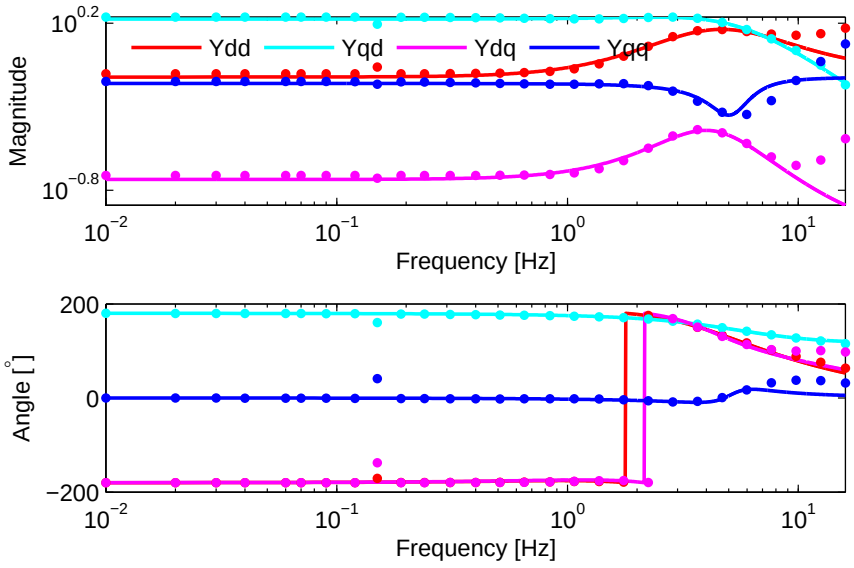

Figure D.6: "Minimum loss", dynamic ϕ, curve fitting performed from 0.5 to 6 Hz.

D.3 Admittance of Equivalent Load - No-Load

Admittance as function of frequency for the complete vehicle model, shown with dots, and the admittance-based equivalent load shown as lines. The control scheme for reactive power have no effect in no-load, only unity power factor is used. The frequency range at which curve fitting is performed is given in the caption for each figure.

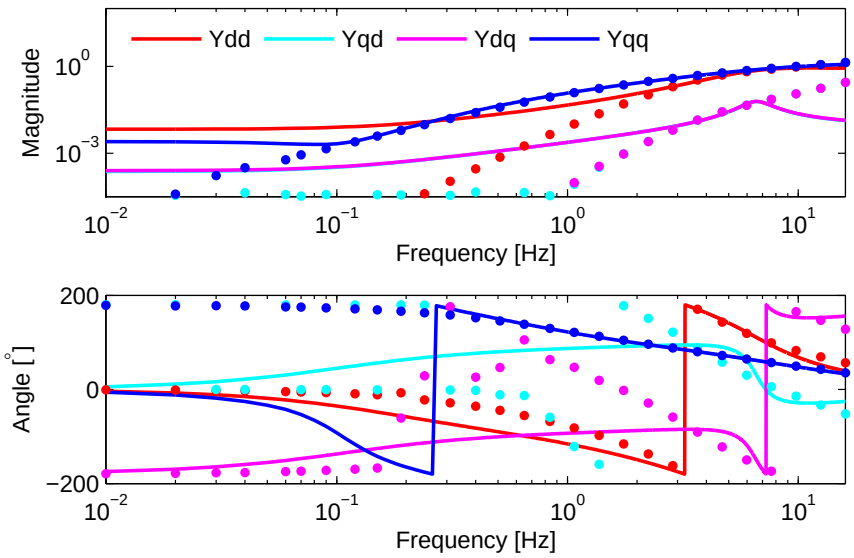

Figure D.7: Unity power factor, no-load, curve fitting performed from 0.01 to 8 Hz.

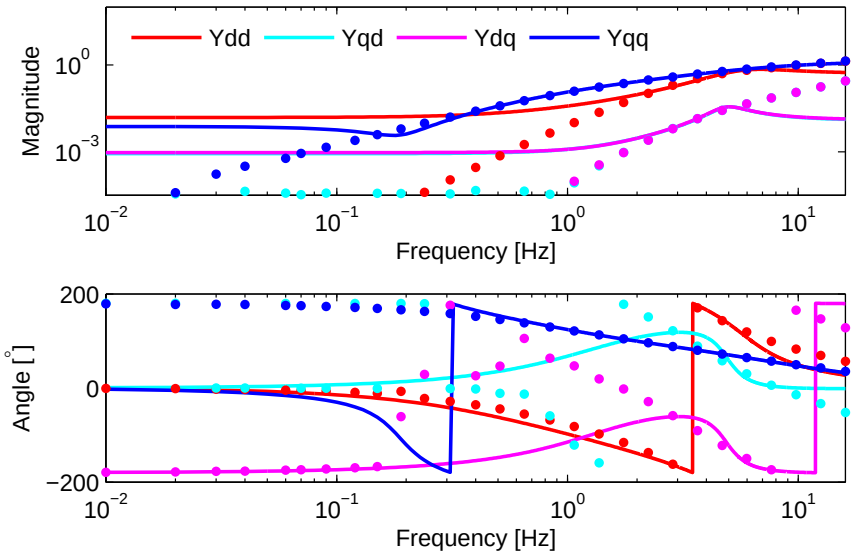

Figure D.8: Unity power factor, no-load, curve fitting performed from 0.5 to 6 Hz.

D.4 DSL-file for Admittance Based Load Model

```
 PROCESS EQLOADMINDYN(BUS,IR0,II0)
REAL IR0,II0,UR0/*/,UI0/*/,URE,UIM
REAL XDD,DXDD,DDXDD,IDD
STATE XDD,DXDD
REAL XDQ,DXDQ,DDXDQ,IDQ
STATE XDQ,DXDQ
REAL XQD,DXQD,DDXQD,IQD
STATE XQD,DXQD
REAL XQQ,DXQQ,DDXQQ,IQQ
STATE XQQ,DXQQ

PLOT XDD,DXDD,IDD,IDQ,IQD,IQQ

REAL b1dd/0.94652633/
REAL b2dd/-51.038308/
REAL b3dd/-697.44033/
REAL b1dq/0.080387254/
REAL b2dq/-9.1762819/
REAL b3dq/-140.69068/
REAL b1qd/-0.043264266/
REAL b2qd/-84.002654/
REAL b3qd/-1055.6519/
REAL b1qq/0.94160579/
REAL b2qq/20.734382/
REAL b3qq/1242.3367/

REAL a1dd/1/
REAL a2dd/50.328897/
REAL a3dd/884.28846/
REAL a1dq/1/
REAL a2dq/33.25846/
REAL a3dq/724.56386/
REAL a1qd/1/
REAL a2qd/56.93943/
REAL a3qd/612.46198/
REAL a1qq/1/
REAL a2qq/46.793905/
REAL a3qq/1749.8464/

EXTERNAL IR0,II0
AC BUS
AC_CURRENT I/BUS/
```

```
IF (TRANSTA) THEN
IF(START) THEN
URO=UPRE(BUS)
UIO=UPIM(BUS)
IPRE(I)=IRO
IPIM(I)=IIO

ELSE
!!YDD d-axis current, d-axis voltage
URE=UPRE(BUS)-URO
UIM=UPIM(BUS)-UIO

DXDD: .D/DT.XDD = DXDD
XDD: .D/DT.DXDD*A1DD=URE-DXDD*A2DD-XDD*A3DD
IDD=B1DD*.D/DT.DXDD+B2DD*DXDD+XDD*B3DD

DXDQ: .D/DT.XDQ = DXDQ
XDQ: .D/DT.DXDQ*A1DQ=UIM-DXDQ*A2DQ-XDQ*A3DQ
IDQ=B1DQ*.D/DT.DXDQ+B2DQ*DXDQ+XDQ*B3DQ

DXQD: .D/DT.XQD = DXQD
XQD: .D/DT.DXQD*A1QD=URE-DXQD*A2QD-XQD*A3QD
IQD=B1QD*.D/DT.DXQD+B2QD*DXQD+XQD*B3QD

DXQQ: .D/DT.XQQ = DXQQ
XQQ: .D/DT.DXQQ*A1QQ=UIM-DXQQ*A2QQ-XQQ*A3QQ
IQQ=B1QQ*.D/DT.DXQQ+B2QQ*DXQQ+XQQ*B3QQ

IPRE(I)=IRO-IDD-IDQ
IPIM(I)=IIO-IQD-IQQ

ENDIF !!End start
ENDIF !!Virker bare i TRANSTA, END - IF (TRANSTA) THEN
END
```